USTI

MAY 3 1 1990

LBL-28930

Lawrence Berkeley Laboratory
UNIVERSITY OF CALIFORNIA

CHEMICAL BIODYNAMICS DIVISION

Repair of Psoralen Crosslinks in *Escherichia coli*: *In Vitro* Studies with the RecA Protein and (A)BC Excinuclease

S. Cheng

Ph.D. Thesis

May 1990

DO NOT MICROFILM
COVER

DISTRIBUTION OF THIS DOCUMENT IS UNLIMITED

Prepared for the U.S. Department of Energy under Contract Number DE-AC03-76SF00098.

DISCLAIMER

This report was prepared as an account of work sponsored by an agency of the United States Government. Neither the United States Government nor any agency thereof, nor any of their employees, makes any warranty, express or implied, or assumes any legal liability or responsibility for the accuracy, completeness, or usefulness of any information, apparatus, product, or process disclosed, or represents that its use would not infringe privately owned rights. Reference herein to any specific commercial product, process, or service by trade name, trademark, manufacturer, or otherwise does not necessarily constitute or imply its endorsement, recommendation, or favoring by the United States Government or any agency thereof. The views and opinions of authors expressed herein do not necessarily state or reflect those of the United States Government or any agency thereof.

DISCLAIMER

Portions of this document may be illegible in electronic image products. Images are produced from the best available original document.

DISCLAIMER

This document was prepared as an account of work sponsored by the United States Government. Neither the United States Government nor any agency thereof, nor The Regents of the University of California, nor any of their employees, makes any warranty, express or implied, or assumes any legal liability or responsibility for the accuracy, completeness, or usefulness of any information, apparatus, product, or process disclosed, or represents that its use would not infringe privately owned rights. Reference herein to any specific commercial products process, or service by its trade name, trademark, manufacturer, or otherwise, does not necessarily constitute or imply its endorsement, recommendation, or favoring by the United States Government or any agency thereof, or The Regents of the University of California. The views and opinions of authors expressed herein do not necessarily state or reflect those of the United States Government or any agency thereof or The Regents of the University of California and shall not be used for advertising or product endorsement purposes.

Lawrence Berkeley Laboratory is an equal opportunity employer.

LBL--28930

DE90 011337

Repair of Psoralen Crosslinks in *Escherichia coli:* *In Vitro* Studies with the RecA Protein and (A)BC Excinuclease

Suzanne Cheng
(Ph.D. thesis)

Department of Chemistry
University of California
and
Lawrence Berkeley Laboratory
University of California
Berkeley, CA 94720

May 1990

This work was supported by the Director, Office of Energy Research, Office of General Life Sciences, Molecular Biology Division, of the U.S. Department of Energy under Contract No. DE-AC03-76SF00098.

MASTER

DISTRIBUTION OF THIS DOCUMENT IS UNLIMITED

Repair of Psoralen Crosslinks in *Escherichia coli:* *In Vitro* Studies with the RecA Protein and (A)BC Excinuclease

Suzanne Cheng

Abstract

RecA, a key protein for recombination in *Escherichia coli*, was utilized to insert short psoralen-monoadducted oligonucleotides into a duplex plasmid molecule through a variation of the homologous pairing reaction. Covalent psoralen crosslinks could then be formed between the inserted oligonucleotide and its complement within the plasmid. The efficiency of the overall process was found to depend upon the nucleoside triphosphate cofactor, the extent of homology, oligonucleotide length, and psoralen location. Deproteinized complexes were also observed to retain a certain degree of unwinding of the plasmid due to the introduction of the crosslinked oligonucleotide.

These three-stranded complexes were used as model substrates for the study of the action mechanism of (A)BC excinuclease (uvrABC endonuclease), the enzyme responsible for nucleotide excision repair in *E. coli*. (A)BC excinuclease incises just one strand of a psoralen-crosslinked duplex, but can be induced to incise the other strand through formation of a three-stranded complex at the crosslink site. DNA polymerase I and ligase can then complete the repair process by filling and sealing the gap left by the incisions. These results support a previously suggested model for error-free crosslink repair, and represent progress toward the *in vitro* reconstitution of the entire pathway for repair of a psoralen crosslink.

In the spirit of those who search for answers and those who ride the roller coaster.

Acknowledgements

In my five years at Berkeley, I have had a multitude of experiences, both academic and social, intellectual and emotional. I owe the successful completion of my graduate career to many individuals, for I have been fortunate enough to have never lacked for words of encouragement.

Regarding my education and initiation into the world of academic science, I particularly want to thank Harvey Schugar from my years as an undergraduate at Rutgers; John Hearst, my research director here at Berkeley; Aziz Sancar, my research director at my lab-away-from-lab at UNC-Chapel Hill; and two former post-docs, Howard Gamper and Ben Van Houten, who paved the way for the work contained in this thesis. I would also like to thank the National Science Foundation and my mentors at AT&T Bell Laboratories for their support.

To my friends and the extended families associated with the Hearst and Sancar labs, the ones who tolerated my bad days and who made graduate life at least bearable, but mostly enjoyable and educational, many thanks. David and Luz, Effie, Yvonne, and Pete and Susie in particular gave me much needed and appreciated support at those times when life seemed bleakest. Above all, I want to thank Ken for his companionship and lessons in life, and both Ken and Ruth for helping me through the most difficult months.

I thank my parents Wen-Kwei and Mei-Fang, and my brother Po-Yuan and sister Julie. To my mother, especially, thank-you for a lifetime of support and encouragement.

My gratitude to those who remain anonymous is no less sincere than to those I have chosen to name here. I thank everyone with whom I have interacted during my stay at Berkeley for a memorable five years. Time will show whether I have learned my lessons well.

Table of Contents

Chapter 1

General Introduction

Given the biological importance of DNA as the keeper of an organism's genetic makeup, RNA viruses excepted, it is not suprising that a variety of repair mechanisms exist to ensure that the genetic information (chemical) and the functionality (physical) of the genome are not compromised. The effect of damage to DNA may be limited to loss of information at the modified or deleted bases, or, as in the case of interstrand crosslinks, the damage may interfere with the processes of replication and transcription.

Formation of interstrand crosslinks is the mechanism by which a number of carcinogenic and chemotherapeutic agents act. Biological effects of crosslink damage have been noted in bacteriophages, bacteria, and in eucaryotic cells. Understanding cellular efforts to repair these potentially lethal lesions is therefore of interest to many researchers. Our own model system for the study of crosslink damage is that of psoralen-adducted DNA.

Plants and seeds containing psoralens have been used in the treatment of skin disorders for thousands of years. *Ammi majus* seeds and sunlight were specifically prescribed for vitiligo as early as in the thirteenth century in Egypt, although the active component 8-methoxypsoralen (8-MOP) was not identified until 1947 [reviewed by Ben-Hur and Song, 1984]. The related compound 5-methoxypsoralen (5-MOP) had already been isolated, from bergamot oil in 1834, but the necessity of light for the observed interaction of psoralens and biological molecules had not been noted until the work of Phyladelphy in 1931 [reviewed by Midden, 1988; Song and Tapley, 1979]. Isolation of 5-MOP, 8-MOP, and a third derivative from *Ammi majus* seeds by Fahmy and coworkers in 1947 marked a beginning in efforts to understand the photobiological action of psoralens [reviewed by Ben-Hur and Song, 1984]. Currently, the most widely used psoralens are 8-MOP and 4,5′,8-trimethylpsoralen (TMP), both readily synthesized chemically. Like 8-MOP, TMP is also found in nature, in a fungus found on diseased celery [reviewed by Cimino *et al.*, 1985].

Interest in the photochemistry and photobiology of psoralens stems from the desire

to understand not only the beneficial medical applications, but also the applications of psoralens in probing nucleic acid structure and function [reviewed by Cimino *et al.*, 1985], and the mechanisms by which psoralens are both mutagenic and carcinogenic [reviewed by Averbeck, 1989; Ben-Hur and Song, 1984]. Although the reactions between photoactivated psoralens and DNA may be primarily responsible for biological effects such as cytotoxicity and mutagenesis, other effects such as skin erythema and inflammation may be due to reactions with other targets. Psoralens are known to bind to and react with proteins [reviewed by Midden, 1988; Parsons, 1980], as well as lipids and membranes [Midden, 1988]. Singlet oxygen, a product of the quenching of photoactivated psoralens by molecular oxygen, may also be responsible for certain lesions [Sage *et al.*, 1989; reviewed by Midden, 1988]. Our concern here is the ability of psoralens to directly damage DNA, and the cellular mechanisms for repair of such damage.

The psoralen derivatives used in photochemotherapy are bifunctional linear furocoumarins, able to form both monoadducts and interstrand diadducts (crosslinks) upon irradiation with ultraviolet (UV-A, 320-380 nm) light. Monofunctional and angular psoralen derivatives also exist. Both mono- and diadduct lesions are mutagenic, typically resulting in base substitutions at the psoralen site or deletion of the adducted thymidine [Piette *et al.*, 1988]. Crosslinks also prevent the unwinding of DNA required for replication and can therefore be lethal lesions. Frameshift mutations induced by high concentrations of certain psoralens in the absence of UV light have also been observed; however, this weak mutagenicity appears to occur by a different mechanism from the UV-dependent induction of base substitutions [reviewed by Saffran, 1988].

The relative mutagenic potentials of monoadducts and crosslinks have been examined by several groups [reviewed by Averbeck, 1988a; Saffran, 1988]. As noted earlier, crosslinks may be lethal, but to the extent that they are repaired, they do often lead to mutations. Monofunctional derivatives are less mutagenic than bifunctional psoralens, suggesting that more mutations result from the presence of crosslinks than from mono-

adducts alone. Selective formation of monoadducts or crosslinks with a bifunctional derivative is possible because of kinetic and wavelength requirements of psoralen photochemistry. Monoadduct formation requires a single photon, while a two-photon absorption is necessary for the diadduct; short versus long irradiations can therefore favor one adduct over the other. Furthermore, irradiation with UV light at wavelengths above 389 nm preferentially yields crosslinkable monoadducts which can later be converted to crosslinks upon irradiation with 365 nm light [Kodadek and Gamper, 1988; Tessman *et al.*, 1985]. Comparisons of monoadduct- and crosslink-rich populations of lesions due to bifunctional psoralens [Averbeck, 1988a; Papadopoulo *et al.*, 1988] support the general conclusion that crosslinks are more mutagenic than monoadducts, but mutagenicity does depend upon the particular psoralen derivative and the biological system in question. Because psoralen crosslinks involve both strands of a DNA helix, such lesions are likely to be more difficult to repair than monoadducts which directly affect only one strand. In the absence of DNA repair activity, monoadducts can be as mutagenic as crosslinks [reviewed by Saffran, 1988].

Our focus here is on the molecular events involved in the excision repair of psoralen-crosslinked DNA in *Escherichia coli (E. coli)*. The amount of genetic and biochemical knowledge that exists makes this organism particularly useful for such an investigation. At a greater level of complexity and correspondingly less detailed level of understanding are the studies of repair in yeast, specifically of *Saccharomyces cerevisiae*. Even more complex is the analysis of repair in mammalian cells. Excision repair in all three systems has been recently reviewed [Friedberg, 1987 and 1988; Myles and Sancar, 1989; Smith, 1988]. Although *E. coli* is a procaryote and hence not the best model for eucaryotic processes, the details that are more readily elucidated in *E. coli* can serve as a foundation for constructing models of eucaryotic mechanisms. Parallels among bacteria, yeast, and mammalian cells have previously been found in fundamental biochemical processes such as replication [Kornberg, 1980].

In *E. coli*, inhibition of DNA replication or damage to DNA, such as that due to exposure to ultraviolet radiation or to alkylating or crosslinking agents, results in the induction of the SOS system of responses [reviewed by Little and Mount, 1982; Ossanna *et al.*, 1987; Peterson *et al.*, 1988; Smith and Wang, 1989; Smith *et al.*, 1987; Walker, 1985]. Other repair systems do exist; however, the SOS system is the largest and the most understood. The SOS network involves a number of unlinked genes. The products of these genes function in a variety of processes, including nucleotide excision repair, mutagenesis via "error-prone repair," recombinational repair (both of daughter-strand gaps and double-strand breaks), and mismatch repair. Yet another SOS response is to delay cell division, to allow the cell to repair its DNA.

Regulation of the SOS system is mediated by interactions between the RecA and LexA proteins. In the uninduced cell, LexA protein represses the SOS genes, permitting only a low level of expression. Both DNA damage and inhibited replication lead to activation of the RecA protein which then promotes cleavage of LexA, thus inactivating the repressor. As a result, expression of the various SOS genes, including the *recA* gene, increases. Certain prophage repressors are also subject to RecA-mediated cleavage, enabling prophage induction upon death of the cell. *In vitro* evidence suggests that RecA may not be functioning as a protease in these reactions. Under alkaline conditions *in vitro*, the LexA and λ repressors spontaneously undergo the same specific cleavages that occur under SOS-induction conditions *in vivo*. Activated RecA may therefore serve to allosterically facilitate the cleavage of LexA at physiological pH. [Little, 1984]

The mechanism of RecA activation is still a subject of investigation, but the inducing signal is most probably nucleic acid. Experimental evidence appears to rule out an oligonucleotide signal resulting from DNA degradation [reviewed by Devoret *et al.*, 1988; Little and Mount, 1982]. Results of *in vitro* and *in vivo* studies have led instead to proposals of both single- (ss) and double-stranded (ds) DNA signal pathways, perhaps initiated by different SOS-induction treatments. These studies have utilized a variety of

RecA mutants, including (i) *recA441* (*tif*) cells which can be thermally induced to express genes at SOS levels despite the absence of any SOS induction, and (ii) *recA430* cells which respond poorly to SOS-inducing treatment. Both mutant proteins as well as wild-type RecA have been purified. Lu and Echols [1987] observed that wild-type RecA preferentially bound to UV-damaged DNA and promoted efficient cleavage of LexA. By comparison, undamaged DNA was sufficient to activate RecA441-induced cleavage of LexA, while RecA430-induced cleavage of the repressor was inefficient even in the presence of UV-irradiated DNA. Lu and Echols hypothesized that RecA recognizes and preferentially binds to lesions over undamaged DNA because of the distortion in the DNA helix. Activated RecA may therefore be lesion-bound protein. Alternatively, either discontinuous replication at lesions or nucleolytic activity by the RecBC enzyme can produce ssDNA which then stimulates RecA to cleave the LexA repressor [Phizicky and Roberts, 1981; reviewed by Devoret *et al.*, 1988; Moreau, 1985]. Both single-stranded DNA binding protein [Moreau, 1987] and binding of a nucleoside triphosphate are also implicated in the activation process. Hydrolysis of the nucleoside triphosphate is not required. One model is that RecA is activated upon formation of a ternary complex with ssDNA and dATP [Moreau, 1985; Phizicky and Roberts, 1981]. Two strongly coprotease-constitutive mutants, both more effective than wild-type RecA in the cleavage of LexA repressor, have been found to accept RNA in addition to ssDNA [Wang *et al.*, 1988b] and also a broad range of nucleoside triphosphates [Wang *et al.*, 1988a] as cofactors for the reaction. Devoret and coworkers have also reported that the PsiB protein from certain conjugative plasmids can inhibit RecA-mediated cleavage of LexA. They propose that the PsiB protein interferes with a conformational change needed for the activation of the RecA protein [Bailone *et al.*, 1988; Célérier *et al.*, 1988; Devoret *et al.*, 1988].

The role of the RecA protein in *E. coli* actually extends far beyond modulation of the LexA repressor activity for SOS induction. In the uninduced cell, RecA is of paramount importance for genetic recombination, hence its very name. As a recombinase,

RecA promotes homologous pairing and strand exchange between various ss and dsDNA molecules (discussed further in Chapter 2). RecA is also required for SOS-induced mutagenesis and certain DNA repair pathways.

SOS-induced mutagenesis is known to require the RecA, UmuC, and UmuD proteins, and genetic studies implicate DNA polymerase III (pol III) [reviewed by Lu and Echols, 1987; Shwartz *et al.*, 1988; Walker, 1985]. This process is also known as "error-prone repair" or "SOS processing". Recent *in vivo* and *in vitro* work has shown that the RecA-dependent cleavage of UmuD protein yields UmuD′ which then associates with UmuC to form the complex that is active in mutagenesis [Burckhardt *et al.*, 1988; Nohmi *et al.*, 1988; Shinagawa *et al.*, 1988; Woodgate *et al.*, 1989]. The site of cleavage of UmuD was actually predicted based upon sequence homology between the UmuD and LexA proteins [Burckhardt *et al.*, 1988]. One model for SOS mutagenesis is that the UmuC/D′ complex, possibly with the aid of RecA, enables pol III holoenzyme to bypass DNA lesions that would otherwise result in termination of replication [Lu *et al.*, 1986; Shwartz *et al.*, 1988a; Woodgate *et al.*, 1989]. Homology between the sequences of UmuC and UmuD′ and those of gp44/gp62 and gp45 of bacteriophage T4, respectively, is suggestive of their function [Battista *et al.*, 1988]. These three T4 gene products (gp) enhance the processivity of the T4 DNA polymerase. The UmuC/D′ complex may similarly make pol III holoenzyme more processive. Pol III is known to possess some ability to bypass apurinic sites and cyclobutane photodimers *in vitro*, an ability attributed to high processivity; accessory proteins such as UmuC/D′ and RecA may increase the efficiency of translesion synthesis [Shwartz *et al.*, 1988a].

In the absence of single-stranded DNA binding protein, RecA has also been observed to inhibit pol III in the replication of ssDNA. RecA may therefore be involved in the temporary suspension of DNA replication that follows UV irradiation, presumably to give DNA repair enzymes time to act on any lesions that could interfere with replication. [Shwartz and Livneh, 1989]

Other SOS-inducible processes involve homologous recombination. Genetic studies have revealed an absolute requirement for the *recA* gene in the repair of both daughter-strand gaps and double-strand breaks, otherwise known as "postreplicational repair," and in nucleotide excision repair. These processes involve a number of inducible recombination gene products.

A daughter-strand gap can arise from termination of replication at a lesion and subsequent resumption of replication downstream from the lesion. Gaps can be 1000 to 40,000 nucleotides long [reviewed by Smith *et al.*, 1987]. Double-strand breaks can result from agents such as ionizing radiation or mitomycin C [reviewed by Walker, 1985], or from incision across from a daughter-strand gap [reviewed by Smith and Wang, 1989; Smith *et al.*, 1987]. A number of genes have been implicated in postreplicational repair, but some of these have yet to be tested for their direct role, and there may be genes as yet unidentified. Based upon the genetic data, four modes of repair have been identified: *recF*- and *polA*-dependent pathways for daughter-strand gaps, and *recF*- and *recBCD*-dependent pathways for double-strand breaks. The extent to which the RecA protein acts in a regulatory versus mechanistic capacity remains unclear, but it is a necessary component of all of these repair processes [reviewed by Smith and Wang, 1989].

Nucleotide excision repair has also been found to proceed by two different pathways [reviewed by Peterson *et al.*, 1988; Smith and Wang, 1989]. Both require the *uvrA*, *uvrB*, and *uvrC* genes. The predominant pathway is characterized by short repair patches 10-30 nucleotides long and *polA*-dependence. The minor pathway involves *recA*, *recF* and *recB*, and results in long patches of 200 to 1500 nucleotides. In a model for short patch repair proposed as early as 1966, gaps produced in the excision of DNA lesions are filled by the product of the *polA* gene, DNA polymerase I [reviewed by Smith *et al.*, 1987]. Although the phenomenon of *rec*-dependent long patch repair synthesis had been characterized previously [Cooper, 1982], a mechanism has only recently been proposed. This process is functional only if the affected portion of the chromosome has been repli-

cated such that the homologous sister duplex exists. This observation suggests a role for recombination in the generation of long repair patches. Long patch repair appears to resemble postreplicational repair, having both a RecF- and a RecB-dependent pathway [Smith and Sharma, 1987].

Although psoralen monoadducts, like UV-induced photodimers, can be readily repaired by the short patch repair pathway, crosslinks present a special problem because both strands of the helix are adducted. Simultaneous excision of both adducted nucleotides results in a double-stranded break, and incision of only one strand leaves a potentially mutagenic template for the polymerase attempting to fill the excision gap. Psoralen-induced mutagenesis may indeed proceed by the UmuC/D′ pathway described earlier. The phenomenon of *uvr*-independent crosslink repair has been observed in *uvr*-deficient cells, and alternate repair pathways involving double-stranded breaks or glycosylase-mediated generation of apyrimidinic sites have subsequently been proposed [reviewed by Smith, 1988]. These mutagenic mechanisms are discussed further in Chapter 4. An explanation for *uvr*-dependent *non*mutagenic crosslink repair was developed during the 1970s by Cole and coworkers.

Cole first noted the particular sensitivity of either excision-defective (*uvr*$^-$) or recombination-deficient (*recA*$^-$) *E. coli* mutants to damage from psoralen (the TMP derivative) plus UV light in 1971. Although wild-type cells could recover from 65 crosslinks per genome, and single mutants survived 6-16 crosslinks, the double mutant *uvr*$^-$*recA*$^-$ was unable to overcome a single crosslink per genome [Cole, 1971]. Cole further investigated the roles of excision activity and strand exchange between homologous duplexes in the repair of such interstrand crosslinks by analyzing the cellular DNA. He observed both *uvrA*- and *uvrB*-dependent cutting of the DNA into discrete segments whose size corresponded to approximately twice the single-stranded distance between the original crosslinks. Using differential density-labeling of the DNA, he observed subsequent *recA*-dependent covalent joining of fragments to yield high molecular weight species. Cole

therefore proposed a mechanism of sequential excision and recombination for the repair of interstrand crosslinks [Cole, 1973]. These observations were later extended to include the *uvrC* and *polA* genes as necessary components for strand incision. In particular, *polA* mutations affecting the 5′→3′ exonucleolytic function of DNA polymerase I rendered cells more sensitive to crosslinks, but deficiencies in the polymerization function had no effect on crosslink repair. Furthermore, no evidence of mechanisms involving double-strand breaks, single incisions at each crosslink, or double incisions all along the same strand was found [Cole *et al.*, 1976].

The *uvrA* and *uvrB* genes were thought to encode an endonuclease responsible for making the strand incision 5′ to a crosslink, leaving the 3′-side incision to be made by the 5′→3′ exonuclease of DNA polymerase I. The role suggested for UvrC was stabilization of the DNA between incision steps. The crosslinked structure that remained on the unincised strand would presumably interfere with repair synthesis and ligation, while possibly stabilizing the gap in the incised strand. However, nucleolytic extension of the gap from the initial incision sites would create a single-stranded region that could serve as a substrate for RecA-mediated strand exchange. This first excision gap would thus be replaced through recombination rather than by mutagenic polymerase-mediated synthesis. Once the duplex structure was restored in the damaged region, the remaining strand of the crosslink could be excised. Repair synthesis could then complete the repair process without introducing mutations. [Cole, 1973; Cole *et al.*, 1976]

In essence, this remains the current model for error-free repair of interstrand crosslinks, a mechanism of sequential incision and recombination steps. Revisions have been made, however, to account for more recent data. Perhaps the most significant revision followed the purification of the UvrA, UvrB and UvrC proteins, technically difficult because of their low cellular concentrations. Sancar and Rupp used overproducing plasmids and then reconstituted the UvrABC excision nuclease (ABC excinuclease) *in vitro*. ABC excinuclease was found to possess the ability to make *both* 5′ and 3′ incisions around

pyrimidine photodimers. Specifically, the enzyme hydrolyzed the eighth phosphodiester bond on the 5′ side and the fourth or fifth bond on the 3′ side, leaving 3′-OH and 5′-P termini. [Sancar and Rupp, 1983] This dual incision mechanism was proposed to apply to all ABC excinuclease-mediated repair, a prediction that has been borne out by numerous studies [reviewed by Sancar and Sancar, 1988; discussed further in Chapter 3].

Recent *in vitro* work provided evidence supporting the short patch pathway for the repair of psoralen monoadducts [Van Houten *et al.*, 1986b and 1988]. In light of these results, a more detailed revised version of Cole's model for crosslink repair was proposed [Van Houten *et al.*, 1986b and 1988]. The overall mechanism is the same: two ABC excinuclease-mediated incision steps separated by RecA-mediated recombination, and completion of the repair process by the accessory proteins DNA pol I, ligase, and helicase II (UvrD). The molecular events associated with each step and the transitions between successive steps have not yet been defined, however.

Our efforts to examine the RecA-dependent steps in this model for error-free repair of psoralen crosslinks are summarized in the following pages. Using the bifunctional psoralen derivative 4′-hydroxymethyl-4,5′,8-trimethylpsoralen (HMT), we constructed site-specifically crosslinked duplex and three-stranded DNA molecules. With purified proteins and these well-defined substrates, we were able to take a close look at RecA-mediated crosslink repair. Our *in vitro* results are consistent with the model proposed by Van Houten and associates, and provide insight to recombination and repair mechanisms at the molecular level.

Chapter 2

RecA-Mediated Formation of Three-Stranded DNA Complexes

Introduction

Removal of a crosslinked site requires two pairs of incisions, one pair on each strand. These incisions may be made simultaneously, to create a double-stranded break, or they may be made sequentially. As was described briefly in Chapter 1, the current model for error-free crosslink repair is a sequential incision and recombination mechanism. RecA-mediated recombination provides a homologous replacement strand for the gap created by the first pair of incisions in one strand of the crosslinked duplex. The result is a three-stranded repair intermediate which then undergoes the second round of incisions. We modeled this three-stranded intermediate with a complex generated by using the RecA protein to insert a psoralen-monoadducted DNA oligonucleotide into a duplex circular plasmid and then irradiating the complex to site-specifically crosslink the oligomer to its complement. Although this procress is feasible in principle, we needed to understand the requirements for RecA-mediated recombination and to determine the effect of having a psoralen-adducted substrate.

Successful cloning of the *recA* gene from *Escherichia coli* in 1976 [McEntee *et al.*, 1976] was a crucial achievement in the effort to understand the biological role of the RecA protein. Prior to this, genetic studies had revealed the importance of the *recA* gene in homologous recombination, DNA repair, and in the SOS response [reviewed by McEntee and Weinstock, 1981]. In the nearly 15 years since the gene was first cloned, purified RecA protein has been studied extensively by a variety of methods. Comprised of a single 352-amino acid chain (37,842 dalton molecular weight), the RecA protein has quite a diverse set of responsibilities. The regulatory role of the coprotease function has already been described in Chapter 1. Our interest here is in RecA-mediated homologous pairing.

RecA protein promotes annealing of complementary single strands and pairing between homologous duplexes or between single-stranded (ss) and homologous double-stranded (ds) DNA. Recent studies characterizing the RecA-mediated renaturation of complementary single strands include those by Bryant and Lehman [1985], Bryant and

coworkers [1989], and McEntee [1985]. Homologous pairing and strand exchange have been reviewed several times by key contributors to the field [Cox and Lehman, 1987; Griffith and Harris, 1988; Kowalczykowski, 1987; McEntee and Weinstock, 1981; Radding, 1982 and 1989; West, 1988].

The homologous pairing reaction may be separated into three stages [reviewed most recently by Radding, 1989]. Initially, RecA monomers cooperatively polymerize along the ssDNA to form a presynaptic complex. Next, the duplex DNA and the complexed ssDNA are brought into homologous alignment. The search for homology appears to occur by a mechanism of facilitated diffusion within networks formed between presynaptic filaments and dsDNA [Gonda and Radding, 1983 and 1986]. Two distinct structures have been noted in this synaptic process [Bianchi *et al.*, 1983; Riddles and Lehman, 1985a and 1985b]. First to form is a paranemic joint in which the complementary strands are aligned without any net interwinding; this structure dissociates at high temperatures or upon deproteinization. Paranemic joints may encompass hundreds of basepairs [Christiansen and Griffith, 1986; Schutte and Cox, 1988]. The paranemic structure is apparently then converted into the more stable plectonemic joint, the interwound complex. The topology of the initial DNA substrates can preclude this conversion, as in the case of two covalently closed circular molecules. The postsynaptic stage involves unidirectional branch migration resulting in extended heteroduplex complexes (D-loops) or complete strand exchange. This 5′→3′ polarity, defined relative to either the incoming strand or the homologous parental strand undergoing displacement, was first noted and characterized in studies of the reaction between circular ssDNA and linear dsDNA [Cox and Lehman, 1981; Kahn *et al.*, 1981; West *et al.*, 1981]. If the plectonemic joint has formed at the 3′ end of the incoming single strand, it will be unwound during branch migration, and the three-stranded complex will dissociate [Wu *et al.*, 1982]. By studying linear ssDNA molecules paired with circular dsDNA, a better model of the *in vivo* substrates, Konforti and Davis more recently noted that homology at the 3′ end of the ssDNA

was required for strand exchange. One explanation is that the 5′→3′ polarity of RecA polymerization onto ssDNA leaves 5′ ends uncoated by RecA and hence unreactive in synapsis. An alternate explanation is that the direction of branch migration is 3′→5′, defined relative to the homologous 3′ end free initially [Konforti and Davis, 1987].

RecA-mediated recombination requires a nucleoside triphosphate cofactor and involves interaction with the single-stranded DNA binding protein (SSB). This is similar to the process of activating RecA for cleavage of the LexA repressor, as mentioned in Chapter 1. In the absence of a nucleoside triphosphate cofactor, RecA will bind to ssDNA, but not to dsDNA. Only ATP and dATP are both efficiently hydrolyzed and effective as cofactors for pairing reactions. ATP is most commonly used *in vitro*, with the essentially nonhydrolyzable analog adenosine 5′-*O*-(thiotriphosphate) (ATPγS) often substituted for hydrolysis-independent reactions. ATPγS can serve as cofactor for RecA·DNA complex formation [Honigberg *et al.*, 1985], but a hydrolyzable cofactor, either ATP or dATP, is required for the formation of plectonemic joints and subsequent branch migration [Riddles and Lehman, 1985b; reviewed by Radding, 1982]. The DNA-dependent ATPase may require a "critical cluster size" of about 15 contiguous RecA monomers bound to DNA for activation [Kowalczykowski, 1986]. Menetski and Kowalczykowski [1989] recently proposed that a dimer of RecA filaments is the functional species in nucleoside triphosphate hydrolysis.

The precise roles of nucleoside triphosphate binding and hydrolysis in RecA-mediated processes have yet to be determined, although several suggestions have been made. Hydrolysis may be a cycling mechanism for RecA, with ATP-dependent binding to ssDNA and ADP-dependent dissociation [Menetski and Kowalczykowski, 1985]. ATP hydrolysis might also be associated with the polarity of branch migration [Kowalczykowski *et al.*, 1987a], or it may provide the energy of rotation for unwinding the parental duplex and forming the heteroduplex [Cox *et al.*, 1987].

Interestingly, recent work indicates that the rate of dsDNA-dependent dATP

hydrolysis is greater than that of ATP [Menetski *et al.*, 1988], and that dATP is more effective than ATP as a cofactor for strand exchange in the absence of SSB or if the ssDNA has been preincubated with SSB. RecA that has bound dATP appears to have a greater affinity for ssDNA than ATP-bound RecA, and more readily overcomes secondary structure in the ssDNA substrate. The effect of dATP is seen even in the presence of excess ATP, as is the case *in vivo* [Menetski and Kowalczykowski, 1989]. Deoxyadenosine 5′-triphosphate (dATP) had previously been found more effective than ATP for LexA cleavage [Phizicky and Roberts, 1981]. The relative roles of dATP- versus ATP-bound RecA remain open to speculation.

In vitro, SSB is not required for the asymmetric strand exchange reaction between a ssDNA and a duplex, but it can enhance the binding of RecA to the ssDNA and thus dramatically affect the overall reaction efficiency [Riddles and Lehman, 1985a; West *et al.*, 1982b]. SSB is believed to facilitate formation of presynaptic filaments by destabilizing secondary structure in the ssDNA [Kowalczykowski *et al.*, 1987b; Kowalczykowski and Krupp, 1987; Muniyappa *et al.*, 1984]. SSB is then displaced by RecA [Register and Griffith, 1985b; Thresher *et al.*, 1988]. If ATPγS is the cofactor for RecA, presynaptic binding is nearly irreversible and the need for SSB is eliminated [Honigberg *et al.*, 1985]. Other helix-destabilizing proteins such as gp32 from phage T4 can be substituted for SSB, indicating that the interaction between the RecA and SSB proteins is not unique [Egner *et al.*, 1987]. RecA and SSB differ in their affinity for ssDNA, and *in vitro*, the reaction temperature and ATP and Mg^{2+} levels can be varied to favor one or the other protein in the competition for ssDNA binding sites [Kowalczykowski *et al.*, 1987b; Kowalczykowski and Krupp, 1987; Morrical *et al.*, 1986; Thresher *et al.*, 1988]. *In vivo* results suggest that although the coprotease activity of RecA is enhanced by excess SSB, recombinational repair is inhibited [Moreau, 1987 and 1988]. The nature of the ternary complex formed between dATP- or ATP-bound RecA and ssDNA may therefore be different for SOS induction and recombinational repair. Analysis of RecA mutants suggests that the copro-

tease and mutagenesis functions are separable [Ennis *et al.*, 1989; Yarranton and Sedgwick, 1982].

Interchromosomal recombination *in vivo* occurs between homologous duplexes. This symmetric strand exchange reaction, which ostensibly has no ssDNA component, does show a limited requirement for SSB. SSB stimulates the initial pairing of strands at a gap, but has little effect in the branch migration process between two duplexes [West *et al.*, 1982b]. The RecBCD enzyme has been proposed to provide RecA with a ssDNA region for initiation of recombination [reviewed by Smith, 1989]. SSB may serve to prevent the reannealing of duplex DNA that has been unwound by the RecBCD enzyme for this purpose [Roman and Kowalczykowski, 1989; Wang and Smith, 1989]. The HU protein, one of the proteins implicated in maintaining the structural organization of the *E. coli* chromosome, has been observed to strongly inhibit plectonemic joint formation *in vitro*, but not presynapsis or paranemic joint formation. It remains unclear whether this is due to the positive supercoiling resulting from the binding of HU protein or to the physical presence of HU protein on the duplex substrate [Ramdas *et al.*, 1989].

Much effort has been devoted to elucidation of the structure of the RecA protein. Although crystals have been grown [McKay *et al.*, 1980], a 3-dimensional x-ray crystallographic structure has yet to be published. Details are known from other methods, however. The primary sequence was predicted from quantitative analysis of the amino acid content of the active protein and the sequence of the *recA* gene. Amino acid sequencing verified the identities of the residues at each terminus [Sancar *et al.*, 1980]. The presence of several functional sites in RecA is suggested by the range of activities attributed to the protein. Unfortunately, active sites formed by the three-dimensional folding of a polypeptide chain are not easily predicted from its amino acid sequence.

The existence of structural domains in RecA is, however, supported by various studies. Analysis of mutations in the *recA* gene that lead to functionally altered proteins [Kawashima *et al.*, 1984; Wang and Tessman, 1986], characterization of RecA fragments

produced by limited proteolytic digestions [Kobayashi *et al.*, 1987; Rusche *et al.*, 1985] or from truncated genes [Rusche *et al.*, 1985], labeling of complexes with photoaffinity analogs of ATP [Banks and Sedgwick, 1986; Knight and McEntee, 1985], and comparison of the sequence of RecA with that of other ATP-dependent enzymes [Walker *et al.*, 1982] or with that of functional homologs isolated from other procaryotes [Knight *et al.*, 1988] are all approaches that have been taken to identify the residues involved in ATP binding and hydrolysis. Several distal regions of the polypeptide chain that may fold together to form the nucleotide-binding site have thus been identified. One model of monomeric RecA was generated using computer algorithms to analyze the amino acid sequence and incorporate a "nucleotide-binding fold," a structural motif that has been observed in several other nucleotide-binding proteins [Blanar *et al.*, 1984]. Mutant and truncated proteins have also been examined to locate DNA-binding sites [Benedict and Kowalczykowski, 1988; Rusche *et al.*, 1985; Wang and Tessman, 1986], and optically detected triplet state magnetic resonance spectroscopy has been used in an attempt to identify specific residues involved in stacking interactions with DNA [reviewed by Khamis *et al.*, 1988]. Overlapping domains have been proposed between the coprotease and recombinase functions and between the ssDNA- and nucleotide-binding regions [Wang and Tessman, 1986]. Such overlap would not be surprising, given the observed functional interrelationships.

Electron microscopy has also been used rather extensively to characterize the complexes formed between RecA and DNA. Within the last ten years, transmission electron micrographs have been published in nearly forty studies. Various mounting procedures and imaging techniques have been employed to minimize introduction of artifacts and maximize resolution, but certain details remain obscure. Additional information may come from the more recent technique of scanning tunneling electron microscopy. The hope is that this developing technology will enable higher resolution imaging of samples such as RecA·DNA complexes within a biological environment, rather than as chemically

fixed entities [Amrein *et al.*, 1988 and 1989].

As this is not meant to be a comprehensive review of electron microscopy studies, only a few are cited here. This technique has provided insight into many aspects of RecA·DNA interaction beyond the physical appearance of the nucleoprotein complexes. Polymerized RecA (protein alone) has been described by [Register and Griffith, 1985a; Stasiak and Egelman, 1986; Williams and Spengler, 1986]. Register and Griffith [1985b] noted the 5′→3′ unidirectionality with which RecA assembles onto ssDNA. Formation of presynaptic RecA·ssDNA complexes under various conditions (ATP versus ATPγS versus no cofactor, and different SSB and Mg^{2+} concentrations) has been characterized [Thresher *et al.*, 1988; Williams and Spengler, 1986]. Complexes of RecA with dsDNA alone have been similarly characterized [Di Capua *et al.*, 1982; Egelman and Stasiak, 1986 and 1988]. A role for ssDNA regions as nucleation sites in the assembly of RecA onto dsDNA has been described [Shaner *et al.*, 1987a and 1987b; West *et al.*, 1980]. Both paranemic and plectonemic joint molecules [Christiansen and Griffith, 1986; Register *et al.*, 1987] as well as Holliday junctions between duplexes [West *et al.*, 1983] have been visualized. The entire strand exchange process has also been followed with time course imaging [Register *et al.*, 1987; Stasiak and Egelman, 1987; Stasiak *et al.*, 1984].

The calculated stoichiometry varies from 3 to 6 nucleotides bound per RecA monomer, depending upon the cofactor and DNA substrate [reviewed by Cox and Lehman, 1987]. Varying contour lengths of RecA·DNA filaments are observed, depending upon methods of sample preparation. RecA·ssDNA filaments can range from 80-140% of the contour length of corresponding protein-free dsDNA, possibly reflecting a spring-like flexibility [Thresher *et al.*, 1988]. This flexibility could be important during the search for homology. Duplex DNA bound by RecA is unwound by 40% in the presence of ATP [Pugh *et al.*, 1989]. In the presence of ATPγS, the contour length is increased by 50%, equivalent to extending B-form DNA with 3.4 Å between basepairs (bp) and 10.5 bp/turn to an average rise of 5.2 Å and 18.6 bp/turn [Di Capua *et al.*, 1982; Stasiak *et al.*, 1981].

Supertwisted duplex DNA released upon the deproteinization of paranemic joints formed between circular dsDNA and either circular ssDNA or linear ssDNA having nonhomologous ends indicated that the helix had been unwound. Since the presynaptic filament and the paranemic joint appeared identical by electron microscopy, the recipient duplex was apparently unwound to match the dimensions of the incoming presynaptic ssDNA [Christiansen and Griffith, 1986]. Unwinding has also been observed in synaptic complexes formed between two duplexes [Conley and West, 1989]. Unwinding of the recipient duplex has been proposed as a step in the search for homology [Cunningham *et al.*, 1979; Leahy and Radding, 1986; Schutte and Cox, 1988; Shibata *et al.*, 1984; Wu *et al.*, 1983]. Synaptic structures had previously been found to contain as many as 100-300 unwound basepairs [Wu *et al.*, 1982]. Furthermore, the size of insertions that RecA can incorporate has indicated that up to 50 turns of DNA may be unwound in advance, thus allowing nonhomologous regions to be looped out [Bianchi and Radding, 1983].

The cooperative nature of RecA binding to DNA was first observed by electron microscopy [Dunn *et al.*, 1982; Stasiak *et al.*, 1981]. Menetski and Kowalczykowski [1985] assumed monomeric RecA free in solution in calculating a cooperativity value from fluorescence measurements of RecA binding to ss ethenoM13 (derivatized to contain 1,N^6-ethenoadenosine which fluoresces at neutral pH). However, their value predicted nucleotide clusters at half-saturation to be much smaller than those observed by electron microscopy. Takahashi and coworkers noted that the experimentally observed oligomerization of RecA could explain the discrepancy. Based upon velocity sedimentation and light-scattering experiments, they postulated the presence of RecA 30-mers under the conditions used by Menetski and Kowalczykowski, but noted that further work was needed to more accurately characterize the protein's behavior [Takahashi *et al.*, 1986]. Brenner and colleagues have since characterized the effects of concentration, ionic environment, and nucleoside triphosphate cofactors on the aggregation state of RecA in solution. Under conditions used for *in vitro* strand exchange, few monomers were observed.

Rings of oligomeric RecA may be the active form in presynapsis [Brenner *et al.*, 1988].

Chemical and nuclease protection studies in the absence of SSB suggest that RecA binds ssDNA along the sugar-phosphate backbone, leaving the bases exposed for homologous pairing [Leahy and Radding, 1986]. Differential reactivities to dimethylsulfate suggest that RecA may bind dsDNA along the minor groove, resulting in some protection against methylation on that side of the nucleoprotein complex; basepairing was found to be intact [Di Capua and Müller, 1987]. These results support an earlier study using anthramycin, a drug known to bind in the minor groove [Dombroski *et al.*, 1983]. The relative susceptibility of the other side may be evidence that the search for homology relies upon base recognition within the major groove. RecA·ssDNA complexes may be similarly asymmetric, having one relatively protected face and one relatively exposed [Di Capua and Müller, 1987].

During strand exchange, RecA additionally binds to the strand undergoing displacement, leaving the complementary strand free to exchange "pairing partners" [Chow *et al.*, 1986]. This binding might also serve to protect the D-looped strand from degradation by the RecBC nuclease [Williams *et al.*, 1981]. In the presence of SSB, the displaced strand is likely to be covered by SSB instead [Pugh and Cox, 1987a]. As branch migration proceeds, RecA dissociates from the end of the new heteroduplex, leaving a 50-100 basepair region susceptible to restriction endonucleases [Chow *et al.*, 1986]. These patterns were observed during both asymmetric (between ss and dsDNA) and symmetric (between two duplexes, one having a ssDNA tail) strand exchange reactions. In the latter case, RecA remained bound to both the ssDNA tail which defined the initiating strand and to heteroduplex regions, but did not associate with the displaced strand of either parental duplex in the resulting Holliday structure [Chow *et al.*, 1988]. As seen by electron microscopy, RecA appears to remain bound to "post D-loop cycle" dsDNA , inactivating it for further recombination. *In vivo*, this might be to inhibit repeated recombination at any given site [Register and Griffith, 1988].

The RecA filaments visualized by electron microscopy have all been right-handed helices, whether the DNA itself is right-handed B-form [Flory *et al.*, 1984; Stasiak and Di Capua, 1982] or left-handed Z-form [Kim *et al.*, 1989]. Models of how the components of these nucleoprotein filaments are arranged and how branch migration proceeds have been developed using measurements and image reconstructions from electron micrographs, with complementing data from studies such as the protection studies described above. Comparisons of filament dimensions and the maximum dimensions to which DNA can be stretched without breaking bonds argue against a model of DNA surrounding the protein. The DNA helix is believed to lie within the deep groove that characterizes the filaments [Howard-Flanders *et al.*, 1984a; Leahy and Radding, 1986]. Experimental evidence for this placement has recently been reported [Di Capua *et al.*, 1989; Egelman and Yu, 1989]. Three-dimensional image reconstructions from electron micrographs also suggested an axial polarity in the orientation of the RecA subunits within the filament; the surfaces 5′ and 3′ to any given DNA basepair are different [Egelman and Stasiak, 1986; Stasiak *et al.*, 1988]. Takahashi and coworkers suggested that at most, RecA binds one ss and one dsDNA substrate simultaneously. In the reaction between two duplexes, therefore, one duplex must be unwound such that one of its strands lies outside the RecA filament [Takahashi *et al.*, 1989]. In synapsis, the duplex DNA must penetrate the presynaptic "cavity" [Di Capua *et al.*, 1982 and 1989; Howard-Flanders *et al.*, 1984b; Williams and Spengler, 1986]. In one proposed model, the axial alignment and proximity needed for hydrogen bonding between the presynaptic ssDNA and the incoming complementary strand require sharp bending of the parental duplex at the point of entry. The homologous duplex then winds into the filament, lying near its axis [Howard-Flanders *et al.*, 1987].

Howard-Flanders and colleagues have argued that a head-to-tail arrangement of RecA monomers, each with two DNA binding sites, was more consistent with the observed directionality of RecA-mediated strand exchange than a model with symmetrical

dimers in which each monomer contributes one DNA binding site. Branch migration might then proceed by cooperative binding of RecA monomers at one end to draw together the DNA substrates, and dissociation of monomers at the other end after strand exchange [Howard-Flanders *et al.*, 1984b]. Recent neutron scattering data has yielded a mass-per-length value that is consistent with a monomeric model, and also provided evidence for conformational changes within the RecA protein upon binding to DNA [Di Capua *et al.*, 1989]. An alternative model places the duplex DNA alongside the presynaptic filament, making contact once per helical turn. Evidence against the treadmill type of model for branch migration proposed by Howard-Flanders and coworkers suggested an alternative model in which the presynaptic nucleoprotein filament need not dissociate [Cox *et al.*, 1987; Pugh and Cox, 1987a]. Some dissociation may be involved in nonhomologous regions [Cox *et al.*, 1987; Schutte and Cox, 1987]. Branch migration may proceed either by rotation of the presynaptic filament and the duplex DNA relative to each other [Cox *et al.*, 1987], or the concomitant rotation of each about its own longitudinal axis, mediated by RecA [Honigberg and Radding, 1988].

To construct our uniquely crosslinked three-stranded substrates, we needed to optimize the presynaptic association of RecA with the psoralen-monoadducted oligonucleotides. RecA has only a weak affinity for oligonucleotides; however, by using an excess of RecA and ATPγS as cofactor, stable complexes with oligomers more than 8 nucleotides long can be formed [Leahy and Radding, 1986]. As noted earlier, presynaptic complexes formed in the presence of ATPγS can be paired with homologous dsDNA, although subsequent branch migration is inhibited [Honigberg *et al.*, 1985]. A potential concern was preferential dissociation of RecA from the oligonucleotide in favor of the dsDNA, disrupting the presynaptic complexes. Unlike the ssDNA reaction, binding of RecA to dsDNA is highly pH-dependent, with a maximum at pH 6.2-6.4 and a requirement for ssDNA or ATPγS at pH 7.5 [McEntee *et al.*, 1981; Weinstock *et al.*, 1981;

reviewed by Pugh and Cox, 1987b]. This difference is attributed to a kinetic barrier at pH 7.5 [Pugh and Cox, 1987b]. ATPγS-bound RecA, however, binds essentially irreversibly to DNA [reviewed by Honigberg *et al.*, 1985]. In reactions at neutral pH, then, the dsDNA was not expected to compete RecA away from the *preformed* presynaptic filaments.

At the time that we initiated these studies, the minimum extent of homology required for efficient RecA-mediated pairing was estimated at between 30 and 150 basepairs [Gonda and Radding, 1983]. We therefore chose a set of eight oligonucleotides to span this size range, and also tested a 13-mer. In addition, a comparison was made between pUC19 and a duplex not containing the region homologous to the oligonucleotides. We also considered the effect of supercoiling in the duplex substrate on the efficiency of formation of the three-stranded complexes. Effects of superhelicity on the kinetics and RecA requirements [Shibata *et al.*, 1981] as well as on the fidelity of homologous pairing [Das-Gupta and Radding, 1982] had all previously been noted.

As noted in Chapter 1, psoralens are photochemically-activated crosslinking agents. Adduct formation requires the planar psoralen molecule to intercalate between stacked DNA basepairs. Because psoralens preferentially react with thymidines in 5′-TpA sites of B-form duplex DNA, adducts can be specifically placed. Bifunctional psoralens possess a furan and a pyrone end, each capable of reacting to form a cyclobutane ring adduct with the 5,6 double bond of pyrimidine bases. Irradiation of psoralen-intercalated DNA with 320-380 nm light therefore produces a mixture of the two monoadducts. Irradiation with UV light above 380 nm yields predominantly furan-side monoadduct. The pyrone-side monoadduct essentially does not absorb above 320 nm; consequently, only the furan-side monoadduct is crosslinkable. Both monoadducts can be photoreversed under 254 nm light [reviewed by Cimino *et al.*, 1985; Song and Tapley, 1979]. The particular derivative used in our studies was 4′-hydroxymethyl-4,5′,8-trimethylpsoralen (HMT, see Figure 2-1). This psoralen has greater solubility in water than the parent com-

Figure 2-1. Structures of 4,5′,8-trimethylpsoralen (TMP), the derivative 4′-hydroxymethyl-4,5′,8-trimethylpsoralen (HMT), and the dT-HMT-dT diadduct (cross-link). The psoralen and thymidines are in the *cis-syn* conformation [Cimino *et al.*, 1985]. The methyl groups in the diadduct have been left unlabeled for clarity. (dR = deoxy-ribose)

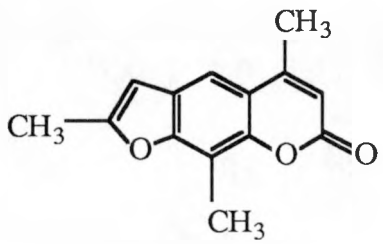

4,5′,8-trimethylpsoralen (TMP)

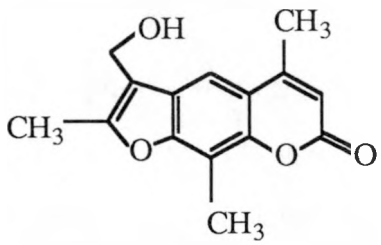

4′-hydroxymethyl - 4,5′,8 - trimethylpsoralen (HMT)

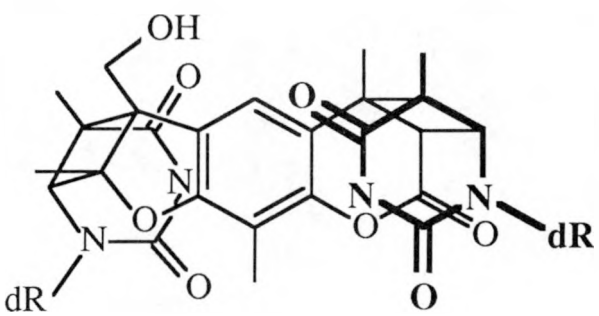

dT-HMT-dT diadduct, *cis-syn* conformation

pound TMP [Isaacs *et al.*, 1977]. By taking advantage of the particular reactivity of 5′-TpA sites and the two-photon requirement for crosslink formation, we constructed site-specifically monoadducted oligonucleotides. These oligonucleotides ensured unique placement of the final crosslink in the three-stranded complexes, a specificity not attainable by adding free psoralen to preformed complexes.

RecA might be predicted to tolerate the psoralen moiety, in view of its observed tolerance for insertions, deletions, and mismatches [Bianchi and Radding, 1983]. We were nonetheless concerned about minimizing the effect of the monoadduct's presence on presynapsis and synapsis while still achieving basepairing and the proper orientation of the psoralen within the paired region for crosslinking of the oligomer to its complement. Placing the psoralen close to the 3′ end would hopefully minimize any disruptive effect on branch migration proceeding in the 5′→3′ direction, and also allow stabilization of the complex through the basepairing at the 5′ end. Polymerization of RecA onto the oligonucleotides in the 5′→3′ direction might also tend to leave the 5′ ends uncoated and hence either inactive in pairing or readily displaced by reannealing of the parental duplex. We therefore examined the effect of the position of the adduct relative to the ends of the oligonucleotide on overall reaction efficiency.

Crosslinked complexes were successfully formed between pUC19 plasmid and psoralen-modified oligomers ranging from 30 to 107 nucleotides in length. The efficiency of this two-step process depended upon several factors, including the nucleotide cofactor for RecA, the length of the oligomeric substrate, and the position of the psoralen adduct relative to the 5′ end of the oligomer. Reaction with linearized pUC19 was much less efficient than with supercoiled pUC19. Absolute homology was not required. This work has been previously published [Cheng *et al.*, 1988a and 1989]. We also qualitatively characterized the extent of unwinding induced by the presence of the inserted oligonucleotides in deproteinized complexes.

Materials and Methods

Proteins and DNA — RecA protein from *E. coli* was a gift of Chi Lu and H. Echols, University of California at Berkeley. T4 gp32 was a gift of B. Alberts, University of California at San Francisco, and SSB was a gift of J. Griffith, University of North Carolina at Chapel Hill. Rabbit muscle creatine phosphokinase (CPK) was obtained from Sigma. T4 DNA ligase was purchased from Amersham; KpnI and XmnI restriction endonucleases and T4 polynucleotide kinase were from New England Biolabs.

Unmodified oligonucleotides were synthesized using phosphoramidite chemistry on either a Biosearch Model 8600 or an Applied Biosystems Model 381A automated synthesizer and purified by polyacrylamide gel electrophoresis. Duplex pUC19 plasmid (approximately 85% FI, 10% FII, and 1-5% FIII and multimers) was purchased from Pharmacia. This FI stock was digested with XmnI endonuclease to generate FIII substrate.

Preparative scale irradiations — The light source used to generate psoralen-adducted DNA was a 2500 W Hg/Xe compact arc lamp (Canrad-Hanovia). For irradiations at 320-380 nm, the light was initially filtered through pyrex and then through a $Co(NO_3)_2$ solution [1.67% (w/v) in 2% aqueous NaCl; approximately 300 mL over a 9-cm pathlength]. The light intensity at the sample was approximately 100 mW/cm^2. The irradiation buffer was 50 mM Tris·Cl (pH 7.6), 150 mM NaCl, 10 mM $MgCl_2$, and 0.1 mM EDTA. Samples (< 0.25 mM total DNA) were irradiated at 4°C for two 4-minute periods. Before each irradiation, a fresh aliquot of HMT (gift of HRI Associates, Berkeley, CA) in ethanol was added. Aliquot volume and the stock concentration were calculated to yield a final 0.12 mM HMT, < 4% ethanol sample solution. To remove unreacted HMT and any photodegradation products, irradiated samples were extracted twice with 1:1 (v/v) chloroform:isoamyl alcohol and once with diethyl ether, then ethanol-precipitated.

To photoreverse crosslinks, 2-mL aliquots of samples at $A_{260} < 1.5$ in water were

placed into the glass lid of an analytical thin-layer-chromatography jar (3 cm diameter) together with a 7-mm flea stirring bar. The solution depth was 2-3 mm. This was covered with plastic wrap and irradiated for 2.5 minutes at a distance of 2.5 cm below a germicidal lamp. The light intensity was not measured. (Procedures courtesy of Y.-B. Shi, personal communication.)

For irradiations at 390 nm, the $Co(NO_3)_2$ solution was replaced by 345 nm and 375 nm cutoff filters and a 389 nm bandpass filter (Oriel). Three 30-45-minute irradiations at 4°C, each preceded by an addition of fresh HMT as described above, yielded predominantly furan-side monoadduct. Buffer conditions and sample work-up were as for the 320-380 nm irradiations.

Preparation of monoadducted substrates — The eight monoadducted oligonucleotide substrates ranged in length from 30 to 107 residues (Figure 2-2). These substrates were prepared from HMT and synthetic oligonucleotides, as described above and elsewhere [Gamper *et al.*, 1987; Shi and Hearst, 1986]. Each was homologous to the polylinker region within the plus strand of pUC19 plasmid (and hence complementary to the plus strand of the phage M13mp19 vector). The pUC19 sequence was obtained from Yanisch-Perron *et al.* [1985]. Common to all eight oligonucleotide substrates was a 13-base sequence containing the unique KpnI recognition site (Figure 2-2a). This 13-mer had been modified with HMT at the central thymidine by one of two methods: (i) The 13-mer was first crosslinked with HMT to the 8-mer 5′-GGGTACCC using 320-380 nm light. Photoreversal of this crosslink using 254 nm light yielded a mixture (approximately 2:3) of pyrone- and furan-side monoadducted 13-mer. Since only the furan-side monoadduct is crosslinkable, the relative yields of each monoadduct were determined by an irradiation with 320-380 nm light in the presence of complement. (ii) Irradiation of the 13-mer with 390 nm light in the presence of HMT and the complementary 8-mer 5′-GGGTACCG yielded the desired furan-side (approximately 98% versus pyrone-side) HMT-monoadduct directly.

Figure 2-2. Monoadducted oligonucleotides. (a) Sequence of the 13-mer contained within all substrates, modified on the 3′ side of the central thymidine (arrow) with HMT. This 13-mer contains the unique KpnI restriction endonuclease recognition site. (b) and (c) Schematics of the final substrates, illustrating the position of the psoralen (denoted by the small vertical bar) within each molecule. The substrates are aligned by sequence. All are homologous to the polylinker region within the plus strand of pUC19. (b) Initial eight substrates. (c) Substrates developed to focus on the effect of the position of the psoralen within the molecule. 57-mer C is the same 57-mer shown in (b).

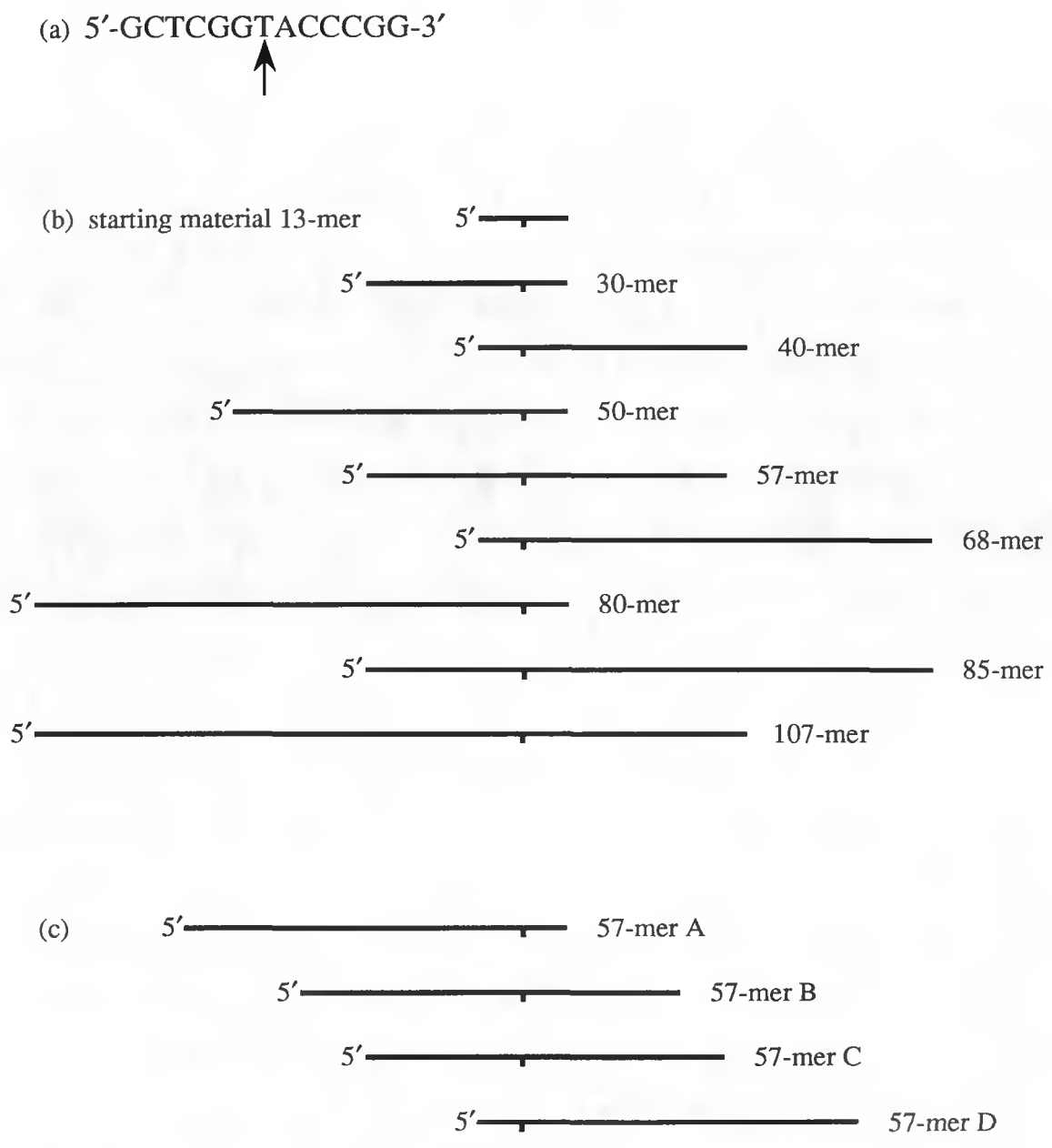

Figure 2-2. Monoadducted oligonucleotides

Monoadducted 13-mer from either method was separated from unmodified material on a 20% polyacrylamide gel (19:1 acrylamide:bis, 7M urea). The substrates for the RecA reactions were then prepared by ligation of extender oligonucleotides onto the monoadducted 13-mer, using T4 DNA ligase in the presence of a slight excess of either a 22- or 26-mer template. The 26-mer, 5′-AGGATCCCCGGGTACCGAGCTCGAAT, provided at least six bases on each side of the 13-mer for aligning the extender oligonucleotides. Prior to reactions with RecA, aliquots of each oligonucleotide substrate were 5′-end-labeled with ^{32}P using T4 polynucleotide kinase and then gel-purified.

Formation of three-stranded complexes — Optimal stoichiometries for the formation of RecA·oligomer complexes were estimated using unmodified oligonucleotides and a nitrocellulose filter assay similar to that described by Leahy and Radding [1986]. The longer the substrate, the smaller the excess of RecA needed to obtain efficient binding (data not shown). A 600:1 ratio of RecA monomer to single-stranded molecule was chosen for the pairing reactions. This stoichiometry gives a net 20:1 ratio of RecA monomer to nucleotide for a 30-mer substrate and a 5.6:1 ratio for a 107-mer.

The general approach to forming three-stranded complexes, depicted in Figure 2-3, was modeled after that of Tsang *et al.* [1985]. Use of an acetate buffer system was suggested by T. Kodadek, now at the University of Texas at Austin; observations of Menetski and Kowalczykowski [1985] and Roman and Kowalczykowski [1986] supported this choice over a chloride system. RecA was freshly diluted at 0°C into 10 mM Tris·acetate, 5% glycerol. For each 50-μL reaction, 2.5 nM ^{32}P-labeled HMT-monoadducted oligonucleotide (DNA concentrations given in terms of molecules) was first incubated with 1.5 μM RecA at 2 mM Mg·acetate in 5% glycerol, 10 mM Tris·acetate buffer (pH 7.5 at 37°C), 1 mM DTT, 50 mM Na·acetate, and either 1-3 mM ATP (with 3 mM phosphocreatine and 5 units/mL CPK, added 1 minute before RecA, as a regenerating system) or 0.8-1 mM ATPγS (Boehringer Mannheim). After 10 minutes, the Mg^{2+} concentration was raised to 12 mM and 2.5-5 nM pUC19 was added to initiate the pairing reaction. As a

Figure 2-3. Formation of three-stranded complexes. As discussed in the text (see 'Methods'), the single-stranded substrate is first incubated with RecA protein at low Mg^{2+}. The homologous pairing reaction is initiated by the addition of the double-stranded substrate with an increase in the concentration of Mg^{2+}. Irradiation with 320-380 nm light drives the inserted monoadduct to form a crosslink. Each oligomer is ^{32}P-labeled at the 5′ end (asterisk). The furan (F) and pyrone (P) ends of the psoralen are indicated; only the furan-side monoadducted substrates will form crosslinks. The actual structure of the final three-stranded molecule was not determined.

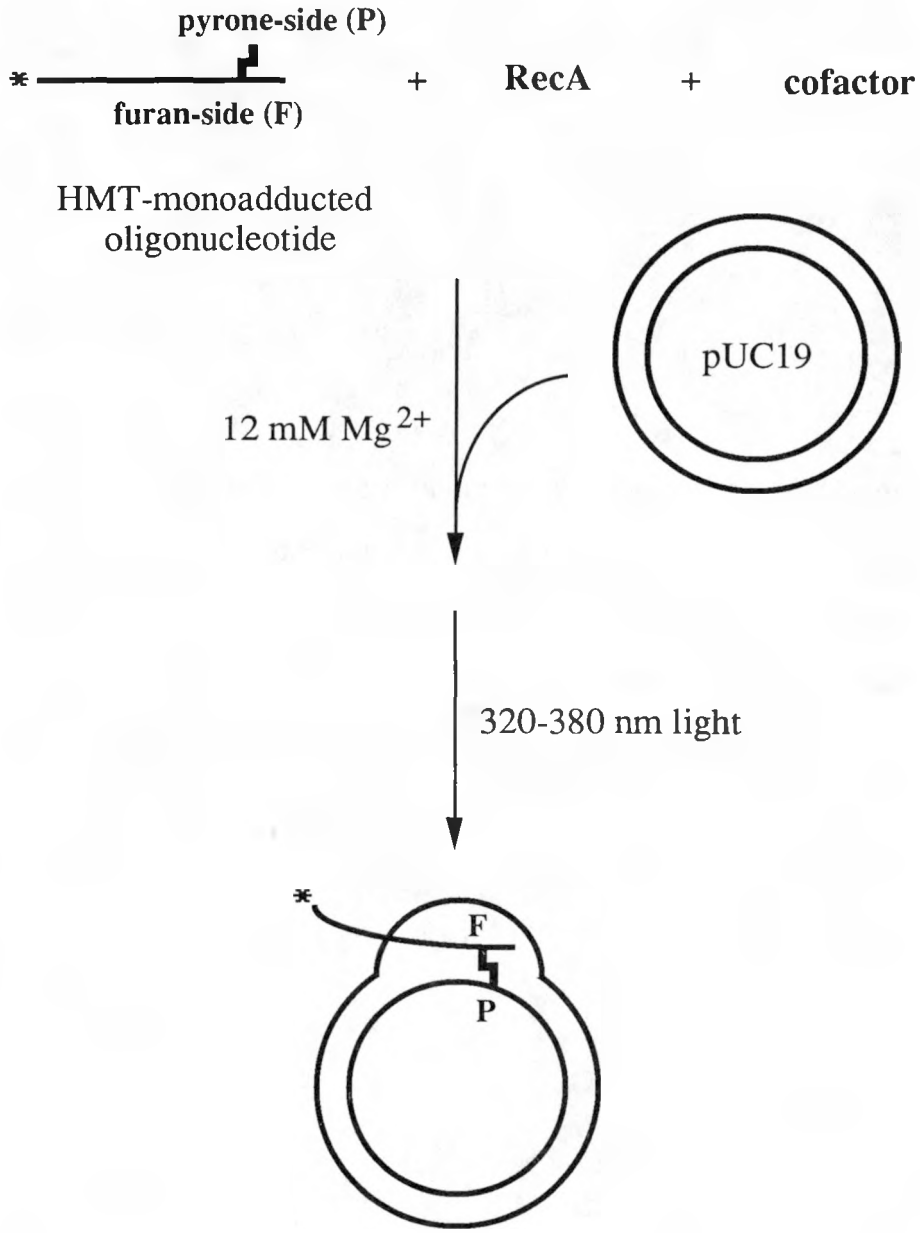

Figure 2-3. Formation of three-stranded complexes

duplex substrate which does not contain the targeted polylinker region, pBR322 was used either instead of or in addition to pUC19. Certain reaction mixtures also included either 0.15 μM gp32 or 20 nM tetrameric SSB, added 1 minute after the RecA. For these reactions, the Mg^{2+} concentration was raised when the single-stranded DNA binding protein was added, rather than when pUC19 was added. After a 12-15-minute incubation, samples were irradiated for 2 minutes with 320-380 nm light at 100 mW/cm^2 to effect crosslinkage. All incubations and irradiations were carried out at 37°C.

Samples were deproteinized by two phenol and one diethyl ether extractions, and the DNA was precipitated with ethanol and 0.3 M Na·acetate overnight at -20°C, then resuspended into 5 mM Tris·acetate (pH 7.5) and 0.5 mM EDTA. Xylene cyanole FF and bromophenol blue dyes in glycerol were added to samples for analysis on horizontal 1.2% agarose gels. KpnI digests of deproteinized and ethanol-precipitated samples were carried out in 10 μL using reaction conditions suggested by New England Biolabs. These digests were stopped with the addition of EDTA and dyes, and samples were loaded directly onto agarose gels. The gels were electrophoresed at a constant 2.2 V/cm in TBE (50mM each Tris·HCl and boric acid, 1 mM EDTA). Gels were stained with 1 μg/mL ethidium bromide in 40 mM Tris·acetate and 1 mM EDTA, then photographed. For autoradiography, gels were dried at 60°C onto Whatman 3MM chromatography paper using a Bio-Rad Model 483 Slab Drier, with a Zeta-Probe Blotting Membrane (Bio-Rad) between the gel and the paper to prevent the loss of oligonucleotide.

Quantitation of complex formation — With the autoradiogram as a guide, plasmid and oligomer bands were excised from dried gels and counted in 5 mL of scintillation fluor [PPO-BisMSB (ICN Radiochemicals), toluene, Triton X-100, and water]. This fluor was later (in the pBR322/pUC19 comparison experiments) replaced by Beckman Ready-Safe fluor. The efficiency of a given reaction was defined as the percentage of the total excised cpm that was contained in the plasmid bands.

Analysis of unwinding in three-stranded complexes — Three-stranded complexes

were formed as described above between pUC19 (Pharmacia or gift of L. Greene, University of California, Berkeley) and six of the HMT-monoadducted oligonucleotides (30, 50, 57(C), 80, 85, and 107 bases in length). Free oligonucleotide was removed on a 1% agarose gel (FMC SeaKem LE agarose) in TBE; the plasmid region was excised and recovered by electroelution (Schleicher and Schuell Elutraps) and ethanol precipitation.

Isolated samples were analyzed by one-dimensional gel electrophoresis, 1% agarose (horizontal) in TANE [40mM Tris·acetate (pH 8 at 25°C), 1 mM EDTA, and 5 mM NaCl] containing varying amounts of chloroquine (0, 0.1, 0.2, 0.5, 1.0, 1.5, 2.0, 2.5, 3.0, 3.5, and 4.0 μg/mL; from Sigma). Since chloroquine has a weaker binding affinity for DNA than ethidium bromide, higher concentrations of chloroquine are needed to effect a given amount of positive supercoiling than of ethidium. Consequently, the conversion of negative superhelical turns to positive ones is more easily controlled with chloroquine [Shure *et al.*, 1977; conversations with C. Boles and J. Dugan of Prof. N. Cozzarelli's lab, Department of Molecular Biology]. A peristaltic pump was used to circulate the buffer at 5-6 mL/minute. Each gel was 25 cm long, and electrophoresis was carried out at 55V (electrodes 45 cm apart) for 24 hours. Typically, FII pUC19 had migrated 14-15 cm from the origin, FI 17-18 cm. Gels were dried onto Whatman 3MM paper at 60°C for autoradiography. Inkspots of known cpm were used as internal standards and to determine that the exposures were within the linear response range of the film (Kodak X-OMAT AR, from Merry X-Ray). Densitometric scans of the autoradiograms were made using either a Hoefer GS300 Transmittance/Reflectance Scanning Densitometer (courtesy of the labs of Profs. H. Echols and M. Botchan, Department of Molecular Biology) with GS350 (IBM) or GS370 (Macintosh) software, or a Kratos Spectrodensitometer Model SD3000 with Kratos SDC300 Density Computer and Hewlett-Packard 3380A Integrator (courtesy of the lab of Prof. G. Ames, Department of Biochemistry). More than one instrument was used in an attempt to sufficiently resolve bands by varying the scanning speed. Using the Hoefer software, peaks were identified either

by a Gaussian fit or by manual peak selection and then integrated; peaks from Kratos scans were excised and weighed on a Mettler analytical balance (±0.0001 g.).

Our data analysis was based upon the method of Keller [1975]. Adjacent bands in each sample distribution were taken to differ by one superhelical turn. The densitometric data was used to determine the center of mass of each FI distribution, that is, the position of 50% of total FI (supercoiled) intensity, relative to position of the FII (nicked circular duplex) DNA. The FII mobility was previously found to be insensitive to the presence of crosslinked oligonucleotide, within experimental error (data not shown). The distance from center to center in neighboring samples was then interpreted to reflect the difference in the mean number of superhelical turns. The center-to-center distances were divided by the average peak-to-peak distance to obtain values in units of turns ($\Delta\tau$). Our interest was not in the absolute number of turns (which could not be obtained from this data alone), but in the trend of increasing extent of plasmid unwinding by increasingly longer oligonucleotides. Therefore, $\Delta\tau^*$ was plotted against the length of the inserted oligomer, where $\Delta\tau^*$ is the value of $\Delta\tau$ defined relative to an arbitrarily chosen reference point. That is, the first point plotted was an arbitrarily chosen value $\Delta\tau^*$ for the 107-mer complex. All other points were then determined relative to this using $\Delta(\Delta\tau)$ as calculated from the $\Delta\tau$ values.

Results and Discussion

Formation of three-stranded complexes — RecA-mediated homologous pairing and strand exchange have typically been studied using substrates at least several hundred bases or basepairs long. Our approach was to use minimal length single-stranded substrates and to trap the three-stranded synaptic intermediate by covalently fixing the inserted single strand to its complement. Our systems for homologous pairing therefore consisted of HMT-monoadducted oligonucleotides (Figure 2-2) and duplex pUC19 plasmid. Incorporation of oligomers into the plasmid was detected on agarose gels. Figure 2-4 shows

the results from various pairing reactions using the 80-mer monoadducted substrate. Qualitatively similar results were obtained with each of the oligonucleotides. The three-stranded complexes migrate with the original pUC19 plasmid DNA, but carry the ^{32}P label from the inserted oligonucleotide (e.g. samples 8 and 10). The resistance of the labeled plasmid DNA to digestion by KpnI, due to the psoralen crosslink within the single recognition site [Gamper *et al.*, 1984], confirmed the insertion of the oligomer at the target site.

The data showed that both RecA and a cofactor are necessary for homologous pairing, that is, the solution hybridization of the monoadducted oligonucleotide to its target. Although spontaneous uptake of ssDNA fragments by superhelical DNA at 75°C has been observed [Beattie *et al.*, 1977], RecA is needed to overcome thermodynamic and kinetic barriers for efficient uptake at physiological temperatures and salt conditions. Three-stranded complexes were formed much more readily in the presence of 1 mM ATPγS (reactions 8 and 10) than in the presence of ATP, either at the same concentration (data not shown) or at 3 mM (reactions 12 and 14). This result is consistent with those of Leahy and Radding [1986] who noted that both excess RecA and the virtually nonhydrolyzable cofactor ATPγS were necessary to overcome the weak affinity of RecA for oligonucleotides. The effect of either SSB (from *E. coli*) or gp32 (from phage T4) was also tested since the efficiency of RecA association with ssDNA is often enhanced by ssDNA-binding proteins [Muniyappa *et al.*, 1984; reviewed by Cox and Lehman, 1987]. Both proteins did facilitate incorporation of the oligonucleotide into pUC19 in the presence of ATP (for gp32, compare reaction 14 to 12; SSB data not shown). Comparison of reactions 10 and 8 suggests little or no enhancement of incorporation in the presence of ATPγS due to the presence of gp32; other experiments did show some enhancement due to the presence of SSB (discussed further below).

Complexes formed in any given pairing reaction were quantitated by determining the amount of ^{32}P-labeled oligomer contained in the plasmid bands after agarose gel electrophoresis. Because this approach detects stable species that have survived depro-

Figure 2-4. Deproteinized samples from RecA-mediated homologous pairing reactions between 5nM pUC19 and 2.5nM HMT-monoadducted 80-mer, using 1.5 μM RecA as described under "Methods," analyzed by nondenaturing agarose gel electrophoresis: (a) photograph of gel stained with ethidium bromide, and (b) the corresponding autoradiogram. The right-hand lane of each pair is the sample following KpnI digestion. Conversion of FI to FII DNA may be attributed to the phenol extractions used to remove RecA.

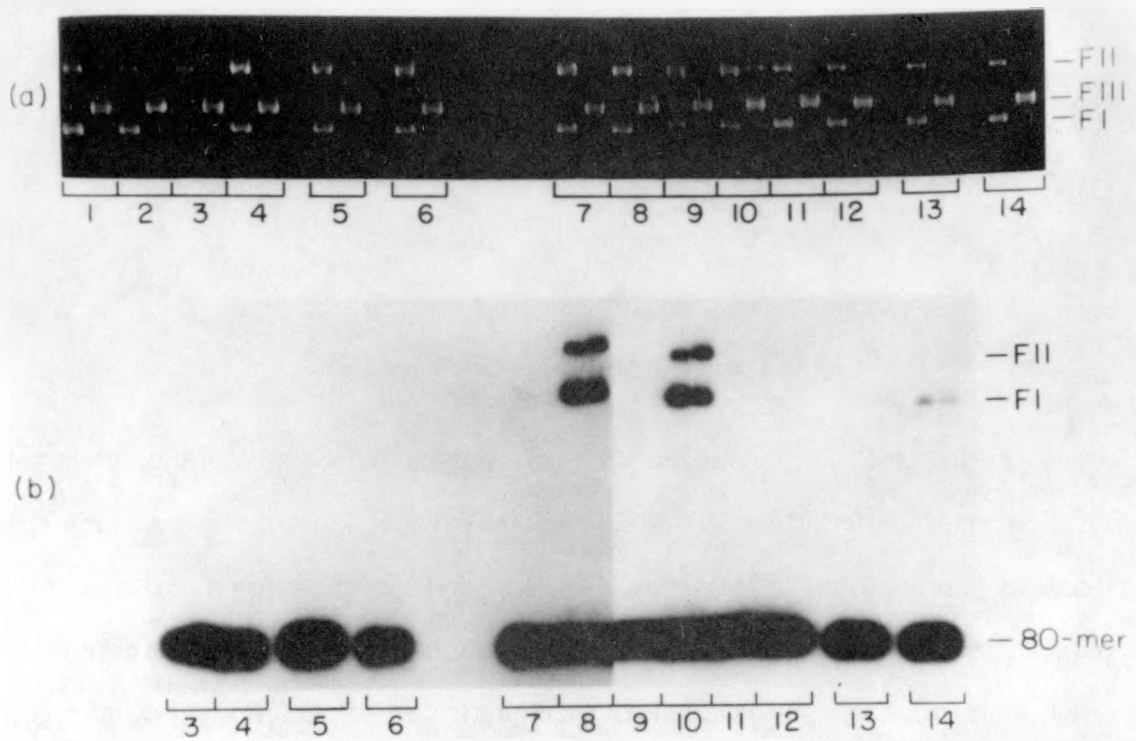

Sample	80-mer	RecA	ATPγS	ATP	gp32	320-380 nm hν
1	-	-	-	-	-	-
2	-	+	-	-	-	-
3	+	-	-	-	-	-
4	+	-	-	-	-	+
5	+	+	-	-	-	-
6	+	+	-	-	-	+
7	+	+	+	-	-	-
8	+	+	+	-	-	+
9	+	+	+	-	+	-
10	+	+	+	-	+	+
11	+	+	-	+	-	-
12	+	+	-	+	-	+
13	+	+	-	+	+	-
14	+	+	-	+	+	+

teinization and nondenaturing electrophoresis, values should reflect the overall efficiency of oligomeric substrate insertion by RecA and subsequent crosslink formation. Such analysis revealed that the 68-mer system yielded similar, although low, levels of complex in both ATP and ATPγS reaction mixtures. In the presence of ATP, the 68-mer formed the most three-stranded complex of all eight substrates, at 15-20% efficiency. Why the two cofactors mediated utilization of this particular substrate to the same extent is not known. Complex formation with any of the other seven substrates was significantly greater with ATPγS rather than ATP as the cofactor.

Samples 12 and 14 in Figure 2-4 show that gp32 enhanced complex formation in the presence of ATP, but had little or no effect on the ATPγS reaction. Quantitative analysis indicated that SSB could also enhance the pairing process in the presence of either cofactor. Up to an additional 10% of oligomer could be incorporated into the plasmid if SSB was present. The effect of SSB was not consistent, but varied among experiments and oligomeric substrates. SSB did reduce interaction and hence background crosslinking between oligomers (data not shown).

Dependence on oligonucleotide length — Figure 2-5(a) summarizes the quantitated results for complexes formed in the presence of ATPγS. These values have been normalized for the differences in percent furan-side (crosslinkable) monoadduct introduced by the two methods of preparation (described under 'Methods'). If RecA has no preference for pairing one type of monoadduct over the other, the values in Figure 2-5(a) can be interpreted as being the yields of three-stranded complex expected from 100% furan-side substrate. These values do not, however, correspond completely to yields of crosslinked complexes because stable uncrosslinked complexes were also detected, as discussed below.

One general conclusion from Figure 2-5(a) is that the longer the invading oligonucleotide, the greater the level of incorporation into the plasmid. This trend was expected based upon predicted relative stabilities of the heteroduplexes which would result

from complete hybridization of each oligomer to its complement. Attempts were made to form three-stranded complexes with the monoadducted 13-mer (Figure 2-2a), but no incorporation was detected (data not shown). The data suggest that efficient incorporation requires a single-stranded substrate of at least 50 residues in length. This is consistent with the observed length-dependence of the dissociation constant for RecA·ssDNA filaments, indicating that efficient binding of RecA requires a site of between 30 and 50 bases [Brenner *et al.*, 1987].

Role of psoralen location — The data presented in Figure 2-5(a) also indicated that the position of the psoralen within the oligonucleotide can significantly affect the efficiency of incorporation. Under the ATPγS reaction conditions, both substrates with the psoralen located very near the 5′ end (40- and 68-mer) were incorporated with a much lower efficiency than might be expected based upon their lengths. In an effort to confirm this observation, 57-mers A, B and D were prepared, each having the psoralen at a different position from the original 57-mer C (Figure 2-2c). The observed efficiencies of reaction under ATPγS conditions are shown in Figure 2-5(b). Upon removal of the RecA protein, both ends of the oligomer are likely to be subject to displacement by the renaturing strands of pUC19, and yet 57-mer A (adducted near the 3′ end) showed a much greater level of complex formation than 57-mer D (adducted near the 5′ end). In combination with the data summarized in Figure 2-5(a), this indicated that a terminally located psoralen adduct could influence the overall reaction efficiency. At the 5′ end, the adduct may inhibit either RecA presynaptic or synaptic complex formation or interfere with basepairing within the synaptic complex such that the monoadduct is unfavorably oriented to form a crosslink. RecA has been observed to both polymerize along ssDNA and branch migrate in the 5′→3′ direction, and the initial insertion of the ssDNA into the duplex substrate appears to occur randomly along the single-stranded molecule [reviewed by Cox and Lehman, 1987; Radding, 1982]. Our data may reflect a directional preference of RecA in the insertion and homologous alignment steps. RecA-mediated strand exchange (a unidirectional process)

Figure 2-5. Histograms showing efficiencies of oligomer incorporation into pUC19. (a) Initial eight substrates (see Figure 2-2b). Values represent the average of 7-9 trials, normalized for the percent of furan-side (i.e. crosslinkable) versus pyrone-side monoadduct in each substrate sample: the 50-, 80-, and 107-mer were 62% furan-side, and the others were 98%. Black bars indicate oligomers with the psoralen on the 7th base in from the 3′ end. White bars indicate that the psoralen was on the 7th base in from the 5′ end. Bars with single hatch marks indicate that the psoralen was on the 24th base in from the 5′ end. The 107-mer (cross-hatched bar) had the psoralen on the 34th base in from the 3′ end. Sample standard deviation values ranged from 2 to 8% incorporation.

(b) Data from 57-mers A-D, plotted as a function of the distance between the monoadducted residue and the 5′ end of the oligomer. As pictured in Figure 2-2(c), 57-mer A was adducted on the 51st residue, B on the 34th, C on the 24th, and D on the 7th residue in from the 5′ end. Values represent the average of 3 trials. Sample standard deviation values were less than 2.1% incorporation. 57-mer C is the same oligonucleotide previously used to generate data shown in (a).

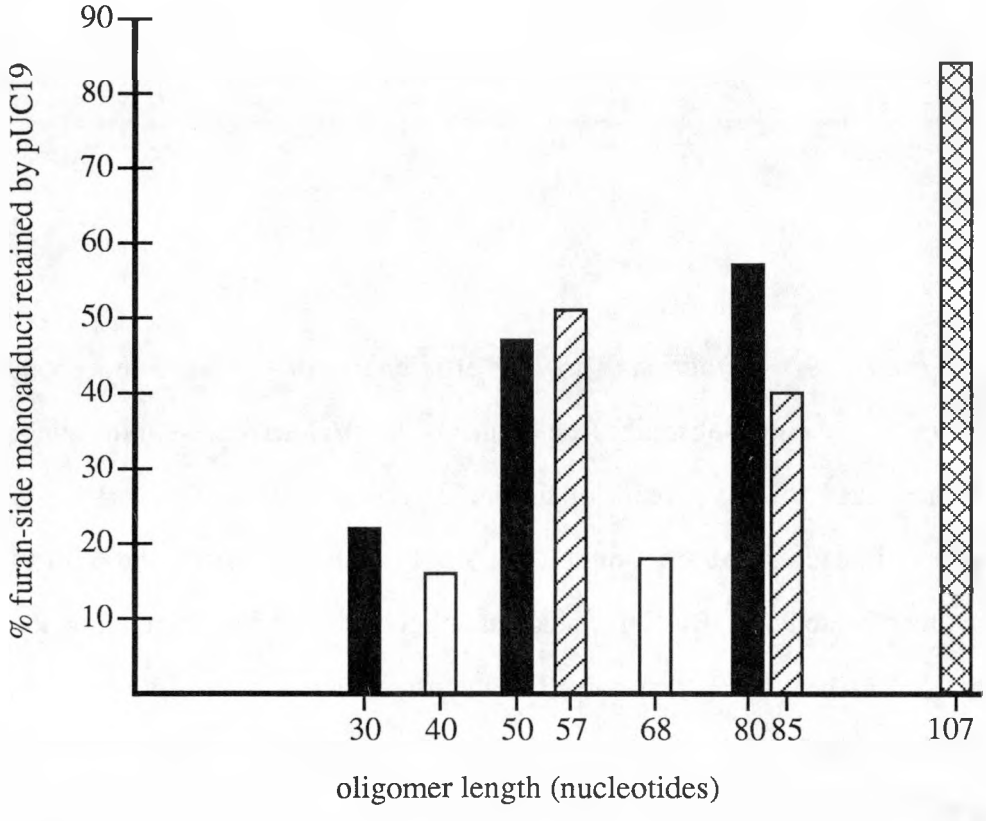
% furan-side monoadduct retained by pUC19
90
80
70
60
50
40
30
20
10
30
40
50
57
68
80
85
107
oligomer length (nucleotides)

(a)

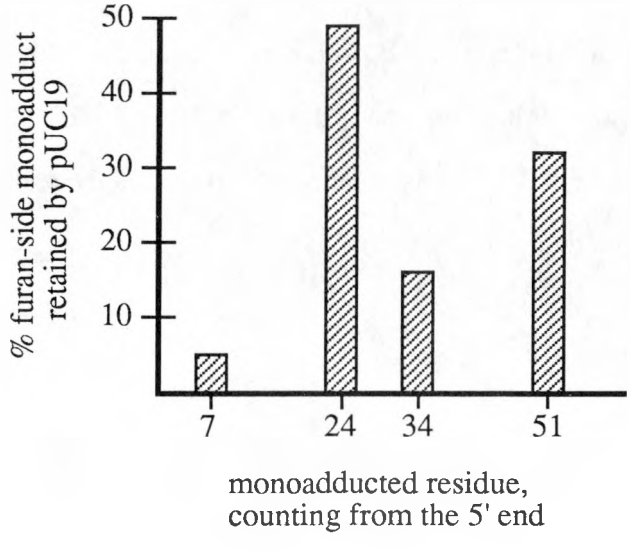
% furan-side monoadduct retained by pUC19
50
40
30
20
10
7
24
34
51
monoadducted residue,
counting from the 5' end

(b)

between long substrates is not observed in the presence of ATPγS [Honigberg *et al.*, 1985]. The role of the sequences of these 57-mers in the stabilities of the three-stranded complexes formed was not addressed, though this might explain the difference between 57-mers B and C. More centrally positioned adducts could presumably be stabilized by basepairing on both sides; yet 57-mer B was poorly retained. Although RecA binding to DNA is generally not sequence-specific, a sequence-dependence was previously noted among four 15-mers [Leahy and Radding, 1986]. This phenomenon may be an artifact due to oligomeric substrates.

Detection of stable uncrosslinked complexes — In the presence of ATPγS, detectable complexes were formed even without an irradiation to effect crosslinkage (longer film exposure of Figure 2-4(b); additional data not shown). The 80- and 107-mer substrates may be incorporated into pUC19 at levels up to 50% of that observed in samples that had been irradiated. For the shorter oligomers, however, crosslink formation was necessary for the three-stranded complexes to survive deproteinization. No formation of complexes with either the 30- or 40-mer substrate was detected in the absence of an irradiation. These observations indicated that the RecA reaction could produce a three-stranded structure stable enough to retain an inserted, yet uncrosslinked oligomer under nondenaturing conditions.

Stable uncrosslinked complexes were also found in irradiated samples. These uncrosslinked complexes could be denatured at 90°C and detected on a denaturing polyacrylamide gel. The 107-mer system yielded the greatest amounts, with up to 35% of complexed oligomer apparently remaining uncrosslinked. The 40- and 68-mer systems also showed significant levels, while in the remaining five systems less than 10-15% of complexes were found to be uncrosslinked. The 30- and 40-mer results were curious since no stable complexes were detected in the absence of an irradiation. Given the low levels of overall complex formation with these two substrates (Figure 2-5), however, 2-3% total uncrosslinked complex falls within experimental error. The 50-, 80-, and 107-

mers were approximately 62% furan-side monoadduct. Uncrosslinked oligomer in these systems could therefore result from insertion of a pyrone-side (uncrosslinkable) monoadducted substrate or from insertion of a furan-side monoadducted substrate with an orientation that precluded crosslink formation. The relative contributions of such complexes to the final populations of uncrosslinked 50-, 80-, and 107-mer is not known. The remaining five substrates (30-, 40-, 57-, 68-, and 85-mer) were approximately 98% furan-side monoadduct. These also yielded uncrosslinked complexes, suggesting that unsuccessful crosslinkage was primarily due to an unfavorable orientation of the monoadduct in the three-stranded complex. Within experimental error, longer irradiation times of up to ten minutes yielded an additional 5% of crosslinked complex, but did not affect total complex formation (data not shown). Incomplete crosslinkage even at light doses in excess of that needed to effect 100% crosslink formation also suggests that within the RecA-stabilized synaptic intermediate, the newly formed DNA helix may have an altered B-form structure which is not favorable to formation of a psoralen crosslink.

Effect of linearizing the duplex substrate — The duplex pUC19 substrate contained approximately 10% FII (nicked circular duplex) in addition to the FI (supercoiled) molecules. As Figure 2-4 shows, both FI and FII complexes were observed, although nicking of FI during phenol extractions would have contributed to the amount of labeled FII detected. The relative efficiencies of complex formation with these two substrates was not determined. To examine the efficiency of oligomer insertion into FIII (linear duplex) DNA, FI pUC19 was linearized with XmnI, leaving 800 base pairs 5′ to the KpnI site for crosslink formation. Increasing the relative amount of FIII to FI pUC19 at a fixed total pUC19 concentration inhibited oligonucleotide incorporation. If only FIII substrate was present, no three-stranded complexes containing the 50-mer were detected. For the 80-mer system, the efficiency of oligomer insertion into FIII pUC19 was 15-20% of that observed for FI (data not shown). Thus, superhelicity appeared to be necessary for efficient formation of the three-stranded complexes.

Requirement for homology — RecA-mediated pairing of the 50- and 85-mer monoadducted oligomers with FI pBR322 was also tested, using ATPγS as the cofactor. This substrate was chosen to examine the degree of specificity in the formation of three-stranded complexes, since most of pUC19 outside of the targeted polylinker region was derived from pBR322. As was discussed above, resistance of pUC19 complexes to digestion by KpnI was one test of the site-specificity of oligomer insertion. Based upon the ability to detect three-stranded pUC19 complexes that were linearized by KpnI, up to 5-10% of the observed complexes may have been formed at sites other than the intended target. The pBR322 plasmid was tested alone and together with pUC19 as the duplex substrate. Three-stranded pBR322 complexes were detected if the reaction mixtures had been irradiated to effect crosslinkage (Figure 2-6). The level of incorporation of the 50-mer into pBR322 was 10-15% of that into pUC19, and the level of 85-mer incorporation was 30% of that usually observed with pUC19. Incorporation into pUC19 was somewhat reduced by the presence of pBR322 (data not shown).

In an attempt to understand these results, the sequences of the two oligomers were compared to that of pBR322 using a program obtained from Pustell and Kafatos [1982]. The pBR322 sites having the greatest homology with the 50- and 85-mers represented 48% and 45% overall homology, respectively. If the search was narrowed to the 26-base sequence centered around the KpnI recognition site (only 19 of the 26 are within the 50-mer), then regions of 50-62% overall homology were identified. The observed formation of stable complexes with pBR322 might be explained by interaction initiated by RecA at any of these sites. Retention of these randomly inserted oligomers in FI plasmid would presumably be favored by the energy of supercoiling.

Computer searches were also performed using the sequence of ϕX174, expected to have less homology with pUC19 than pBR322 has. Sites having the greatest overall homology with the oligomeric substrates were at 50% for the 50-mer, and 45% for the 85-mer. If the analysis focused again at the 26-base sequence around the crosslinking site,

Figure 2-6. Deproteinized samples from RecA-mediated pairing reactions between either 2.5 nM pUC19 (lanes 1, 2, 7, and 8) or 2.4 nM pBR322 (lanes 3, 4, 9, and 10) or 3.0 nM both (1:1 mixture; lanes 5, 6, 11, and 12) and either the 50- or 85-base HMT-monoadducted oligomer, as indicated. (a) photograph of gel stained with ethidium bromide, and (b) the corresponding autoradiogram.

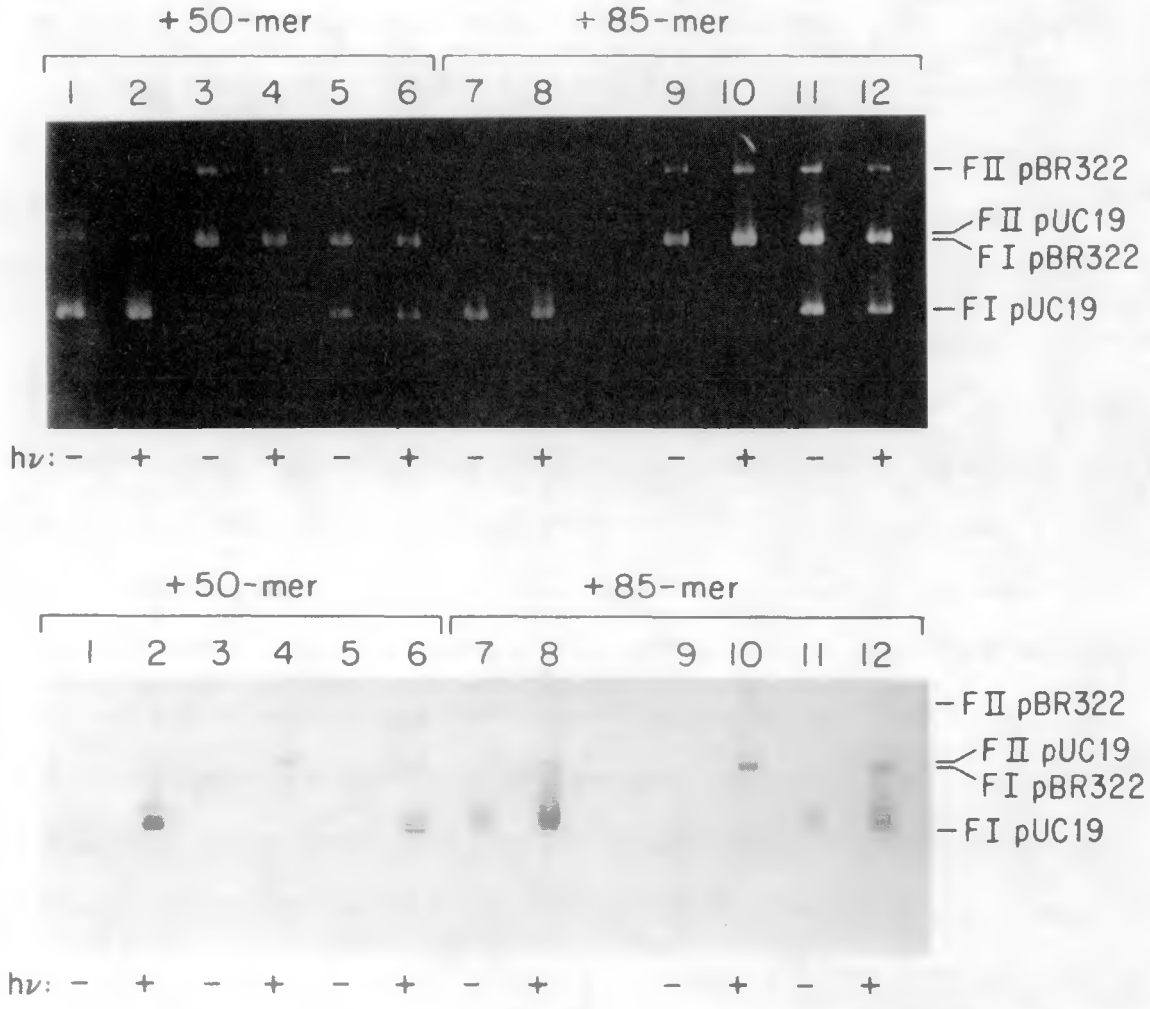
+50-mer
+85-mer
1 2 3 4 5 6 7 8 9 10 11 12
– FII pBR322
FII pUC19
FI pBR322
– FI pUC19
hν: – + – + – + – + – + – +
+50-mer
+85-mer
1 2 3 4 5 6 7 8 9 10 11 12
– FII pBR322
FII pUC19
FI pBR322
– FI pUC19
hν: – + – + – + – + – + – +

XBB903-2445

regions of 50-54% homology were identified. Apparently, then, regions of 40-60% overall homology are likely to be found in randomly chosen DNA, and this extent of homology may be sufficient for interaction between the RecA-coated oligonucleotides and a duplex substrate.

Extent of unwinding — In various analytical agarose gels of the three-stranded complexes, the FI plasmid was observed to migrate as a multiplet of bands if the inserted oligonucleotide was the 85- (as in Figure 2-6) or the 107-mer. This suggested that the deproteinized samples retained some of the unwinding induced by the presence of the third strand. To resolve these bands, the samples were electrophoresed in buffers containing various amounts of chloroquine, in effect titrating the superhelical turns of the three-stranded complexes. Representative autoradiograms are shown in Figure 2-7. In an initial study, commercially prepared pUC19 was used as in all the preceding work, but this had too broad an initial distribution of topoisomers to permit complete resolution in the gel system used. It was also necessary to ensure that the entire initial distribution was capable of accommodating each oligonucleotide completely. With 2686 basepairs, pUC19 at a superhelical density of about -0.05 could be expected to have 13 superhelical turns, and could therefore accommodate the 107-mer (maximum 10 turns). A noncommercial preparation of pUC19 was used to generate the data shown in Figures 2-7 and 2-8. With increasing amounts of chloroquine, the topologically different species within complexes containing shorter oligonucleotides were resolved while those with longer oligomer inserts became superimposed (see Figure 2-7).

As described under "Methods," densitometric traces were taken of all resolved samples in each autoradiogram. The center-of-mass for each FI distribution was then determined relative to the FII position (for example, see Figure 2-8a). The relative insensitivity of the FII bands to the presence of the third strand (as in Figure 2-7; additional data not shown) was evidence that the additional mass, at most 2% of the total, was not responsible for the observed changes in FI band mobilities. At each chloroquine

Figure 2-7. Four of the eleven autoradiograms used for the analysis of unwinding in the crosslinked three-stranded complexes. Lanes 1–6 in each are complexes containing, respectively, a 30-, 50-, 57-, 80-, 85-, or 107-mer insert. All gels were run in TANE (see 'Methods') at varying concentrations of chloroquine: (a) 0.5 μg/mL, (b) 1.0 μg/mL, (c) 2.0 μg/mL, and (d) 3.5 μg/mL. The position of FII (nicked circular duplex) is labeled.

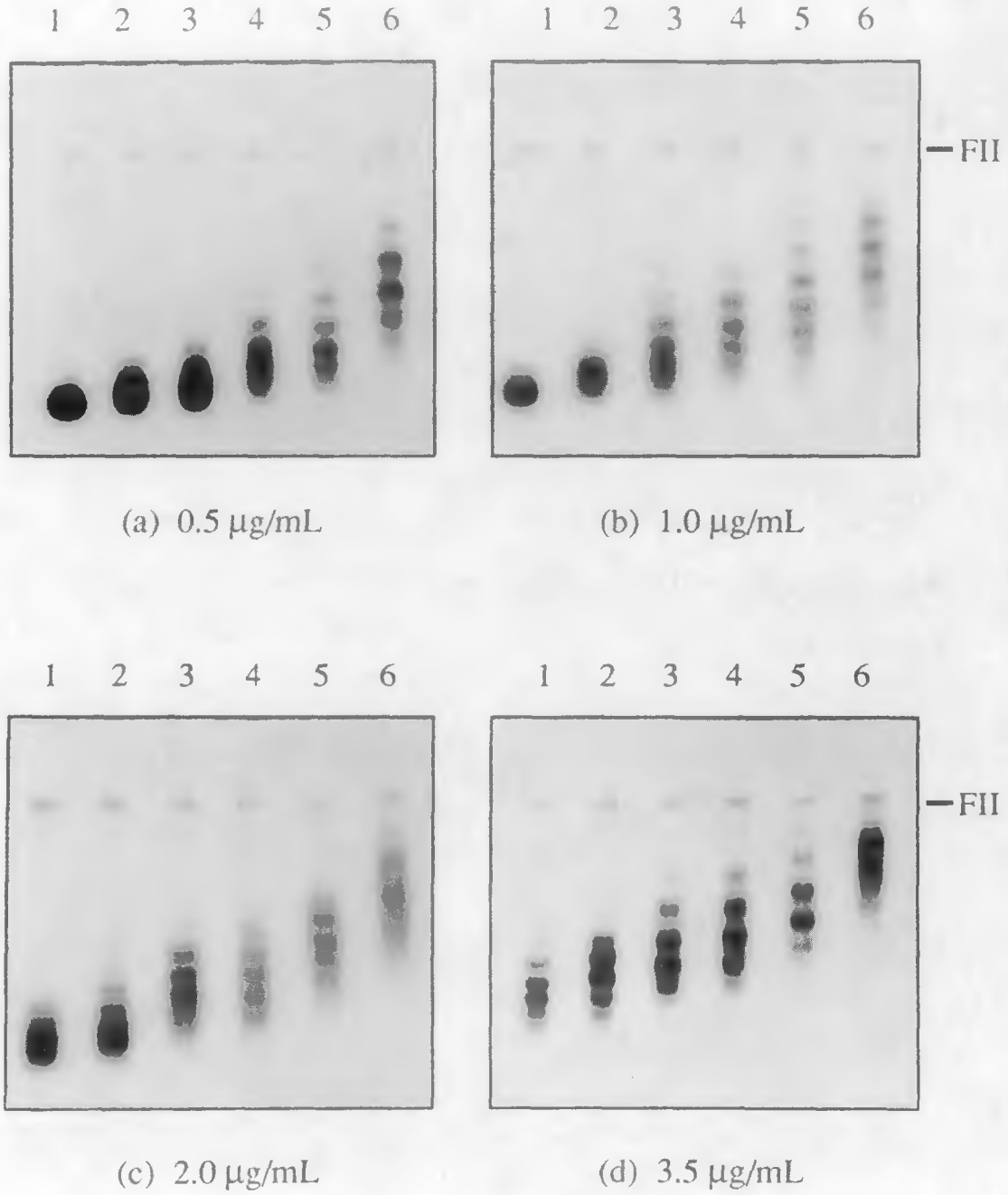

Figure 2-7. Unwinding analysis

XBB903-2446

Figure 2-8. Sample densitometric traces from either (a) Hoefer or (b) Kratos instruments (see 'Methods'). Shown here is the crosslinked complex between pUC19 and the monoadducted 85-mer, electrophoresed in 1.0 μg/mL chloroquine (lane 5 in Figure 2-7b). The positions of 50% FI intensity are marked, as is the position of the FII peak. (c) Summary of data obtained as discussed under "Methods," originally plotted using Cricket Graph 1.3 (Cricket Software, PA). Square boxes represent single data points; rectangular boxes represent two identical data points. Please refer to text for discussion.

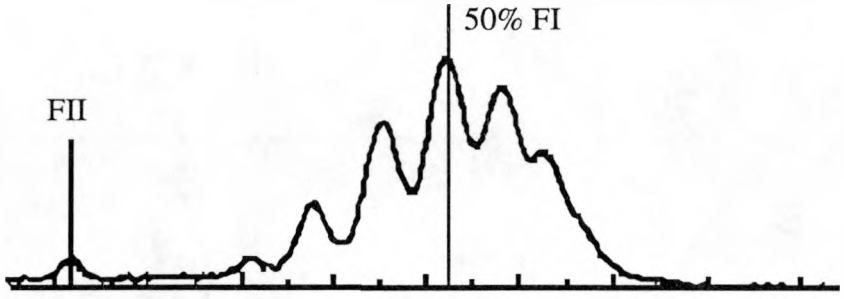
50% FI
FII

(a)

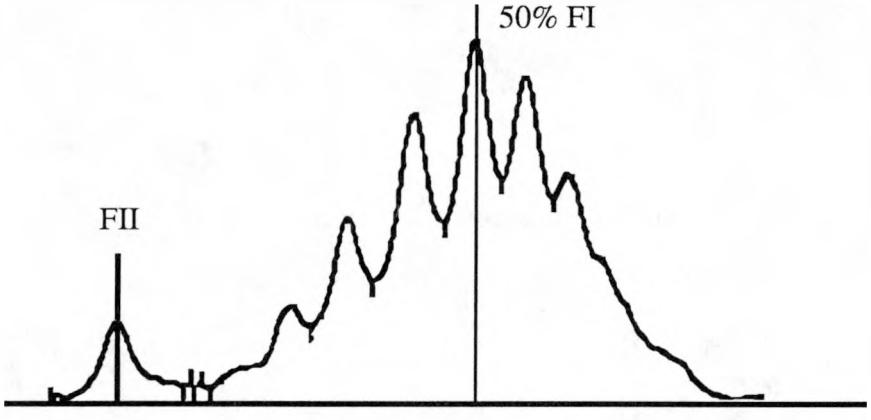
50% FI
FII

(b)

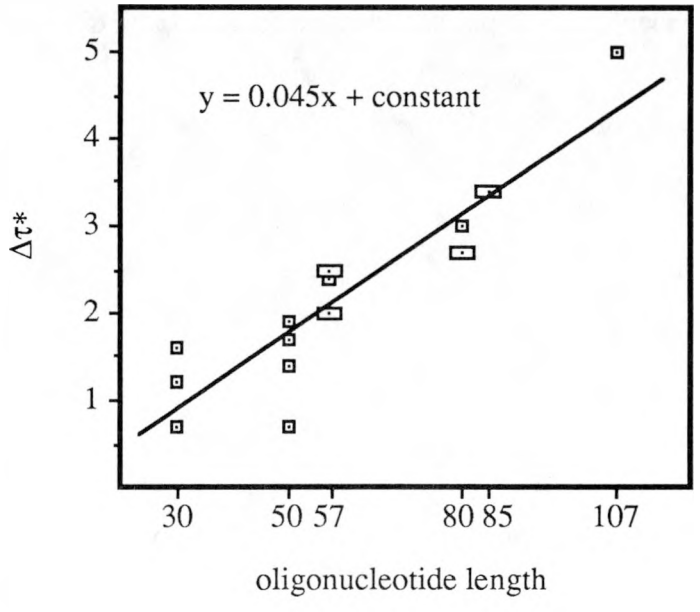
y = 0.045x + constant
Δτ*
5
4
3
2
1
30
50 57
80 85
107
oligonucleotide length

(c)

concentration, changes in the position of the center-of-mass between lanes were attributed to the differences between the inserted oligonucleotides. The trend of increasing extent of unwinding with length of the third strand was plotted for each gel (not shown) and collectively (Figure 2-8). The actual number of basepairs between the inserted oligomer and its complement was not determined, and presumably would depend upon the position of the crosslink within the three-stranded region. If the effect of psoralen position is not considered, and a linear function rather than a multiphasic or nonlinear relationship is assumed, then Figure 2-8 indicates that on average, approximately 0.45 turns of deproteinized plasmid were unwound per 10 bases inserted over the range of 30 to 107 bases. If the psoralen location is taken into account and held constant, as in comparison of the 30-, 50-, and 80-mers which share a 3′-end location of the adduct, then the value is approximately 0.3-0.4 turns per 10 bases inserted. For technical reasons, RecA-coated complexes were not amenable to a similar analysis. In the deproteinized complexes, then, the inserted strand was not fully basepaired to its complement with the concomitant complete unwinding of nearly 10.5 bp/turn (B-form helix). Nor did the three-stranded region appear confined to within five basepairs on either side of the crosslink.

Attempts were made to determine more precisely the extent to which each inserted oligomer was basepaired to its complement using restriction digests. Since the homologous sequences lie within the polylinker region, both the plasmid and oligonucleotide components of the three-stranded complexes could, in principle, be assayed for their susceptibility to each of the adjacent restriction enzymes. However, there is an unknown dependence on flanking sequences and on DNA conformation for each restriction enzyme. Results of these experiments were inconclusive (data not shown).

Summary — The data presented here demonstrate that psoralen-monoadducted oligomers of between 30 and 107 bases can be hybridized to their complement within a duplex plasmid via the homologous pairing reaction of RecA protein. The psoralen mono-

adduct can then be photochemically activated to form a crosslink, covalently fixing the oligomer to its complement in the RecA-stabilized, three-stranded DNA complex. Several factors affecting complex formation were identified. In contrast to reactions involving longer fragments, excess RecA and ATPγS were needed, presumably to overcome the weak affinity of the protein for oligonucleotide substrates. Single-stranded DNA binding proteins were observed to enhance this process. Both the overall length of the substrate and the position of the psoralen-monoadducted residue affected reaction efficiency. The issue of sequence-dependent stability of the final complexes was not addressed. Absolute homology was not required, since complex formation was observed with a duplex which did not contain the specific target region. This observation may reflect a reduced fidelity of homologous pairing that has been previously noted with supercoiled substrates [DasGupta and Radding, 1982]. The energy of supercoiling would presumably favor D-loop formation, but the kinetics and mechanism of RecA-mediated synapsis may also be affected by superhelicity [Shibata *et al.*, 1981].

Successful formation of psoralen crosslinks within synaptic RecA·DNA complexes is evidence that the invading DNA strand was basepaired to its complement at the crosslink site, and that any psoralen-induced structural distortions have been tolerated by the RecA protein. NMR has recently been used to probe the structure of psoralen-crosslinked DNA, specifically an 8-basepair duplex crosslinked by 4′-aminomethyl-4,5′,8-trimethylpsoralen (AMT) [Tomic *et al.*, 1987]. The presence of the centrally located crosslink distorted the helix only locally, within two to three basepairs on either side. HMT resembles AMT as a 4′-substituted derivative of TMP, although AMT is also a charged molecule at neutral pH. Extending the NMR results to describe HMT-adducted DNA suggests that RecA is unlikely to be inhibited by the psoralen, particularly since the protein is known to proceed with pairing reactions despite the presence of large insertions or mismatches [Bianchi and Radding, 1983]. The site of psoralen crosslink formation is presumed to be B-form DNA. The role of Z-form DNA in synapsis, as suggested by

Blaho and Wells [1987] and Fishel [1988] remains a possibility. How well these three-stranded structures model *in vivo* synapsis remains to be seen, particularly since ATPγS is not the natural cofactor for RecA. As noted earlier, RecA·DNA filaments formed in the presence of ATPγS cannot branch migrate to fully displace the homologous strand of the duplex and produce long heteroduplex regions, but such filaments are known to undergo homologous pairing [Honigberg *et al.*, 1985]. The deproteinized molecules characterized here may be unusually stable species, interesting as three-stranded DNA complexes, but playing no mechanistic role in recombination. Analysis of the covalently fixed three-stranded molecules in the presence of RecA might reveal more information about the structure of the initial joint molecule formed by RecA.

Chapter 3

Repair of Crosslinked Three-Stranded DNA Complexes

Introduction

The error frequency of DNA replication, determined by the specificities of DNA polymerases and accessory proteins, is necessarily very low to ensure that genetic information is properly passed on to the next generation. Perhaps one in 10^7 nucleotides is incorrectly copied. Post-replication mismatch repair pathways further reduce the error frequency to one in 10^{10} nucleotides. However, DNA can be damaged in a number of ways. "Spontaneous" chemical changes to the bases themselves include deamination (C→U), tautomerization which may affect basepairing, and depurination. Furthermore, the environment may subject the cell to a variety of chemical and physical agents that can adversely affect both the bases and the sugar-phosphate backbone. [reviewed by Friedberg, 1985]

In *Escherichia coli*, a number of repair pathways have been identified, some more specialized than others. Damage to DNA can sometimes be reversed, as in photolyase-mediated monomerization of *cis-syn* pyrimidine dimers [reviewed by Sancar and Sancar, 1988] or ligation of single-stranded breaks. Other lesions must be excised or somehow bypassed. Replicative bypass is usually a mutagenic process. Base excision repair, in which the damaged base alone is removed, is mediated by DNA glycosylases that hydrolyze the N-glycosidic bond between the base and the sugar-phosphate backbone. Apurinic/apyrimidinic (AP) endonucleases recognize the absence of a base and hydrolyze the adjacent 5′ and 3′ phosphodiester bonds [reviewed by Friedberg, 1985]. Mismatched basepairs can also be corrected through excision repair pathways [reviewed by Friedberg, 1985; Modrich, 1989; Myles and Sancar, 1989]. In nucleotide excision repair, the damaged bases are typically removed as part of a small oligonucleotide.

ABC excinuclease is the multisubunit enzyme which mediates nucleotide excision repair in *E. coli* [recently reviewed by Sancar and Sancar, 1988; Myles and Sancar, 1989]. Psoralen adducts (both monoadducts and crosslinks) are among the various lesions targeted in this process. Other lesions recognized by ABC excinuclease include those due to

the drug CC-1065 [Selby and Sancar, 1988], numerous other alkylating agents, and *cis*-$Pt(II)NH_2Cl_2$, as well as UV irradiation-induced pyrimidine dimers and 6-4 photoproducts [reviewed by Sancar and Sancar, 1988]. One possible basis for the recognition of such lesions is a distortion of the DNA helix. The observed efficiencies of incision at a site-specifically placed psoralen monoadduct, thymine dimer, and O^6-methylguanine (listed in order of decreasing efficiency) appear to correlate with the degree of resulting helical distortion, but the sequence-dependence of these efficiencies is unknown [Voigt *et al.*, 1989]. Furthermore, ABC excinuclease will recognize damage that does not cause significant distortion of the helix, including thymine glycol and AP sites [Lin and Sancar, 1989], as well as the N^2-guanine adduct formed by anthramycin [Walter *et al.*, 1988] and O^6-methylguanine [Voigt *et al.*, 1989]. DNA damage sites may be targeted through a process in which lesions alter helix dynamics and thus influence binding of the excinuclease rather than through enzymatic recognition of a particular static structural distortion of the helix [Lin and Sancar, 1989; Pu *et al.*, 1989].

As was noted in Chapter 1, two types of nucleotide excision repair have been identified, one characterized by short repair patches and a dependence on DNA polymerase I (pol I), the other characterized by long patches and a dependence on recombination proteins [reviewed by Peterson *et al.*, 1988; Smith and Wang, 1989]. Psoralen monoadducts can readily be repaired by the short patch pathway in which ABC excinuclease makes two incisions in the damaged strand to remove the adduct and pol I replaces the resulting gap using the undamaged strand as its template. Error-free repair of interstrand crosslinks is intuitively more difficult because the genetic information in both strands at the damaged site is compromised.

Cole and coworkers demonstrated that cell survival following psoralen-crosslinking treatment depended upon excision repair (*uvrA*, *uvrB*, and *uvrC* genes), recombination (*recA* gene), and the 5′→3′ exonuclease function of pol I (*polA* gene) in the 1970s [see Chapter 1; Cole, 1971 and 1973; Cole *et al.*, 1976]. Sancar and Rupp

determined that ABC excinuclease, the enzyme reconstituted *in vitro* from the products of the *uvrA*, *uvrB* and *uvrC* genes, was capable of making both of the incisions needed to remove pyrimidine photodimers [Sancar and Rupp, 1983]. Subsequent studies have confirmed that ABC excinuclease typically makes two specific incisions, one at the eighth (and occasionally the seventh) phosphodiester bond on the 5′ side and one at the fourth or fifth bond on the 3′ side of a lesion, leaving a gap with 3′-OH and 5′-P termini that is then filled in by polymerase and sealed by ligase [reviewed by Sancar and Sancar, 1988]. The 5′ and 3′ incisions can be uncoupled, depending upon pH and the ionic strength of the reaction buffer [Van Houten *et al.*, 1987]. Variations in the incision pattern can also be induced by nearby mismatches and small extrahelical loops [Thomas *et al.*, 1986].

The three genes encoding the subunits of ABC excinuclease are genetically unlinked. The *uvrA* and *uvrB* genes are both individual operons regulated by the LexA repressor, and *uvrC* is cotranscribed with two genes whose products are as yet uncharacterized. The UvrA protein is the largest subunit, at 104 kilodaltons. From the sequence of the *uvrA* gene, three purine recognition sequences which are putative ATPase domains and at least two Zn-finger domains can be identified [reviewed by Sancar and Sancar, 1988]. UvrA was known to contain two Zn atoms per monomer, but the existence of these two Zn fingers in the native protein has only recently been confirmed, by x-ray absorption fine structure analysis and site-specific mutagenesis [Navaratnam *et al.*, 1989]. These structural domains are consistent with the protein's observed ATPase and DNA-binding activities. UvrA shows a high affinity for ssDNA and dsDNA ends. Band-shift and DNA footprinting assays indicate that the specific binding constant (that is, to damaged DNA) is 10^3-10^4 times that for nonspecific binding to DNA. ATP has been observed to enhance the specificity of UvrA binding to damaged DNA [reviewed by Sancar and Sancar, 1988]. This subunit is believed to be responsible for scanning DNA to locate sites of damage. Evidence in support of a processive versus distributive scanning mechanism for ABC excinuclease has been reported [Gruskin and Lloyd, 1988].

The UvrB protein (76 kilodaltons) also contains a consensus ATPase sequence, but appears to neither bind nor hydrolyze ATP [reviewed by Myles and Sancar, 1989; Sancar and Sancar, 1988]. Stress-induced *E. coli* cell extracts do, however, yield a specific proteolysis product UvrB* which is a UvrA-independent DNA-dependent ATPase. Activation of this cryptic ATPase activity in the intact UvrB protein was proposed as an explanation for the increase in ATPase activity that is observed upon the addition of UvrB to UvrA in the presence of DNA [Caron and Grossman, 1988a]. However, the UvrB* protein does not form a complex with UvrA and UvrC that leads to DNA strand incision [Caron and Grossman, 1988b; Orren and Sancar, 1990]. More recent work indicates that the UvrB* protein does not exist *in vivo*. The protease responsible for cleaving UvrB to UvrB* is the outer membrane protein OmpT; the cleavage occurs only after cell lysis [reviewed by Myles and Sancar, 1989]. Further study with intact proteins indicates that mutation of a key lysine within the UvrB ATPase sequence interferes with excision repair. One hypothesis is that such mutants are defective in DNA-binding specificity [Seeley and Grossman, 1989]. UvrB alone shows little affinity for DNA. Both UvrA and ATP are required for UvrB to bind to DNA damage [Orren and Sancar, 1989]. Interestingly, a 14-amino acid C-terminal segment shares 93% (13 of the 14 residues) homology with a segment in the center of the UvrC protein [reviewed by Sancar and Sancar, 1988].

UvrC (68 kilodaltons) binds strongly to ssDNA, and is similar to UvrA in its affinity for dsDNA, but shows no particular specificity for damaged DNA. DNase I footprinting studies indicate that UvrC has little effect on the binding of either UvrA or UvrB to damaged DNA. The UvrC subunit is believed to be the nucleolytic subunit of the excinuclease, although intrinsic nuclease activity remains to be clearly demonstrated. [reviewed by Sancar and Sancar, 1988]

ABC excinuclease is so named because all three subunits were believed to be present at the time of DNA incision. An intriguing observation within this context was that while the DNase I footprint of UvrA on a site-specifically psoralen-monoadducted

137-basepair duplex was 33 basepairs, the footprint of UvrA and UvrB together was only 19 basepairs. At that time, UvrA was thought to perhaps initially associate as a dimer and to then release one monomer upon the addition of UvrB. An alternative explanation was that UvrA alone was imprecise in its binding, but became more precise in the presence of UvrB; both situations would be detected in the collective footprint of many molecules [Van Houten *et al.*, 1987].

Recent work has demonstrated that the UvrA subunit is in fact no longer present at the time of strand incision [Orren and Sancar, 1989 and 1990]. In solution, free UvrA protein readily dimerizes. Addition of UvrB leads to formation of a $(UvrA)_2(UvrB)_1$ complex. The dimerization process can be stimulated by ATP, ADP, or ATPγS, but association with UvrB is an ATP hydrolysis-dependent reaction. The function of UvrA appears to be catalytic, to deliver the UvrB subunit to the site of DNA damage and then dissociate once UvrB binds to the lesion. *In vivo*, the UvrA dimer may instead bind to DNA before associating with UvrB in the ATP hydrolysis-dependent reaction. The previously observed stimulation of ATPase activity upon addition of UvrB to UvrA and DNA can now be attributed to hydrolysis during the formation of the $(UvrA)_2(UvrB)_1$ complex [Orren and Sancar, 1989]. Assembly of DNA polymerase III holoenzyme similarly involves the ATP-dependent delivery of the β subunit by a complex comprised of five polypeptides [Maki and Kornberg, 1988]. Lesion-induced unloading of UvrB by the UvrA dimer may be a mechanism for damage recognition [Lin and Sancar, 1989].

The active enzyme may therefore more properly be named (A)BC excinuclease. At saturating concentrations of UvrB, the observed stoichiometry was one UvrB monomer bound per lesion [Orren and Sancar, 1989]. The 19-basepair footprint that was previously observed can now be interpreted as that of UvrB alone. Footprinting analyses had also revealed that the eleventh phosphodiester bond 5′ to a psoralen monoadduct became hypersensitive to DNase I in the presence of both UvrA and UvrB. This might reflect a conformational change in the DNA induced by the binding of UvrB to a lesion. The

footprint intensities also indicated that UvrA and UvrB associated more closely to the undamaged strand than to the adducted strand [Van Houten *et al.*, 1987]. The ability of the ABC enzyme to remove a CC-1065 molecule, which lies in the minor groove approximately four bases on the 5′ side of the adenine to which it is bound, suggests that this minor groove location is not important for (A)BC interaction with the DNA [Selby and Sancar, 1988].

Addition of the UvrC subunit to the UvrB·DNA complex leads to incision of the damaged strand, but only in the presence of ATP or the nonhydrolyzable analog ATPγS. This nucleotide cofactor requirement (K_M = 2-3 μM) is, however, quite different from the ATP requirement for the initial binding of UvrB to DNA (K_M = 120 μM) [Orren and Sancar, 1990]. No interaction of UvrC with UvrA, UvrB, or the $(UvrA)_2(UvrB)_1$ complex is detected in the absence of DNA [Orren and Sancar, 1989]. The observations by Seeley and Grossman [1989] regarding the importance of lysine-45 in the cryptic ATPase sequence of UvrB might reflect the role of ATP in the productive association of UvrC to UvrB-bound DNA that leads to incisions.

Left alone *in vitro*, (A)BC excinuclease dissociates very slowly from the incised DNA. Addition of both DNA polymerase I (pol I) and helicase II (UvrD protein), two proteins implicated in excision repair *in vivo*, was sufficient to achieve a turnover rate (approximately 0.07 adduct per nucleoprotein complex per minute) comparable to that observed *in vivo* [Husain *et al.*, 1985]. These two accessory proteins were thought to perhaps form a "repairosome" complex with the excinuclease [Caron *et al.*, 1985]. DNase I footprinting was used to further examine the requirements for turnover of (A)BC excinuclease following the dual incisions. The results indicate that *in vitro*, pol I alone is capable of displacing the post-incision complex during repair synthesis [Van Houten *et al.*, 1988]. Helicase II may serve to enhance the processivity of pol I and assist in the dissociation of the excinuclease from the oligomeric excision product [Husain *et al.*, 1985; Van Houten *et al.*, 1988]. Although helicase II showed little specificity for binding

psoralen-modified DNA and had little effect on the UvrA and UvrB footprints, the protein did induce a new DNase I-sensitive site on the undamaged strand. The location of this site may reflect helicase II binding near the 5′ incision site. Additional support for this interpretation comes from the observation that helicase II partially blocks ligase from the 5′ incision site. No evidence of a multienzyme "repairosome" was found [Van Houten *et al.*, 1988].

The short repair patch pathway that predominates nucleotide excision repair is characterized by repair patches of 10-30 nucleotides [reviewed by Peterson *et al.*, 1988; Smith and Wang, 1989]. Van Houten and coworkers found that following incision of a uniquely monoadducted duplex, 83% of the repair patches were 12 nucleotides long. This was precisely the size of the gap between the two (A)BC incision sites. An additional 10% of the patches were 12-20 nucleotides long, and no patches longer than 45 nucleotides were detected [Van Houten *et al.*, 1988]. These results are quite consistent with a short repair patch pathway for psoralen monoadducts.

Several of the recent studies on the action mechanism of (A)BC excinuclease have utilized substrates containing site-specifically placed psoralen adducts [Jones and Yeung, 1988; Van Houten *et al.*, 1986a and 1986b; Yeung *et al.*, 1987]. Both furan- and pyrone-side psoralen monoadducts are recognized and similarly incised at the eighth phosphodiester bond 5′ and the fifth bond 3′ to the adduct [Van Houten *et al.*, 1986a]. A unique pattern is observed with psoralen-crosslinked DNA, however. (A)BC excinuclease incised a site-specifically HMT-crosslinked 40-basepair duplex only on the furan-side strand, and at the ninth (5′) and third (3′) phosphodiester bonds from the crosslink [Van Houten *et al.*, 1986b].

Early *in vivo* data suggested that psoralen crosslinks are removed through two incision steps with an intervening RecA-mediated recombination step [Cole, 1973]. The above *in vitro* data suggested refinements of this model for error-free crosslink repair. The resulting mechanism is shown in Figure 3-1. Initially, (A)BC excinuclease spe-

Figure 3-1. Model for the error-free repair of psoralen crosslinks mediated by (A)BC excinuclease. (A)BC excinuclease initially makes dual incisions adjacent to the crosslink on one strand of the helix. Displacement of the resulting fragment leaves a gap which is filled through a recombination event mediated by the RecA protein. (A)BC excinuclease then makes a second set of incisions, isolating the crosslink in the three-stranded post-recombination intermediate. Finally, the enzyme and the crosslinked fragment dissociate, and the gap is filled by the combined action of DNA polymerase I (pol I), ligase and helicase II, in the presence of all four deoxyribonucleoside triphosphates (dNTP's: dATP, dCTP, dGTP, and dTTP). [Van Houten *et al.*, 1986b]

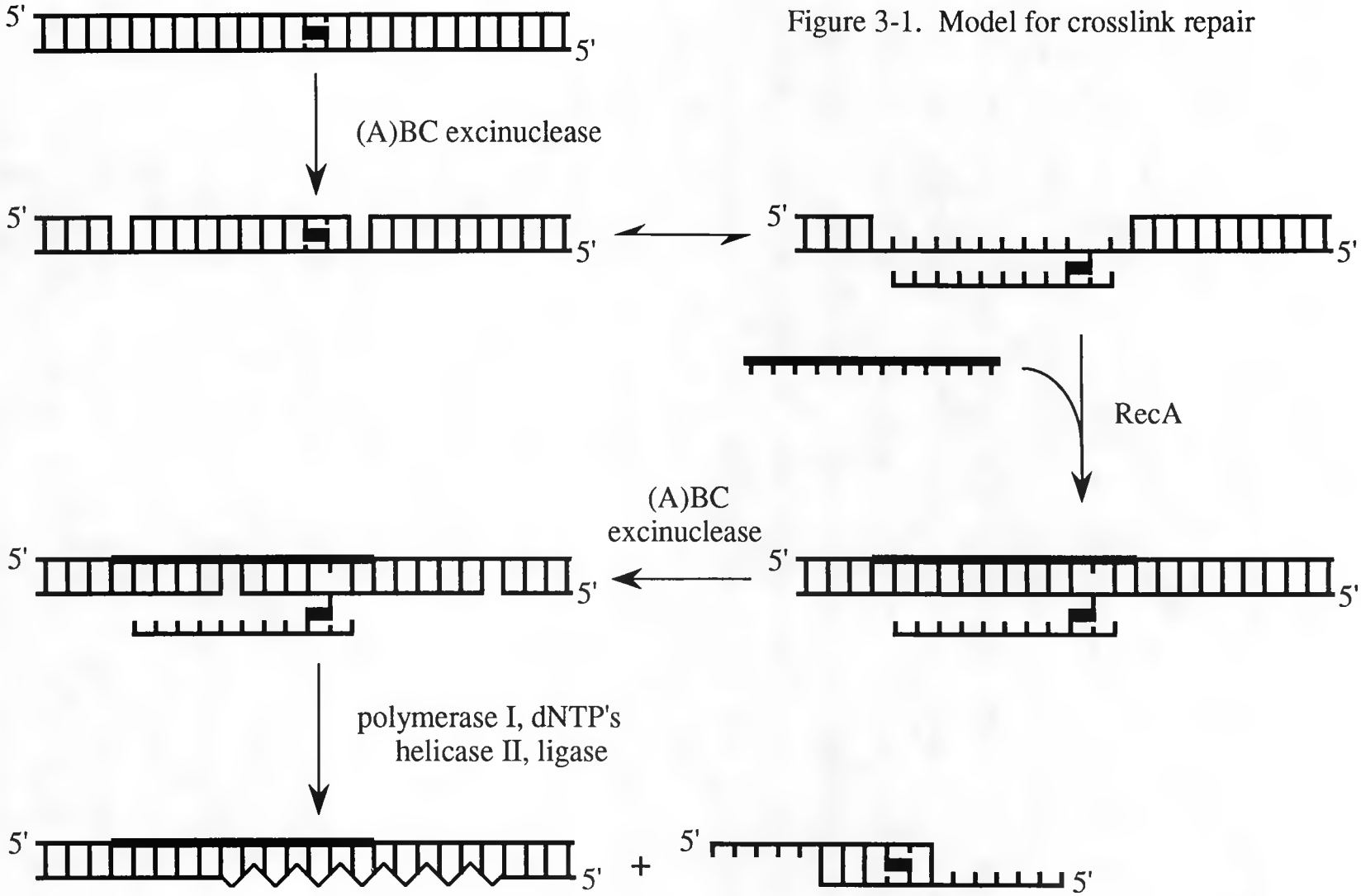

Figure 3-1. Model for crosslink repair

cifically incises one strand of the crosslink. As the recent data indicates, this would be the furan-side strand of HMT crosslinks. For error-free repair, the excision gap is replaced through recombination rather than mutagenic translesion synthesis. Following the recombination step, (A)BC excinuclease must recognize a three-stranded substrate and incise the one strand which will enable removal of the crosslinked site. This second excision gap can then be filled in by polymerase and ligase.

This revised model predicts that (A)BC excinuclease will differentiate between a crosslinked three-stranded substrate and a crosslinked duplex, and incise one or the other strand of the crosslink accordingly. We chose to model the post-recombination substrate using the site-specifically crosslinked three-stranded molecules generated through RecA-mediated homologous pairing and psoralen photochemistry (Chapter 2). The crosslinked oligonucleotide is analogous to the fragment produced by the first incision step, and the homologous strand of the original duplex is analogous to the undamaged strand that has been inserted through recombination. We tested both the post-recombination incision step and the completion of crosslink repair through the combined action of the accessory proteins DNA pol I, DNA ligase, and helicase II. This work has been previously published [Cheng *et al.*, 1988a and 1988b].

Materials and Methods

Proteins and DNA — UvrA, UvrB, and UvrC proteins, purified as described earlier [Thomas *et al.*, 1985], were gifts of A. Sancar, University of North Carolina at Chapel Hill. These aliquots were kept frozen at -80°C. Aliquots of each subunit were thawed as needed; these were subsequently stored at -20°C. Typically, UvrC was inactive after 2 weeks at -20°C, UvrA after 4 weeks. Loss of UvrB activity was noted only after several months at -20°C. All of the remaining proteins listed here were stable at -20°C.

Helicase II (UvrD) was a gift of S. Matson, University of North Carolina at Chapel Hill. DNA polymerase I was obtained from Boehringer Mannheim Biochemicals,

and the T4 DNA ligase was from either Promega Biotec or Bethesda Research Laboratories (BRL). KpnI and PvuII restriction endonucleases and bovine serum albumin (BSA) were purchased from BRL.

Three-stranded complexes were formed in the presence of ATPγS and crosslinked as described in Chapter 2. Complexes were deproteinized, separated from unreacted oligonucleotides on a 9 cm high x 1 cm diameter Bio-Gel A-5m (Bio-Rad) gel filtration column, and then ethanol-precipitated. Site-specifically HMT-monoadducted duplex M13mp19 (described further in Chapter 4) was a gift of B. Van Houten and H. Gamper.

Calibration of (A)BC excinuclease subunit concentrations — Each batch of the three subunits was tested to optimize the relative concentrations of each for (A)BC excinuclease repair activity. The test substrate was 100 ng of pBR322 that had been irradiated with approximately 125 J at 254 nm, to produce an average of 10 photodimers per molecule (Sancar lab, personal communication). The UvrA concentration was varied to find the minimum necessary for incision activity, typically ≥ 10 nM. UvrB and UvrC levels were then optimized at this concentration of UvrA. Reactions were run as described below, for 15 minutes. Aliquots were removed and loaded onto 1% agarose gels with 0.4% SDS, 4 mM EDTA, and 0.04% tracking dyes (bromophenol blue and xylene cyanole FF) in 5% glycerol (final concentrations) to follow the conversion of FI pBR322 to FII. Unirradiated pBR322 was used to test the final concentrations for nonspecific exonuclease contaminants.

Incision of crosslinked DNA — Conditions for (A)BC excinuclease reactions have been described previously [Van Houten *et al.*, 1986a]. The final reaction buffer contained 50 mM Tris·Cl (pH 7.4 at 25°C), 50 mM KCl, 10 mM $MgCl_2$, 2 mM ATP, 5 mM DTT, and 200 μg/mL BSA. In each 50 μL-reaction, 0.5 pmol of UvrA, 1.3 pmol of UvrB and 1.5 pmol of UvrC were used. Each protein was freshly diluted into reaction buffer at 0°C, then mixed and preincubated at 37°C for 5 minutes prior to the addition of the DNA, 25-30 ng (15-20 fmol) of plasmid. Reactions were stopped after 20-30 minutes, and the DNA

was extracted with phenol and diethyl ether, then ethanol-precipitated. The samples contained both unreacted plasmid and three-stranded complex; however, only the complexes were ^{32}P-labeled (from the oligonucleotide). Crosslinks were photoreversed by irradiating samples with 254 nm light (germicidal lamps) at 2 mW/cm^2 for 15 minutes. To detect the excision products, samples were suspended in formamide/dyes, heat-denatured at 90°C for 2 minutes and cooled on ice, then analyzed by 8% denaturing PAGE (19:1 acrylamide:bis, 7.5 M urea). For autoradiography, the gels were transferred onto Whatman 3MM chromatography paper and dried at 80°C using a Bio-Rad Model 483 or SE1125B Slab Drier. Aliquots were also analyzed on nondenaturing 1% agarose gels to detect changes in the FI plasmid population resulting from treatment with (A)BC excinuclease.

Identification of the excised fragment — (A)BC excinuclease reactions were carried out on samples of 300-400 ng (0.20-0.25 pmol) of DNA, using the enzyme concentrations noted above. Crosslinked excision product was recovered from the 8% polyacrylamide gels by soaking the gel slices in 10 mM NaCl and 0.1 mM EDTA, then precipitating the DNA. These crosslinked samples were photoreversed under 254 nm light (3-3.5 minutes at 5 cm below a germicidal lamp) and then combined. Only by combining the samples was enough material obtained for characterization. The fragments were labeled on the 3′ end with [α-^{32}P]-cordycepin 5′-triphosphate using terminal deoxynucleotidyl transferase (kit purchased from NEN Dupont). The samples were first heated at 65-70°C for 5 minutes, then placed on ice. Reactions were scaled down 50% from the NEN protocol. The labeled fragments were isolated on a 20% polyacrylamide gel. The recovered DNA was sequenced at 25°C using the methods of Maxam and Gilbert [1980]. Because of the small size of the fragments, reaction times were extended 2-3 fold. The ethanol-precipitation procedures were also adjusted to include 10 mM $MgCl_2$, a minimum chilling period of 1-2 hours at -70°C or overnight at -20°C, and 30-45-minute spins in a microcentrifuge to pellet the samples efficiently. Sequencing reaction samples were ana-

lyzed on either a 20% or 22.5% polyacrylamide gel.

Complete repair — To completely repair the crosslink site, 0.5-2.5 pmol of helicase II, 2 units of DNA polymerase I, dNTP's (2 nmol each of dATP, dGTP, and dTTP, with 20-30 μCi or 10 pmol of [α-^{32}P]dCTP), and 2-4 units of DNA ligase were added to the post-incision (A)BC excinuclease reaction mixture, and the samples were incubated at 37°C for another 10-20 minutes. The [α-^{32}P]dCTP was included to label the repair patch. For analysis by PvuII and KpnI digestions, the DNA was first deproteinized by two phenol and one diethyl ether extractions, ethanol-precipitated, then resuspended into REact4 buffer (BRL) and 100 μg/mL BSA. Double digests were carried out simultaneously, for two hours at 37°C. SDS to 1%, EDTA to 10-15 mM, and tracking dyes in glycerol (to 3-5%) were added directly to the reaction mixtures and the samples were analyzed by 8% nondenaturing PAGE. X-ray film (see Chapter 2) was exposed at 4°C.

Results and Discussion

Incision of crosslinked three-stranded complexes — (A)BC excinuclease was observed to act only on the furan-side of an HMT-crosslink in a linear duplex [Van Houten *et al.*, 1986b]. For complete crosslink repair, however, the pyrone-side strand must also be incised. As Figure 3-1 illustrates, the current repair model predicts that (A)BC excinuclease will recognize the orientation of the crosslink within a three-stranded complex and make the necessary pyrone-side incisions to remove the damage. To test this prediction, each of eight psoralen-crosslinked three-stranded complexes was incubated with (A)BC excinuclease. These complexes (prepared as in Chapter 2) differed only in the length of the oligonucleotide that was covalently crosslinked to the pUC19 plasmid. The set of possible incision products is diagrammed in Figure 3-2. In each complex, the oligonucleotide component carried a 5' end-label.

Figure 3-2. Summary of possible products of (A)BC excinuclease digestion of the crosslinked three-stranded complexes, depending upon which strand is incised. In each complex, the furan-side strand of the crosslink is the ^{32}P-labeled oligonucleotide insert, and the pyrone-side strand is the plasmid. Furan-side incisions would therefore release a shortened oligonucleotide and leave the supercoiled plasmid intact. Pyrone-side incisions, however, would release a fragment of the plasmid crosslinked to the oligonucleotide and convert the supercoiled plasmid into a gapped circular duplex. The plasmid species could be followed by native agarose gel electrophoresis, the oligonucleotides by denaturing polyacrylamide gel electrophoresis (PAGE).

Figure 3-2. Products expected from the (A)BC excinuclease reaction

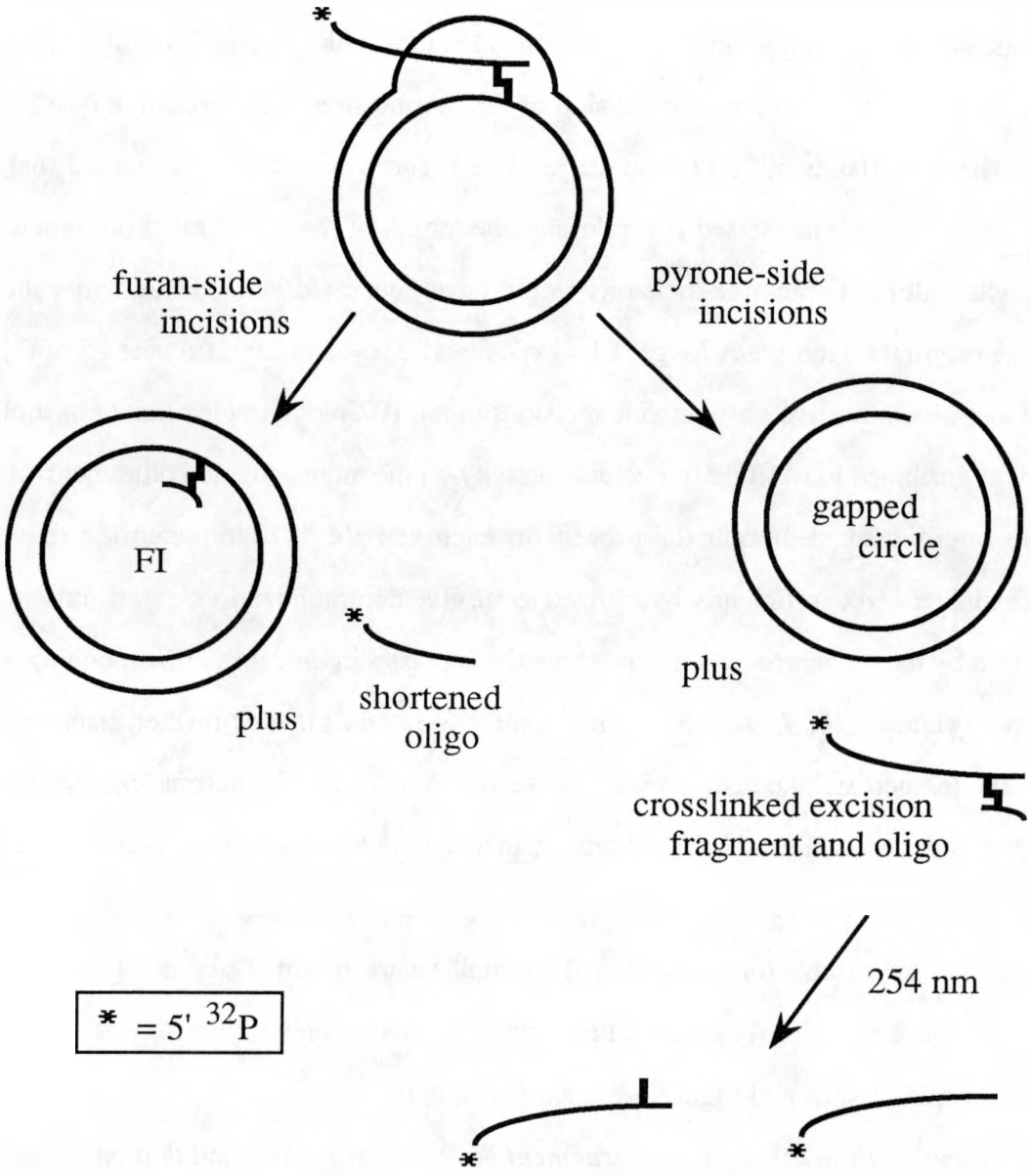

As Figure 3-3 shows, (A)BC excinuclease made incisions on the plasmid side of the crosslink in each complex, releasing a product which migrated more slowly than the free oligonucleotide in a denaturing polyacrylamide gel, and which yielded the full-length oligonucleotide upon photoreversal of the psoralen crosslink. Recognition of damage on the plasmid strand corresponds to incision of the pyrone-side of the crosslink (see Figure 3-2). The data (lanes 3, 7, 11, and 15 in both Figures 3-3a and b) indicated that the pyrone-side strand was incised regardless of the length of the crosslinked oligomer (30-107 nucleotides). Furan-side incisions would have generated labeled fragments shorter than the original oligomer. A longer film exposure did reveal a band (in lane 15 of Figure 3-3b) that was indicative of furan-side incisions in the 107-mer complex (data not shown). This was attributed to (A)BC excinuclease activity on the monoadducted oligomer retained within uncrosslinked complexes present in each sample. Oligonucleotide that was uncrosslinked – yet sufficiently hybridized to survive deproteinization, gel filtration, and detection by native agarose gel electrophoresis – appears in the lanes corresponding to no treatment (lanes 1, 5, 9, and 13 in both Figures 3-3a and b). For further discussion of these stable uncrosslinked complexes, please see Chapter 2. The autoradiograms shown in Figure 3-3 were analyzed by densitometry in an attempt to quantify the incision efficiencies. No correlation between incision frequency and either oligomer length or psoralen position was discernible (data not shown). Samples were also analyzed on agarose gels to follow the plasmid. Conversion of FI to gapped circular duplex was observed, consistent with the PAGE results and Figure 3-2 (data not shown).

Identification of the excised fragment — Previous studies had demonstrated that (A)BC excinuclease incisions yield a specific fragment either 11 or 12 bases in length (for example, Van Houten *et al.*, 1986a; Yeung *et al.*, 1987). To determine the product from (A)BC excinuclease digestion of the three-stranded complexes, the crosslinked oligomer and excision fragments were isolated by gel electrophoresis, photoreversed, and labeled at the 3′ end using terminal deoxynucleotidyl transferase and [α-^{32}P]-labeled cordycepin 5′-

Figure 3-3. Results of (A)BC excinuclease action on each of the eight three-stranded complexes (RecA-free), analyzed on 8% denaturing polyacrylamide gels. The oligomer contained within each is listed at the top: (a) 30-, 40-, 50-, and 57-mer complexes; (b) 68-, 80-, 85-, and 107-mer complexes. Lanes 3, 4, 7, 8, 11, 12, 15, and 16 contain samples digested with (A)BC excinuclease (ABC). Samples in the even-numbered lanes 2–16 were irradiated with 254 nm light to photoreverse crosslinks, yielding both unmodified and monoadducted (hence the doublet) full-length oligonucleotide. Bands migrating more slowly than these full-length oligomers are the crosslinked excision products (XL) which arose from pyrone-side incision (i.e. of the plasmid). Uncut plasmid remains at the origin.

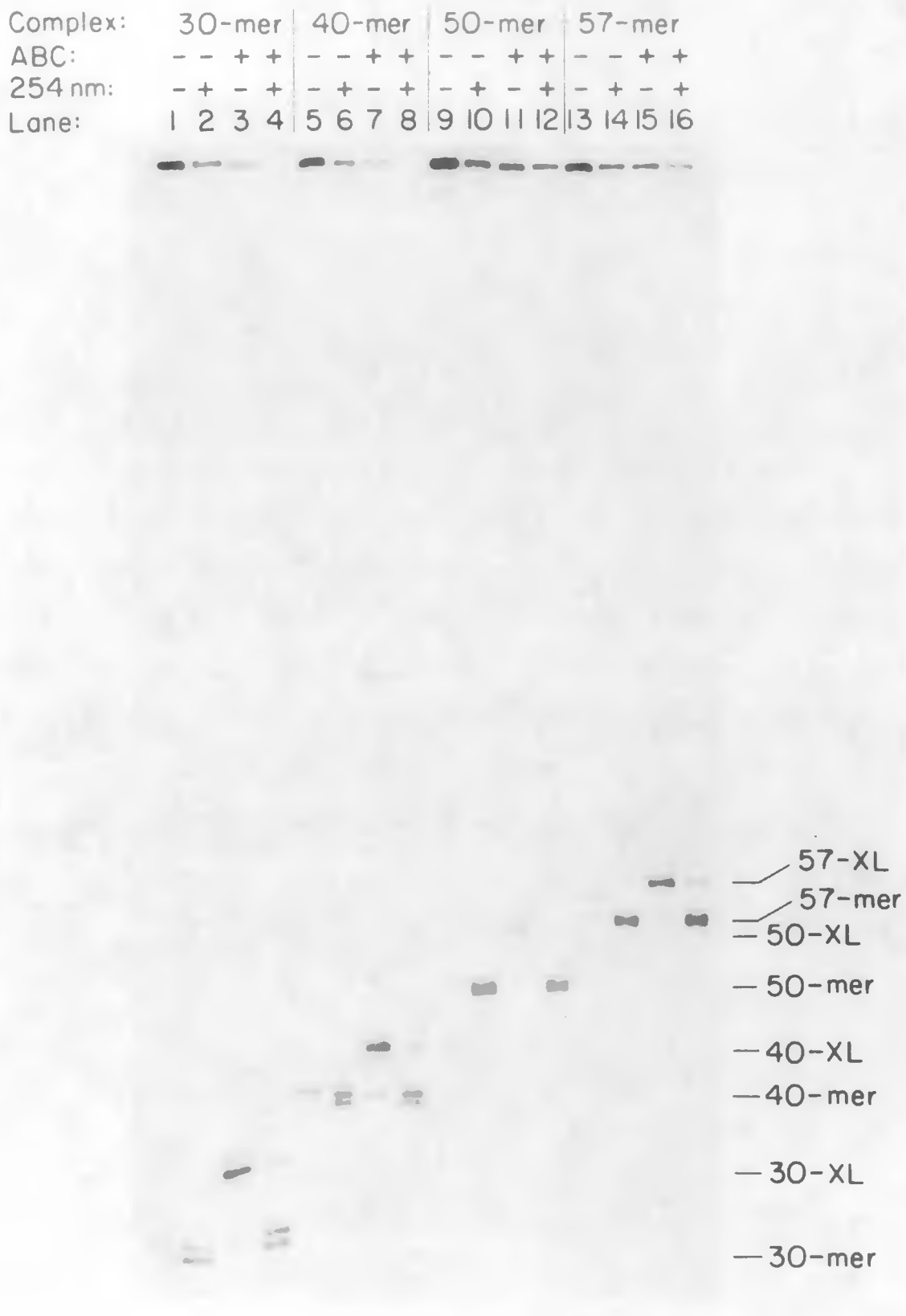

(a)

XBB903-2454

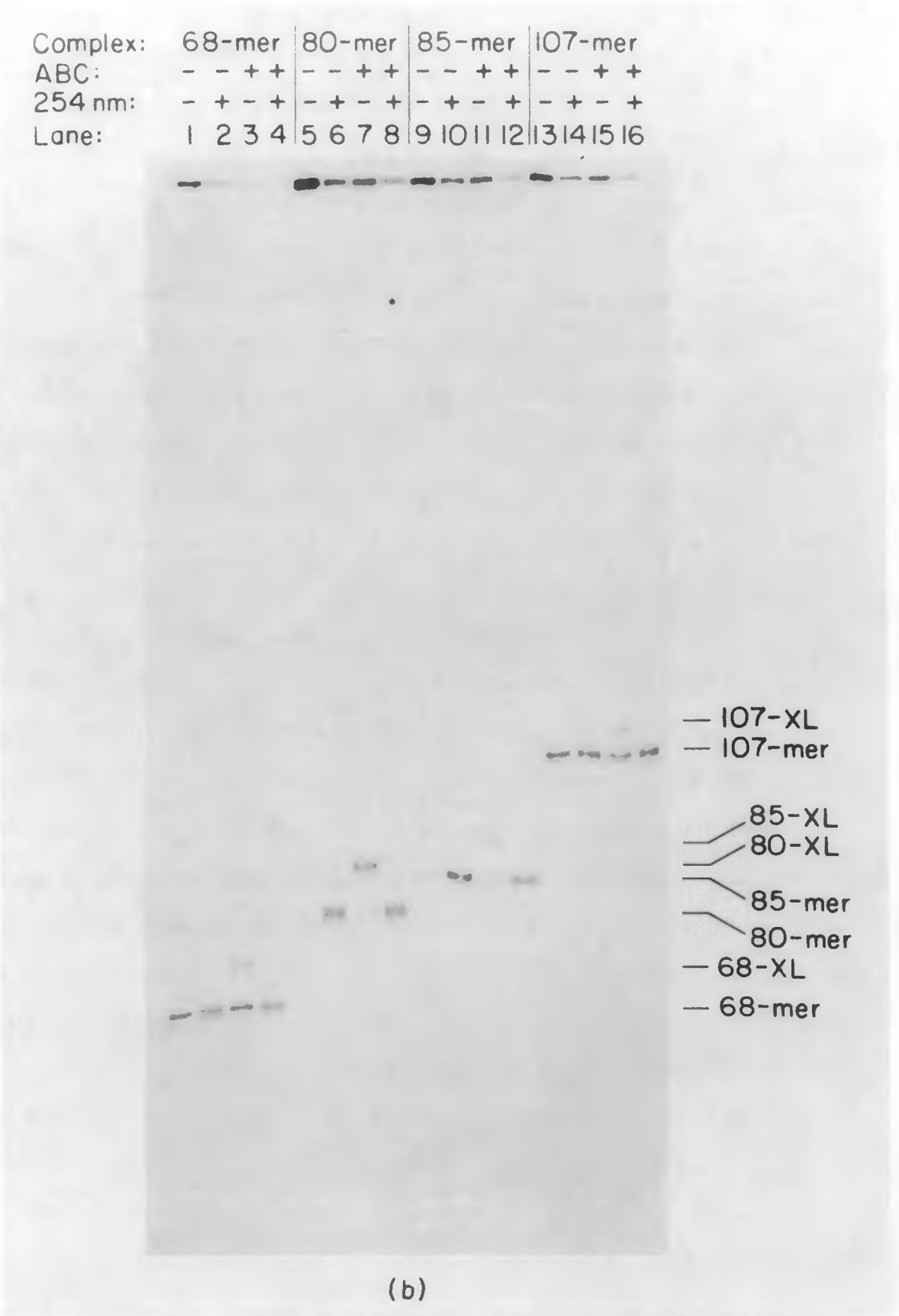

(b)

XBB903-2455

triphosphate (3′-dATP). As seen in Figure 3-4, the two major products which were obtained migrated as an 12- and a 14-mer. Since cordycepin had been added onto the 3′ ends, these corresponded to 11- and 13-base incision products. Sequence analysis by the methods of Maxam and Gilbert [1980] identified the 12-mer band in Figure 3-4 as the product of incisions at the 8th phosphodiester bond on the 5′ side of the crosslink and the 5th bond on the 3′ side, as had been previously observed in linear substrates [Van Houten *et al.*, 1986a]. Similarly, the longer fragment seen in Figure 3-4 was identified as the same 12-base incision product containing an HMT-monoadducted thymidine from photoreversal of the crosslink (data not shown). The faint 11-mer band visible in Figure 3-4 may have resulted from incision at the fourth rather than the fifth phosphodiester bond on the 3′ side of the crosslink. Stagger of the 3′ side incisions has been observed previously [reviewed by Sancar and Sancar, 1988].

Completion of crosslink repair — To completely repair the crosslink, DNA polymerase I, DNA ligase, helicase II, and deoxyribonucleoside triphosphates were added to the post-incision excinuclease·DNA complex (see Figure 3-5). To label the repair patch, [α-^{32}P]dCTP was included. Helicase II has since been found unnecessary for *in vitro* completion of repair [Van Houten *et al.*, 1988]. Repair by (A)BC excinuclease removes the crosslink between the thymidines within the KpnI recognition sequence, thus reactivating this restriction site [Gamper *et al.*, 1984; Van Houten *et al.*, 1988]. This provides a straightforward assay for successful crosslink repair: digestion of pUC19 with PvuII releases a 322-basepair fragment containing the polylinker region. Following repair of the crosslink, a PvuII/KpnI double digest should yield a unique pair of fragments, 100 and 218 basepairs in length. The results of such an assay are presented in Figure 3-6. In principle, the relative intensities of the KpnI bands should reflect the size of the repair patch generated by DNA polymerase I. Quantitative interpretation was, however, complicated by side reactions. Nick-translation or extension off the 3′ end of the cross-linked oligomer by polymerase was suggested by the observed incorporation of the [α-

Figure 3-4. Analysis of fragments excised by (A)BC excinuclease from three-stranded complexes containing either the 30-, 57-, 68-, or 85-mer. Crosslinked excision products recovered from gels such as those in Figure 3-3 were irradiated to photoreverse the crosslinks, then 3′-end-labeled with [α-^{32}P]-cordycepin 5′-triphosphate (discussed under 'Methods'). Shown here is the lower portion of the 20% denaturing PAGE gel that was used to isolate the fragments. Lane 2 contains oligomeric size markers which were 5′-end-labeled using T4 polynucleotide kinase. In lane 1, two excision fragment bands were observed, migrating as 11- and 13-base fragments that have been lengthened by cordycepin (3′-dATP). Sequencing analysis revealed that these product bands were un-modified and HMT-monoadducted 12-mer resulting from incisions of the pyrone-side strand at the eighth phosphodiester bond on the 5′ side of the crosslink and the fifth bond on the 3′ side. The upper portion of the gel contained the originally monoadducted oligo-nucleotides.

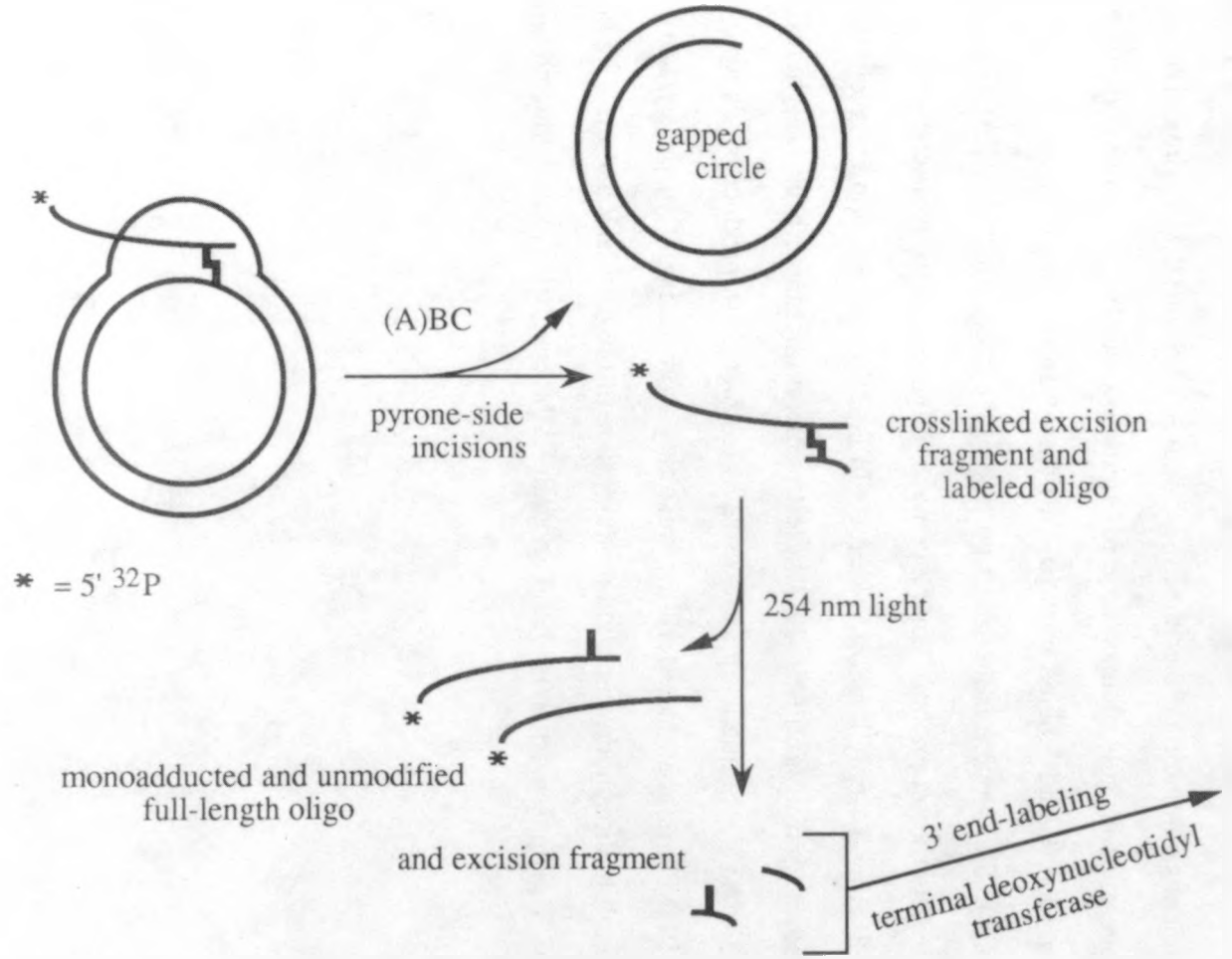
gapped
circle
(A)BC
pyrone-side
incisions
crosslinked excision
fragment and
labeled oligo
* = 5' 32P
254 nm light
monoadducted and unmodified
full-length oligo
and excision fragment
3' end-labeling
terminal deoxynucleotidyl
transferase

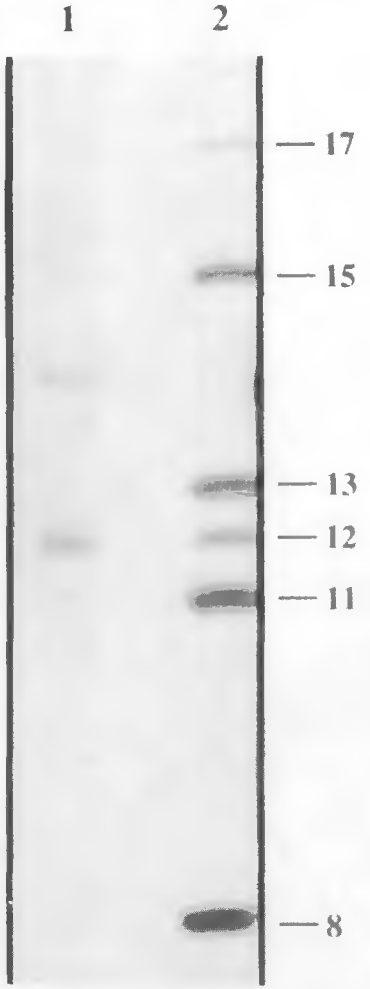
1
2
17
15
13
12
11
8

XBB903-2447

Figure 3-5. Assay to detect complete repair of the crosslinked three-stranded complexes. Following the incision reaction with (A)BC excinuclease, pol I is added to fill in the gap. The repair patch is labeled by including [α-^{32}P]dCTP in the reaction mixture. Samples are then assayed for their sensitivity to KpnI digestion. If the crosslink has been removed and the gap correctly filled, the KpnI restriction site within the polylinker region of pUC19 will be restored. To focus upon the polylinker region for analysis, reaction samples are additionally digested with PvuII restriction endonuclease. The sizes of the DNA fragments of interest are thus reduced from 2686 to 322 basepairs or less.

Figure 3-5. Assay for complete repair of the crosslinked substrate

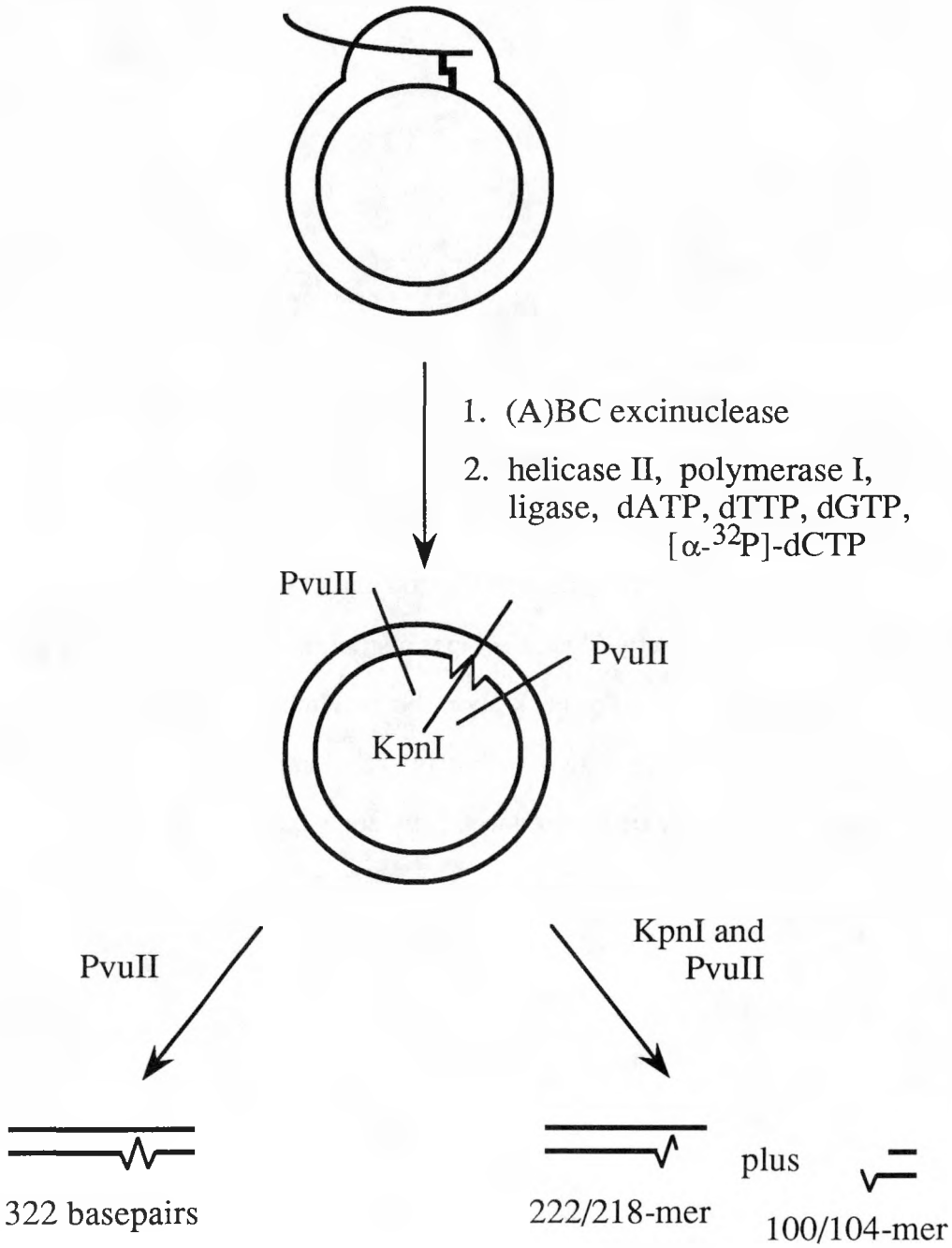

Figure 3-6. Native 8% acrylamide gel demonstrating complete crosslink repair. Beginning on the left, the first lane contains a 137-basepair marker; the faint secondary band is due to partially single-stranded material. The next four sets of three lanes are of samples treated to effect crosslink repair and then digested by the restriction enzymes indicated at the top. The first set is of three-stranded complexes containing crosslinked 30-mer, and the second is of complexes with crosslinked 80-mer. The third set of three lanes shows the positive control, replicative form M13mp19 DNA containing a site-specific psoralen monoadduct [Kodadek and Gamper, 1988; Van Houten *et al.*, 1988]. The final three lanes show the results of adding the accessory enzymes and dNTP's to the 30-mer complex in the absence of (A)BC excinuclease. The ^{32}P label comes from [α-^{32}P]dCTP incorporated by pol I during the repair reaction, as described in Figure 3-5.

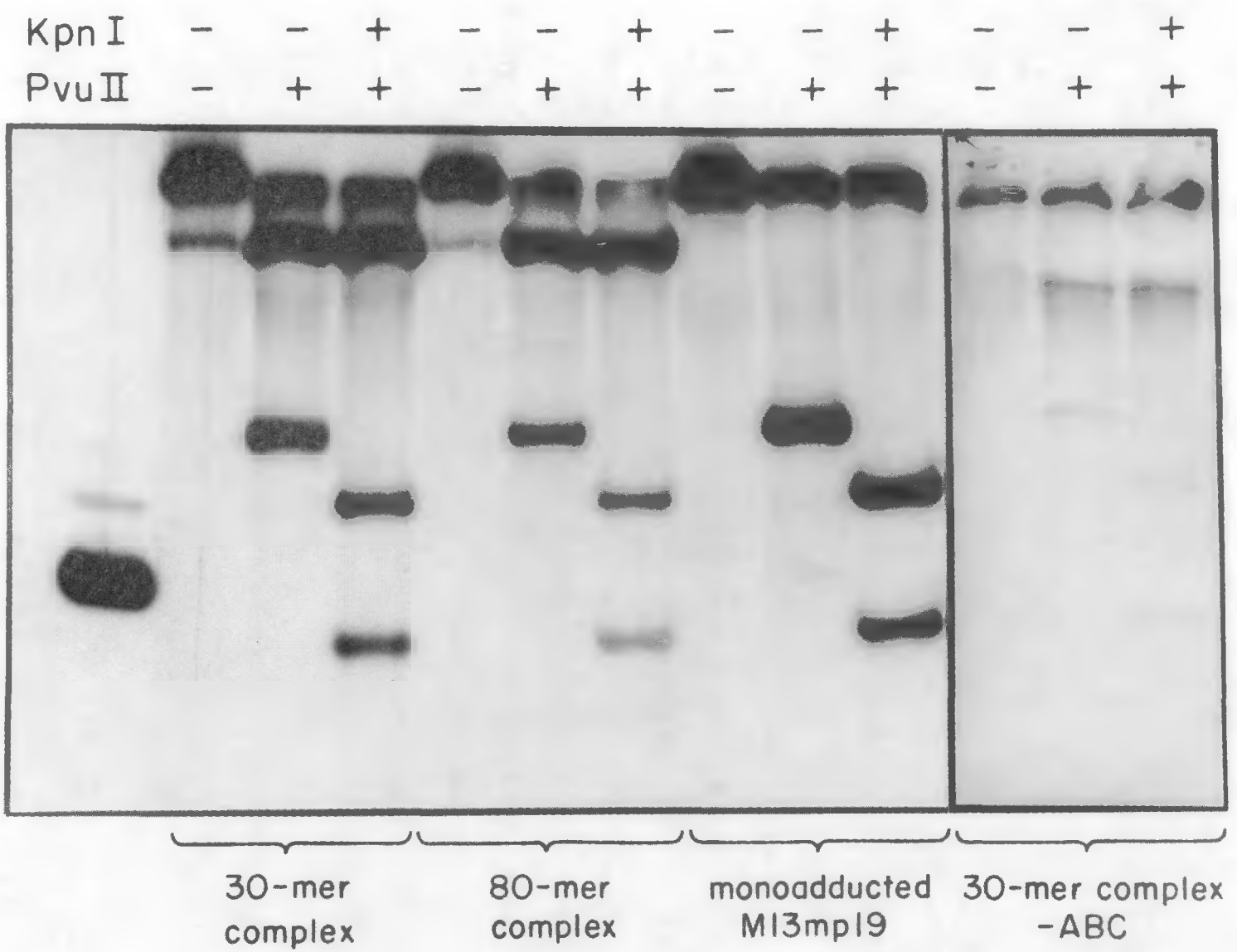
KpnI
PvuII
30-mer complex
80-mer complex
monoadducted M13mp19
30-mer complex -ABC

XBB903-2448

^{32}P]dCTP into the 30-mer sample despite the absence of (A)BC excinuclease. (A)BC excinuclease-mediated repair of UV-induced lesions elsewhere in pUC19 would also lead to incorporation of label that would not be associated with crosslink repair. Control digestions of untreated stock pUC19 did indicate that such lesions were present (data not shown).

Summary — Both the post-recombination incision step and completion of repair as described in the model for crosslink repair (Figure 3-1) proposed by Van Houten and colleagues [1986b] were tested using the three-stranded complexes prepared through RecA-catalyzed homologous pairing and psoralen photochemistry (Chapter 2). The results were consistent with the model's predictions that (A)BC excinuclease will recognize an HMT-crosslinked three-stranded complex and specifically incise the pyrone-side modified strand to release the crosslinked fragment. This reaction was insensitive to the length of the furan-side strand between 30 and 107 bases. A preliminary effort to digest three-stranded complexes in the absence of phenol-extractions to remove RecA indicated that (A)BC excinuclease will also act on complexes in the presence of RecA (data not shown; further study described in Chapter 4). Once the second set of incisions has been made, DNA polymerase and ligase are able to effect complete error-free repair of the crosslink site.

The results of Jones and Yeung [1988 and 1990] suggest that for psoralens lacking a 4′ substituent, the initial incisions may occur on either strand, whereas for HMT the furan-side strand is recognized first. In either case, a three-stranded substrate may be required before the excinuclease will make the necessary second set of incisions. To incise the original duplex twice without replacing the excised fragments would introduce a double-stranded break.

The first step and the last two steps of the model shown in Figure 3-1 have thus been carried out successfully *in vitro*, in work by Van Houten and associates [Van Houten

et al., 1986a and 1986b] and as described here. Remaining unanswered are questions of how RecA or other recombination proteins would actually interact with (A)BC excinuclease and a substrate undergoing crosslink repair. RecA has been observed to bind preferentially to UV-damaged DNA [Lu and Echols, 1987] and HMT-crosslinked DNA [Y.-B. Shi, unpublished observations]. Psoralen crosslinks are apparently more effective than monoadducts in inducing λ phage-prophage recombination under conditions which block replication of the damaged DNA [Cassuto *et al.*, 1977]. This induction is characterized by a requirement for the RecA protein and *uvr*-mediated excision repair (active (A)BC excinuclease) [Lin *et al.*, 1977].

Chapter 4

Toward *in Vitro* Crosslink Repair

Introduction

As described in the previous chapter, one mechanism for error-free crosslink repair in *Escherichia coli* consists of sequential incision and recombination events (Figure 3-1). Individual steps in this mechanism have been successfully modeled *in vitro* using well-defined psoralen-modified substrates. (i) (A)BC excinuclease preferentially incises an HMT-crosslinked duplex on the furan-side strand [Van Houten *et al.*, 1986a and 1986b]. This constitutes the first incision event. (ii) Three-stranded crosslinked complexes in which the furan-side strand is less than 110 bases long are preferentially incised on the pyrone-side strand [Cheng *et al.*, 1988a]. This is analogous to the post-recombination incision event. (iii) Incision gaps can be filled in by DNA polymerase I and ligase using the undamaged complementary strand as a template, thus completing the repair process [Cheng *et al.*, 1988a; Van Houten *et al.*, 1988]. Helicase II (UvrD) is not required, but does appear to facilitate strand synthesis and the dissociation of the post-incision nucleo-protein complex [Van Houten *et al.*, 1988].

A natural follow-up question was whether this complete crosslink repair process could be effected *in vitro* using purified proteins. The key transitions not yet characterized concerned the interaction of recombination proteins such as RecA with (A)BC exci-nuclease and the damaged DNA. Recombinational bypass of pyrimidine dimers [Livneh and Lehman, 1982] and mismatches and insertions [Bianchi and Radding, 1983] has been previously observed. We therefore embarked on a series of experiments to investigate (i) whether RecA would recognize an incised crosslinked duplex in the presence of (A)BC excinuclease and specifically catalyze homologous recombination at the incision gap, and (ii) whether (A)BC excinuclease would recognize the three-stranded post-recombination complex in the presence of RecA and specifically incise the remaining strand of the crosslink.

Sladek and coworkers [1989b] recently reported important findings regarding the requirements for efficient RecA-mediated strand exchange using an incised crosslinked

duplex. First, a single-stranded circle crosslinked to a complementary 19-mer was used to demonstrate that the presence of the psoralen-crosslinked oligonucleotide would not block RecA-mediated strand exchange with a linear duplex. Secondly, a crosslinked circular duplex containing one nick on each side of the adduct was designed to model the product of (A)BC excinuclease's first pair of incisions. The two nicks in this substrate were found to be insufficient to activate the substrate for strand exchange. Initiation of RecA-mediated recombination required extension of the nicked region to form a ssDNA gap. The 5′→3′ exonuclease activity of pol I was capable of generating this gap, and since the polymerase would be present *in vivo*, this may be the role of its exonuclease activity. Furthermore, the proximity of the furan-side end of the psoralen (HMT) to the nick on the 3′ side apparently precluded synthesis off the 3′-OH terminus of the crosslinked oligomer.

Cole and coworkers had previously postulated the need for generating a single-stranded region for RecA [Cole, 1973], and had observed a requirement for the pol I exonuclease activity in crosslink repair [Cole *et al.*, 1976]. Pol I was thought to make the incision 3′ to the crosslink [Cole *et al.*, 1976], an incision now known to be made by (A)BC excinuclease [Sancar and Rupp, 1983]. Pol I does stimulate the turnover of (A)BC excinuclease *in vitro* [Husain *et al.*, 1985], and is able to displace the excised oligomer during repair synthesis [Van Houten *et al.*, 1988]. A recent explanation for the excision repair deficiency noted in *polA*ex1 mutants is that the mutant polymerase, a temperature-sensitive 5′→3′ exonuclease, is unable to convert excision gaps to ligatable nicks [Wahl *et al.*, 1983]. The 5′→3′ exonuclease activity of pol I may therefore be needed for nick-translation and complete gap closure during repair synthesis if the DNA lesion involves only one strand, and for generation of a gap to initiate recombinational repair if both strands are involved. Initiation of RecA-mediated strand exchange from a single-stranded gap is also believed to occur in post-replication repair [West *et al.*, 1982a]. In this case, the gap is created when polymerase is blocked by a lesion, dissociates, and begins replication anew further downstream.

Combining nucleotide excision repair and homologous recombination to remove crosslink damage in an error-free manner represents just one possible cellular response. Other pathways are particularly important when the absence of a homologous duplex precludes recombinational repair. As noted in Chapter 1, psoralen damage typically induces base substitutions or deletion of the adducted thymidine. The mechanisms responsible for generating these mutations remain unclear, although SOS-induction appears to be involved [Saffran and Cantor, 1984a and 1984b; Zhen *et al.*, 1986; reviewed by Saffran, 1988].

Recent evidence suggests that (A)BC excinuclease-incised crosslinks are key intermediates in psoralen-induced mutagenesis. Yatagai and coworkers [1987] noted that the spectrum of mutations induced by psoralen lesions in a *uvr*$^+$ strain differed from that in a *uvrB*$^-$ strain. Furthermore, the types of mutations observed in the *uvrB*$^-$ strain did not include mutations characteristic of psoralen crosslink formation. Their results indicated that crosslinks contribute to mutagenesis only in *uvr*$^+$ strains, thus linking excision repair of crosslinks with mutagenesis. More recently, Sladek and colleagues [1989a] concluded that the product of (A)BC excinuclease incisions is an intermediate in both crosslink-induced homologous recombination (mentioned at the end of Chapter 3) and crosslink-induced mutagenesis. In the presence of a homologous chromosomal gene, psoralen-induced mutations in a plasmid were reduced to background levels in *E. coli*, indicating that recombinational repair competed with mutagenic processes. In the absence of homologous recombination, mutations were either large (kilobases) deletions in uninduced cells, or point mutations in cells with the SOS system constitutively induced. The large deletions were thought to reflect a cellular mechanism for saving the gapped strand in the absence of either recombination to fill the excision gap or SOS mutagenesis to bypass the crosslinked oligonucleotide that remained.

Uvr-independent crosslink repair (survival of *uvr*$^-$ cells) has also been observed. One proposed explanation for this relatively rare phenomenon is that cells possess a

glycosylase which is able to recognize and excise psoralen-adducted thymines [reviewed by Smith, 1988]. The resulting apyrimidinic sites might be further repaired by AP endonucleases, or they might lead to mutagenic replication. Such a mechanism is proposed for the removal of pyrimidine dimers by "UV endonucleases" from *Micrococcus luteus* and bacteriophage T4 [Grafstrom, 1986]. In general, glycosylases are fairly specific in target recognition [reviewed by Friedberg, 1985; Smith, 1988]. A glycosylase activity that targets psoralen damage has yet to be identified, although at least one effort has been made [Sladek, 1988].

Alternatively, *uvr*-independent cell survival may depend on mutagenic replicative bypass. Replication typically terminates directly opposite or near a site of DNA damage, but occasionally the polymerase is able to continue strand synthesis despite the presence of damage. *In vitro* [Piette and Hearst, 1983] and *in vivo* (yeast) bypass of psoralen monoadducts have been observed [reviewed by Moustacchi, 1988]. *E. coli* possesses DNA polymerases I, II, and III. Each is capable of carrying out repair synthesis to fill in excision gaps, and pol I and pol III both contribute to the excision of pyrimidine dimers [reviewed by Friedberg, 1985]. All three enzymes have also been reported to possess a limited ability to bypass certain lesions.

Pol I, present at about 400 molecules per cell, is believed to play a key role in both short and long patch repair synthesis. Mutants in the *polA* gene are particularly sensitive to UV radiation [reviewed by Friedberg, 1985]. The fidelity of pol I can be altered *in vitro* by substitution of Mn^{2+} for Mg^{2+} and by deoxynucleoside monophosphates. These conditions reduce the error discrimination of the 3′→5′ editing exonuclease and also the specificity of nucleotide incorporation [Boiteux and Laval, 1982; El-Deiry *et al.*, 1988; Larson and Strauss, 1987; Rabkin *et al.*, 1983]. Under these conditions, the altered pol I shows some ability to replicate past apyrimidinic sites [Boiteux and Laval, 1982] and UV radiation-induced lesions [Larson and Strauss, 1987; Rabkin *et al.*, 1983]. More recently, bypass of *cis-syn* thymine dimers was observed under standard conditions for *in vitro*

replication. The rate of bypass depended upon the dNTP and pol I concentrations [Taylor and O'Day, 1990]. A recent study of the parameters affecting replicative bypass of thymine glycol lesions by pol I implicated sequence context, the length of the template beyond the lesion, and absence of 3′→5′ exonuclease activity [Clark and Beardsley, 1989]. Inclusion of RecA was observed to have only a minor effect on the ability of pol I to bypass UV radiation-induced damage *in vitro*; SSB had no effect [Larson and Strauss, 1987]. Pol I also has a limited ability to bypass apurinic sites *in vitro* [Schaaper *et al.*, 1983]. An SOS-inducible form, pol I*, has also been isolated [Lackey *et al.*, 1982]. Pol I* is comparable to pol I in its 5′→3′ and 3′→5′ exonuclease activities, but has a characteristically higher error frequency that has been attributed to reduced specificity of nucleotide incorporation. Pol I* does not appear to be a product of RecA-mediated cleavage of pol I [Lackey *et al.*, 1985]. The role of this protein remains to be clarified; no further characterization has been reported.

Bonner and coworkers reported purification of an SOS-inducible polymerase (pol X) from an *E. coli* strain lacking the *polA* gene (pol I). Pol X was able to insert nucleotides opposite abasic sites and then continue strand synthesis much more efficiently than pol III. This initial study suggested that this polymerase might in fact be pol II [Bonner *et al.*, 1988]. Pol II, present at about 40 molecules per cell, has no 5′→3′ exonuclease activity [reviewed by Friedberg, 1985]. The ability of pol II to initiate synthesis from the excision gap left by (A)BC excinuclease is not known.

Pol III, present at about 10 molecules per cell [reviewed by Friedberg, 1985], is believed to participate in the UmuC/D pathway for SOS mutagenesis (see Chapter 1). UmuC has been implicated in enabling *uvr*⁻ cells to survive psoralen damage [reviewed by Moustacchi, 1988]. Of the ten or so subunits comprising pol III holoenzyme, two in particular have been implicated in replicative bypass. The ε subunit (3′→5′ exonuclease associated with editing) and the β subunit dimer (associated with initiation of replication and processivity) appear to modulate the ability of the polymerase to bypass apurinic and

UV radiation-induced cyclobutane pyrimidine dimers. An efficiency of 10-20% has been observed [reviewed by Shavitt and Livneh, 1989]. The RecA and UmuC/D proteins have been found to interact functionally with pol III, specifically inhibiting the proofreading subunit and thus reducing the fidelity of replication [Foster and Sullivan, 1988; Lu *et al.*, 1986]. Bypass efficiency, however, may not be primarily determined by the interactions which affect the fidelity of pol III. Rather, termination at dimer lesions appears to result from formation of relatively unstable initiation-like complexes [Shwartz and Livneh, 1987; reviewed by Shwartz *et al.*, 1988a]. The efficiency of replicative bypass by pol III may therefore be primarily a function of processivity mediated by the β subunit [Shavitt and Livneh, 1989], although it may be enhanced by the inhibition of the ε subunit [Shwartz *et al.*, 1988b].

This chapter summarizes various approaches taken toward the goal of reconstituting crosslink repair *in vitro*. We focused on the fate of a well-defined substrate, a site-specifically HMT-crosslinked circular M13mp19 duplex. We sought first to characterize the pattern of incisions made by (A)BC excinuclease in this crosslinked substrate, and then to understand how RecA-mediated recombination might proceed to enable complete repair of the crosslinked site. In the course of our studies, we examined the possibility of replicative bypass of incised crosslinks by pol I.

Since the post-recombination complex has not been defined in detail, it was possible that a "transiently" positioned third strand at the crosslinked site would be sufficient to induce (A)BC excinuclease to make its second pair of incisions. Sladek and coworkers did observe a significant population of intermediates resulting from strand exchange reactions with gapped crosslinked duplexes. They suggested that these intermediates might have a mechanistic role in the repair process [Sladek *et al.*, 1989b]. We investigated this possibility by testing the ability of an oligonucleotide to serve as a "transient" third strand and thus induce pyrone-side incisions of the crosslink.

Materials and Methods

Proteins and DNA — Bacterial alkaline phosphatase (BAP), BSA, and all restriction enzymes except KpnI were purchased from Bethesda Research Laboratories (BRL). KpnI and T4 polynucleotide kinase were from New England Biolabs. RecA was obtained from Pharmacia, and DNA ligases (T4 and *E. coli*) and *E. coli* DNA polymerase I were from Boehringer Mannheim Biochemicals (BMB). Klenow fragment was purchased from United States Biochemical (USB). T4 gp43 was a gift of B. Alberts, University of California at San Francisco. *E. coli* DNA photolyase, UvrA, UvrB, and UvrC were gifts of A. Sancar, and helicase II (UvrD) was a gift of S. Matson, both at the University of North Carolina at Chapel Hill. Rabbit muscle creatine phosphokinase (CPK) was purchased from Sigma.

DNA oligonucleotides were prepared as described in Chapter 2, using either unmodified or monoadducted 13-mer. Site-specifically HMT-monoadducted M13mp19, prepared using the primer extension method of Kodadek and Gamper [1988], was a gift of I. Husain and A. Sancar, University of North Carolina at Chapel Hill. RF M13mp19 plasmid was purchased from BMB, and single-stranded (+) circular M13mp19 from BRL. Plasmids pUC19 and pBR322 and modified (α-thio) deoxynucleoside triphosphates (αS-dNTP's) were obtained from Pharmacia. [α-^{32}P]dCTP and dATP were from Amersham.

Preparation of crosslinked covalently closed M13mp19 — Site-specifically HMT-monoadducted M13mp19 was purified on a nondenaturing 1% agarose gel in TANE buffer (see Chapter 2) containing 1 μg/mL ethidium bromide. Aliquots of 1 μg in 40 μL were converted to crosslinked M13mp19 using a 3-minute irradiation at room temperature (23-25°C) with 320-380 nm light at approximately 125-150 mW/cm^2 (see Chapter 2). Neither the monoadducted nor the crosslinked molecules were supercoiled. (Figure 4-1)

Transformations — One of two variations of a general procedure was used, depending upon whether the experiment was done in the lab of Prof. A. Sancar at the University of North Carolina at Chapel Hill, or in Berkeley.

In Chapel Hill, competent CSR603 cells (*recA⁻uvrA⁻phr⁻*) and JM103 cells were a gift of the Sancar lab. Competent cells (0.5 mL) were mixed with 50-μL aliquots of DNA (20-25 ng M13) and incubated on ice for 40 minutes. The cells were incubated for 2 minutes at 42°C and then left to grow at 37°C in 2 mL of Luria broth (Gibco). Meanwhile, 10 mL of YT medium (4 g. Bacto tryptone, 2.5 g. Bacto yeast extract (both from Gibco), and 2.5 g. NaCl per 500 mL) were inoculated with JM103 cells and incubated at 37°C until $A_{550} = 0.3$, approximately 2 hours. Serial dilutions of the CSR603 cells were made with pH 7.4 phosphate buffer saline (1.5 mM KH_2PO_4, 6.5 mM Na_2HPO_4, 137 mM NaCl, 2.7 mM KCl). IPTG to 0.7mM and X-gal to 0.7% (both from BRL) were added to YT soft agar (YT medium with 0.6% agar). To 3 mL of this soft agar solution, 0.1 mL of diluted CSR603 and 0.3 mL of JM103 cells were added. The entire mixture was then poured into a petri dish. After 30 minutes at room temperature, the plates were inverted and incubated at 37°C overnight. Colonies were counted using a New Brunswick Scientific Model C-110 Counter.

In Berkeley, 5–10-μL aliquots (1-5 ng DNA or water) were added to 50–100-μL aliquots of competent HB101 cells. Cells were grown as described above. For each sample, 3.3 mL of LC (10 g. tryptone and 5 g. each of yeast extract and NaCl per 1 L) soft agar, 0.3 mL of JM103 cells, 50 μL of 2% X-gal in *N,N*-dimethylformamide, 10 μL of 0.1 M IPTG, and the HB101 cells were combined and poured into petri dishes. All cells were gifts of M. Alberti, Hearst lab. Colonies were counted after an overnight incubation at 37°C.

Photolyase treatment — Photolyase buffer consisted of 50 mM Tris·Cl (pH 7.4 at 25°C), 50 mM NaCl, 1 mM EDTA, 5 mM DTT, and 50 μg/mL BSA. The enzyme was freshly diluted on ice with 50 mM Tris·Cl, 50 mM NaCl, 1 mM EDTA, 10 mM DTT, and 50% glycerol. Each 100-μL reaction contained 200 ng crosslinked M13mp19 and 150 ng photolyase (54 kilodaltons), an estimated 20:1 enzyme to dimer ratio if five dimers per plasmid were assumed. Samples were irradiated for 15-17.5 minutes at room temperature

with 365 nm light at 0.5 mW/cm^2. The DNA was then deproteinized with two phenol and two diethyl ether extractions, ethanol-precipitated, and resuspended in 5 mM Tris·Cl (pH 7.5 at 25°C) and 0.5 mM EDTA.

Analysis of incision and repair synthesis with crosslinked M13mp19 — (A)BC excinuclease reactions were carried out as described in Chapter 3, with 180 μg/mL BSA in 40 μL. DNA pol I (1 unit) and dNTP's were then added to the post-incision complex, with or without either ligase (0.5 unit *E. coli* enzyme with 1.5 mM NAD (from Sigma) or 1 unit T4 ligase) or helicase II (0.5 pmol). Repair patches were labeled by including [α-^{32}P]dCTP. Samples were deproteinized by two phenol extractions, ethanol-precipitated twice, then resuspended in 19 μL REact4 (BRL) buffer with 100 μg/mL BSA. Each sample was digested with HindIII and PvuII, 5 units each, for 1-2 hours at 37°C. SDS to 0.4%, EDTA to 4 mM, and 5x dyes in glycerol were then added. Digests were loaded directly onto a 1.2 mm thick native 8% polyacrylamide (19:1 acrylamide:bis) gel to separate the restriction fragments. Since the polylinker region of interest was contained within the 139/143-mer restriction fragment, the band containing the 139/143-mer duplex from each reaction was excised. The DNA was recovered by electroelution (Schleicher & Schuell Elutrap apparatus) and ethanol-precipitated.

Our first thought was to either label all of the repair patches with trace [α-^{32}P]-dCTP or to fully label certain samples for use as gel standards. Each strand of the isolated restriction fragment could then be dephosphorylated and kinased, and sequenced using the techniques of Maxam and Gilbert [1980]. Initially, we observed a pattern of polymerase pauses that appeared to correspond to the pattern of C's within each strand, eliminating the need for the corresponding sequencing reaction. We then learned that dCTP is a particularly poor substrate for the polymerase, so radioactive quantities (approximately 0.1 μM) could contribute to termination at each C in the sequence and also affect the rate of polymerization (D. Cook, personal conversation). Abbotts *et al.* [1988] reported that with 0.25 nM Klenow fragment and 10 nM template, a much higher frequency of termination

occurred with 0.1 μM levels of each dNTP than with 1.0 μM. We therefore raised the total concentration of dCTP by including two aliquots of 0.5 μM unlabeled triphosphate each. Higher levels did enhance polymerization, but also reduced the total signal since the label was being diluted. The remaining three triphosphates were at 25 μM. We also extended the reaction time and compared [α-^{32}P]dATP with [α-^{32}P]dCTP (data not shown). Our final conclusion was that random termination also occurred, interfering with data interpretation.

Our second approach was to use the αS-dNTP sequencing method developed by Gish and Eckstein [Gish and Eckstein, 1988; Nakamaye *et al.*, 1988]. We used a slightly modified version of a procedure obtained from Sibghat-Ullah, then a member of Prof A. Sancar's lab at the University of North Carolina at Chapel Hill. Each sample was run in quadruplicate, one for each αS-dNTP. All four dNTP's in each sample were at 25 μM. If trace [α-^{32}P]dCTP was to be incorporated, the cold dCTP concentration was initially 0.5 μM for 20 minutes, then raised to 1 μM for the remaining 15 minutes of the synthesis. Samples were twice phenol-extracted, precipitated, and then digested with HindIII and PvuII and gel-purified as described above. Recovered 139/143-mer was heat-denatured at 90°C for 3 minutes and placed on ice ('heat/cooled'), then dephosphorylated in 50 μL of 25 mM Tris·Cl (pH 8.2 at 25°C) at 65°C for 1 hour, with one or two additions of 25 units BAP each. Samples were again deproteinized, precipitated, and "heat/cooled", then 5′-end-labeled in 10 μL with 3-5 units of kinase in the presence of 4.7% PEG8000 (polyethylene glycol, average molecular weight 8000) for 3-3.5 hours. Because the HindIII end (5′ overhang) was a more efficient substrate for kinase than the PvuII end (blunt), the pyrone-side strand was preferentially labeled. Dyes in formamide (10 μL) were added directly to the reactions and the mixtures were reduced to volumes of 9-12 μL in a Speed Vac. The samples were "heat/cooled" and electrophoresed on a denaturing (7M urea) 8% or 10% polyacrylamide gel to resolve the 139-mer (furan-side strand) from the 143-mer (pyrone-side). These two bands were excised, eluted, and precipitated. The pellets were

resuspended with 5-6 μL of 3% 2-iodoethanol (Sigma) in formamide/dyes, heated at 95°C for 3 minutes to promote cleavage at the αS positions and placed on ice, then electrophoresed down a second denaturing 8% gel for sequence analysis.

Preparation of labeled M13mp19 FIII — RF M13mp19 was linearized and subsequently labeled at the 3′ ends based upon a procedure from H. Gamper (now at Microprobe Corporation, Bothell, WA) and the protocol published by O'Farrell [1981]. Six different labeled linear duplexes were prepared to provide homologous ends at different locations relative to the (A)BC excinuclease incision sites. In 20 μL, 750 ng of RF M13mp19 was incubated with 5-10 units of restriction endonuclease (AvaII, EcoRI, HindIII, KpnI, PvuI, or XbaI – see Figure 4-1) and 100 μg/mL BSA in 10 mM Tris·acetate, 10 mM Mg·acetate, 65 mM K·acetate, 2 mM DTT, 0.5 mM spermine, and 0.3 mM spermidine. After 1 hour at 37°C, 380 ng of T4 gp43 was added, without dNTP's to promote the 3′→5′ exonuclease activity. Five minutes later, dATP, dGTP and dTTP to 0.17 mM each were added, with approximately 25 μCi of [α-^{32}P]dCTP. After 30 minutes, 0.17 mM unlabeled dCTP was added, and the synthesis reaction was continued for another 15 minutes. The reactions were stopped with the addition of NaCl to 80 mM and EDTA to 20 mM. Samples were phenol-extracted twice, then ethanol-precipitated twice. The DNA was isolated from unincorporated dNTP's on a nondenaturing 1% agarose gel and recovered by electroelution.

Preparation of gapped M13mp19 — Uniquely gapped M13mp19 was prepared by previously published procedures [Sladek *et al.*, 1989b; West *et al.*, 1982a], with slight modifications. The approach is outlined in Figure 4-2. RF M13mp19 (2.5 μg aliquots) was first linearized using 15 units each of KpnI and HindIII in REact4 buffer (BRL) with 100 μg/mL BSA. The two resulting fragments were separated on a nondenaturing 1% agarose gel in TBE (see Chapter 2). The longer plasmid fragment was excised and electroeluted (Schleicher & Schuell Elutrap apparatus) for 2 hours at 200 V in TBE. The DNA was then ethanol-precipitated. A mixture of KpnI/HindIII-linearized M13mp19 (5 μg) and

Figure 4-1. Schematic of M13mp19 plasmid showing location of unique HMT crosslink and various restriction sites. The HindIII/PvuII restriction fragment whose sequence is partially shown is actually a 143/139-mer duplex. Within this fragment, the furan-side monoadduct is on T_{102} from the PvuII 5′ end. This thymidine is covalently attached through the psoralen to T_{41} from the HindIII 5′ end in the crosslinked substrate. The remaining two PvuII sites on the other side of the HindIII site within the M13mp19 are not shown. AvaII, EcoRI, HindIII, KpnI, PvuI, and XbaI were each used to generate FIII substrates for strand exchange experiments. The HindIII and KpnI enzymes were used to generate the gapped M13mp19 substrate depicted in Figure 4-2. (see 'Methods')

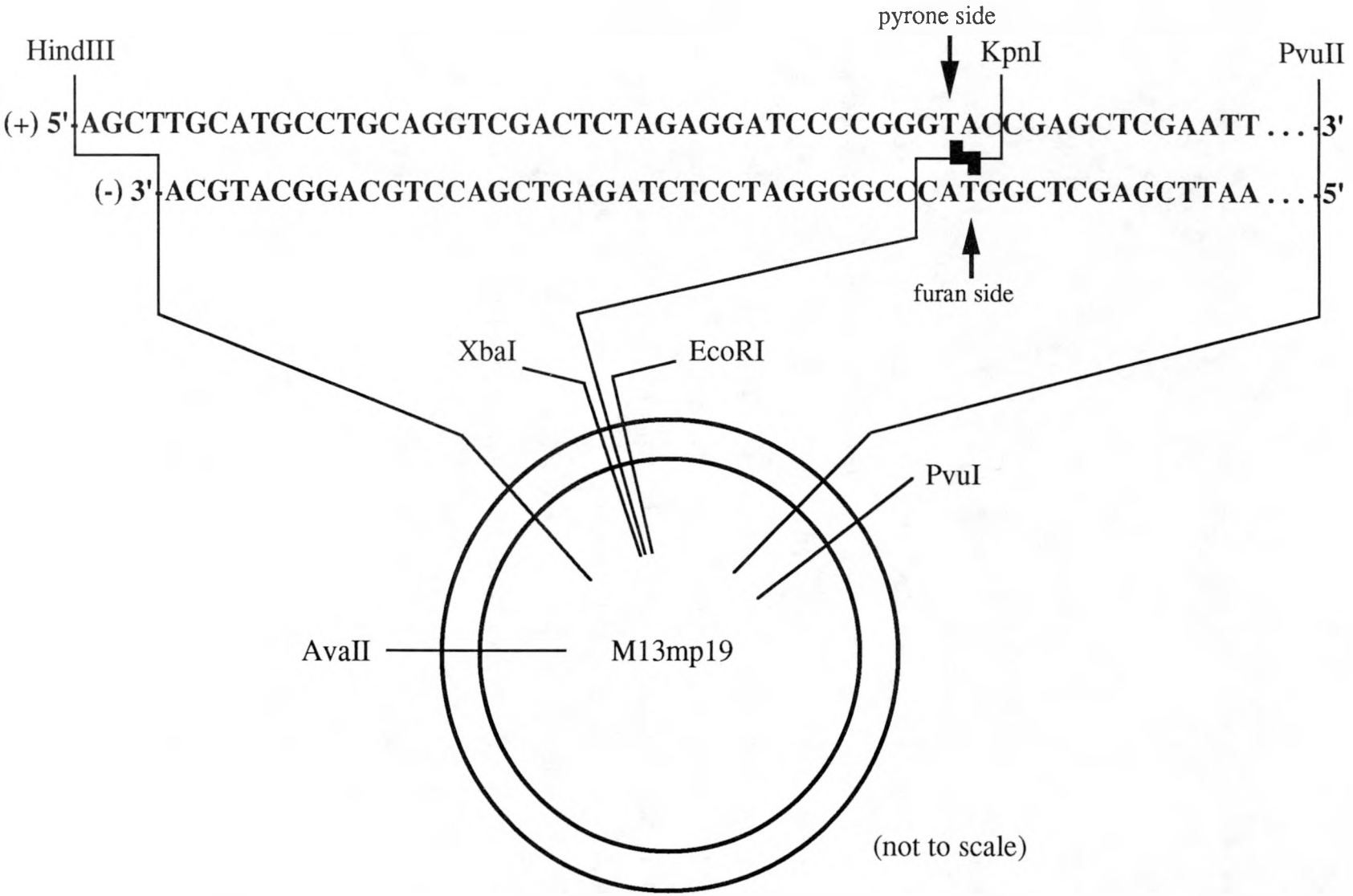
pyrone side
HindIII
KpnI
PvuII
(+) 5'-AGCTTGCATGCCTGCAGGTCGACTCTAGAGGATCCCCGGGTACCGAGCTCGAATT . . . -3'
(-) 3'-ACGTACGGACGTCCAGCTGAGATCTCCTAGGGGCCCATGGCTCGAGCTTAA . . . -5'
furan side
XbaI
EcoRI
PvuI
AvaII
M13mp19
(not to scale)

ss (+) circular M13mp19 (10 μg) was suspended in 115 μL of 50% formamide, 10 mM EDTA. (Formamide was deionized by stirring at 4°C for three hours with Bio-Rad AG501-X8 (20-50 mesh) Analytical Grade Mixed Bed Resin, 1 g. per 15-20 mL of formamide.) The DNA mixture was divided across three wells of a Health Products Microdialyzer (25-mL buffer volume, 100 μL-capacity wells) containing a membrane with a 12-14,000 dalton cutoff. The sample was first dialyzed against 98% formamide, 10 mM EDTA for 2.5 hours at room temperature. After being heated at 65-70°C for 10 minutes, the sample was dialyzed against 50% formamide, 10 mM EDTA, and 0.2 M Tris·Cl (pH 8 at 25°C) for another 2.5 hours at room temperature. Next, the sample was left overnight at 4°C to equilibrate with 0.1 M Tris·Cl (pH 8 at 4°C), 10 mM EDTA, 0.1 M NaCl. Finally, the sample was dialyzed for 3 hours at room temperature against 10 mM Tris·Cl (pH 8 at 25°C), 1 mM EDTA. The same membrane was used for all four dialysis steps, and as much as possible, the same three sample wells were used. The mixture was concentrated in a Savant Speed Vac, then purified on a nondenaturing 1% agarose gel in TBE. The DNA was recovered as before, with a final 40-50% yield of the gapped M13mp19 (35-base gap). Presumably, the yield could have been greater if a larger excess (unavailable at the time) of the ss circle had been present initially.

Four-stranded exchange reactions — We attempted to effect complete strand exchange between labeled M13mp19 FIII (preparation described above) and covalently closed circular monoadducted or crosslinked M13mp19 duplex. The modified duplex was first treated with (A)BC excinuclease and then with pol I to extend the incisions into gaps [Sladek *et al.*, 1989b]. With the knowledge that UvrA was necessary only for the initial binding of UvrB to the damaged DNA [Orren and Sancar, 1989], the order of addition of UvrC and the DNA substrate was reversed from previous experiments.

(A)BC excinuclease reactions were carried out in the buffer described in Chapter 3, in 30 μL and with 167 μg/mL BSA. UvrA and UvrB were preincubated for two minutes at 37°C prior to the addition of the damaged DNA substrate (175 ng of crosslinked or 200

Figure 4-2. Construction of specifically gapped circular M13mp19. As explained under "Methods," FI duplex M13mp19 was linearized with KpnI and HindIII and isolated from the small restriction fragment. The linear duplex was then mixed with circular (+) single-stranded M13mp19, denatured in formamide and gradually equilibrated against Tris·Cl buffers. The final product contained a 35-base gap.

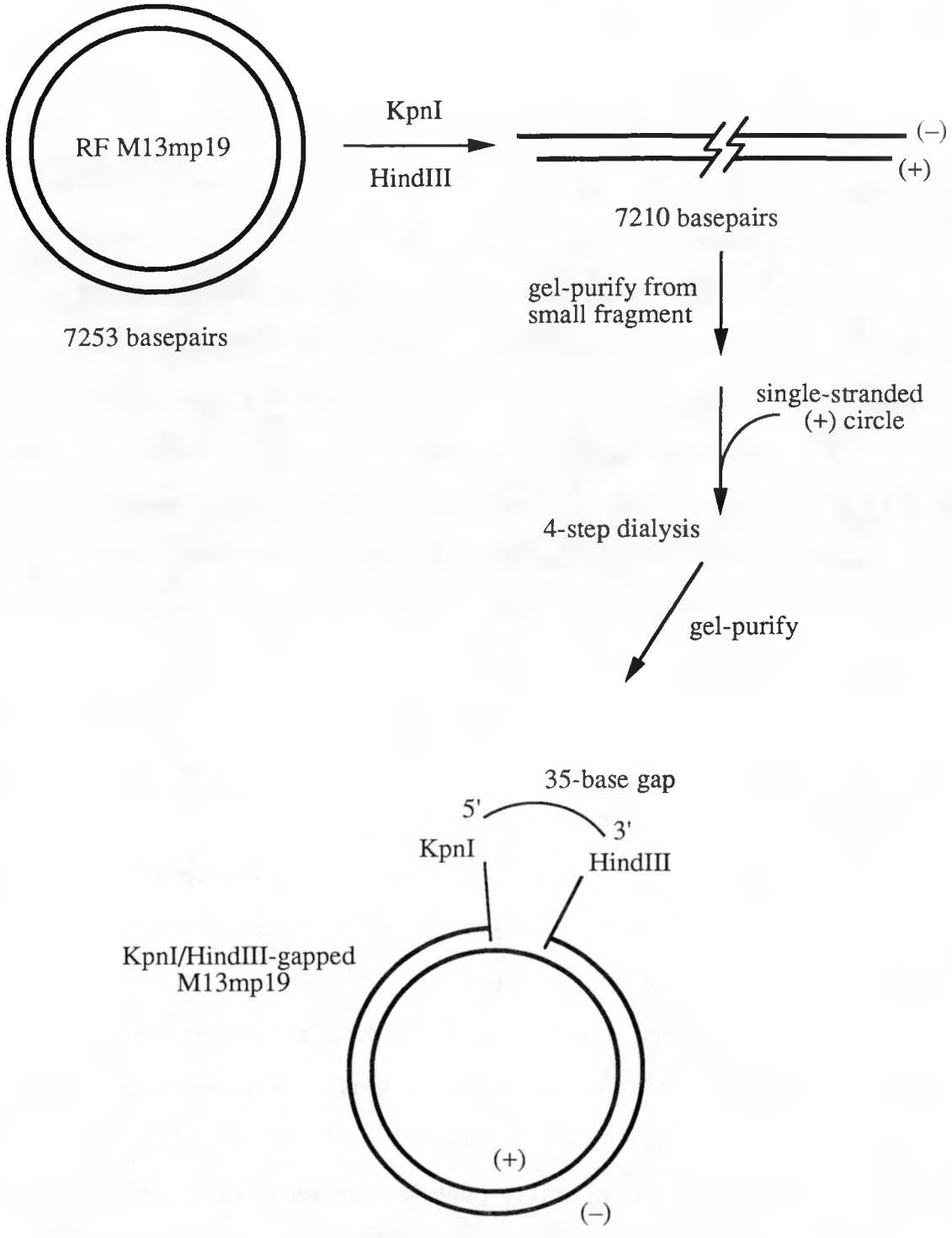
RF M13mp19
7253 basepairs
KpnI
HindIII
(–)
(+)
7210 basepairs
gel-purify from
small fragment
single-stranded
(+) circle
4-step dialysis
gel-purify
35-base gap
5'
3'
KpnI
HindIII
KpnI/HindIII-gapped
M13mp19
(+)
(–)

ng of monoadducted M13). UvrC was added after 5 minutes, and the reaction was incubated for 15 minutes. Pol I (1 unit) was then added, and the 5′→3′ exonuclease was allowed to act: for 6 minutes for samples to be reacted with the HindIII- and EcoRI-linearized M13, 8 minutes for PvuI- and 12 minutes for the AvaII-linearized substrate. Five-μL aliquots were then transferred to RecA reaction tubes. CPK (1 unit) and RecA (to 1.7 μM) and SSB (to 80 nM) were added and after a 15-minute presynapsis period, the ^{32}P-labeled FIII substrates were added. The 20-μL reactions were then incubated for 90 minutes. The final buffer concentrations (representing 0.25x (A)BC buffer added to RecA buffer) were 2.5% glycerol, 42 μg/mL BSA, 12.5 mM each Tris·Cl and Tris·acetate, 50 mM Na·acetate, 12.5 mM KCl, 2.5 mM $MgCl_2$ and 6.25 mM Mg·acetate, 3 mM CP, 2.5 mM DTT, and 2 mM ATP (concentration in absence of UvrA ATPase activity). SDS to 0.4%, EDTA to 4 mM, and dyes in glycerol were added and aliquots were analyzed on nondenaturing 1% agarose. Gels were dried at 60°C for autoradiography, as described in Chapter 2. Strand exchange between FIII and gapped M13mp19 in the presence of 20 mM Mg^{2+} [Conley and West, 1989; Hahn *et al.*, 1988] was also attempted.

Quantitation of strand exchange — Bands were excised from dried agarose gels for analysis as in Chapter 2. Samples were counted in 5 mL of Ecolume fluor (ICN Biomedicals).

Preparation of crosslinked oligomer-M13 complexes — The KpnI/HindIII-gapped M13mp19 was crosslinked to HMT-monoadducted 40- or 50-mer (as pictured in Figure 2-2b) essentially as described for pUC19 in Chapter 2. Although the gap permitted hybridization of the oligonucleotide at the crosslink site (KpnI recognition sequence) in the absence of RecA, the reaction was generally more efficient if RecA was present (data not shown). Each 20-μL reaction was 5% glycerol, 25 mM Tris·acetate (pH 7.5 at 37°C), 50 mM NaCl, either 2.5 mM ATPγS or ATP (with 5mM phosphocreatine and 0.75 units of CPK), 2 mM DTT, and initially 1 mM Mg·acetate for presynaptic association of RecA with the oligonucleotide. Each oligonucleotide substrate was freshly 5′-end-labeled with

kinase and gel-purified prior to use. RecA was at 2.5 μM, and each oligonucleotide was at 6.25 nM (concentration in molecules), corresponding to an 8:1 protein monomer to nucleotide ratio for the 50-mer. After a 10-minute presynaptic incubation at 37°C, 220 ng of gapped M13 substrate was added and the Mg^{2+} concentration was raised to 12.5 mM for synapsis. The final oligomer to plasmid ratio was 5:1. After 13-15 minutes, each sample was irradiated for 2 minutes with approximately 100 mW/cm^2 of 320-380 nm light. Plasmid was separated from unreacted oligomer on a nondenaturing 1% agarose gel. As controls, three-stranded complexes between each oligonucleotide and FI pUC19 (ss:ds at 2:1) were also formed and crosslinked. The final products are referred to as M13/40 and M13/50 (Figure 4-3) or pUC/40 and pUC/50 for simplicity.

RecA-dependent (A)BC excinuclease incisions — RecA-mediated presynapsis with unmodified 107-mer (variant of the 107-mer in Figure 2-2b) and subsequent synapsis reactions with M13/40 or M13/50 were carried out under the ATP conditions described above for the preparation of crosslinked oligomer-M13 complexes. The 107-mer (12.4 ng), CPK (0.75 units) and RecA (5.2 μg) were incubated in 20 μL. After the 10-minute presynapsis, 5-μL aliquots were removed and added to prewarmed tubes containing 5 μL (5-7000 Cerenkov cpm) M13 substrate and 1 μL of 0.115 M Mg·acetate to initiate synapsis. (A)BC reaction tubes were prepared to yield final concentrations of 50 mM Tris·Cl (pH 7.4 at 25°C), 50 mM KCl, 10 mM $MgCl_2$, 2 mM ATP, 150 μg/mL BSA, and 5 mM DTT (excluding the contributions from the RecA reaction buffer) in the final 40 μL. UvrA and UvrB were diluted in (A)BC buffer, then mixed and prewarmed in the (A)BC tubes during the final minutes of the 15-minute synapsis period. The 11-μL synapsis reactions were then added to the UvrA/UvrB mixtures. After 5 minutes, freshly diluted UvrC was added. Incision reactions were incubated for 15 minutes at 37°C. Samples were deproteinized by two phenol extractions and ethanol-precipitated. The DNA was resuspended in formamide/dyes, "heat/cooled," and analyzed on denaturing 10% polyacrylamide gels. In control reactions with the three-stranded pUC19 complexes, the RecA steps were omitted.

Figure 4-3. Formation of complexes between KpnI/HindIII-gapped M13mp19 and monoadducted oligonucleotides. This RecA-mediated reaction (see 'Methods') was essentially carried out as in Chapter 2. The same 40- and 50-mers shown in Figure 2-2(b) were used here. These oligonucleotides were homologous to the (+) strand of pUC19 and hence complementary to the (+) strand of M13mp19. The final M13/40 and M13/50 products may be compared to the three-stranded pUC19 complex pictured in Figure 2-3. None of these structures has been precisely characterized.

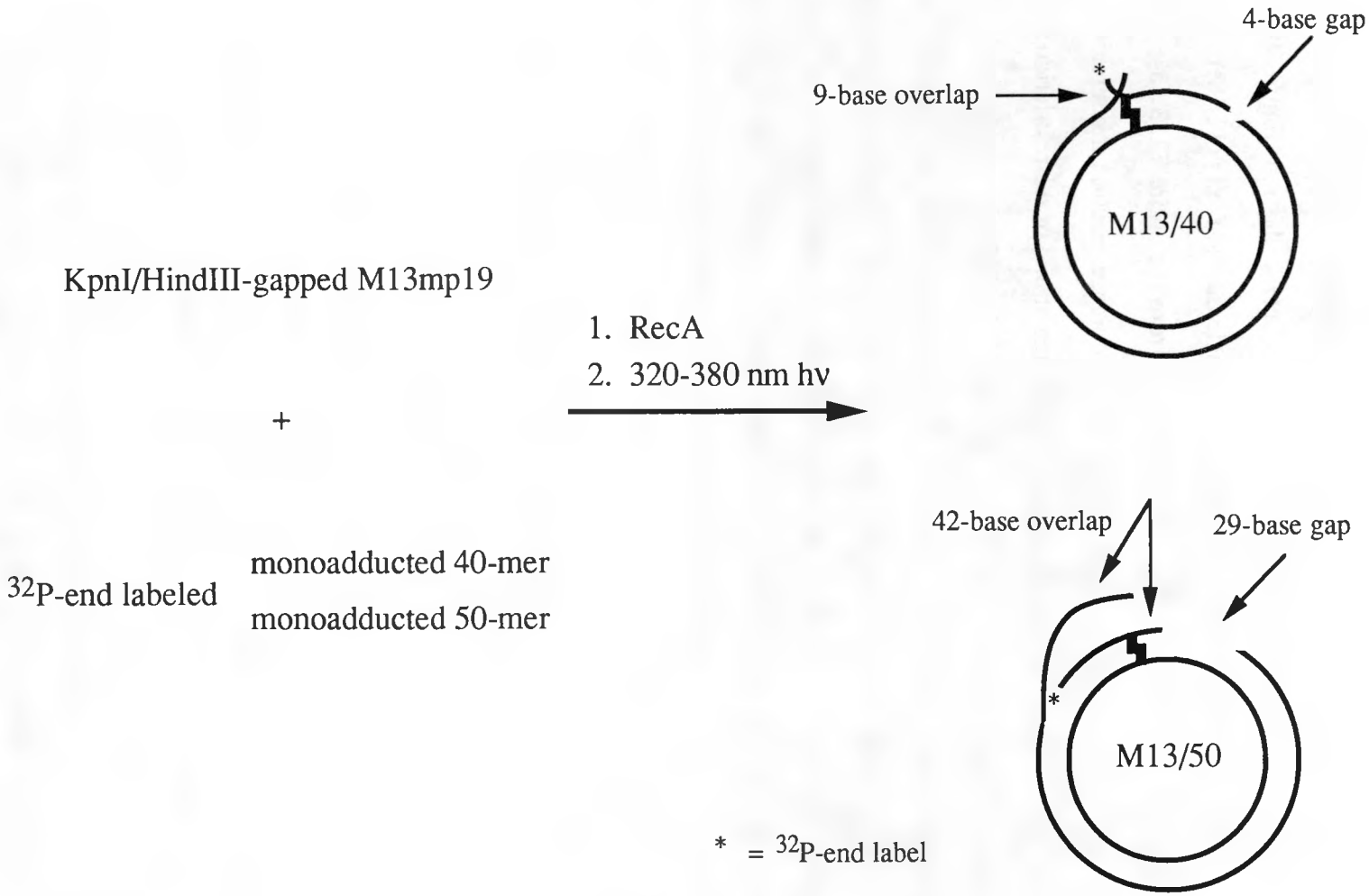
4-base gap
9-base overlap
*
M13/40
KpnI/HindIII-gapped M13mp19
1. RecA
2. 320-380 nm hν
+
32P-end labeled
monoadducted 40-mer
monoadducted 50-mer
42-base overlap
29-base gap
*
M13/50
* = 32P-end label

Results

Our first goal was to simply characterize the incisions made by (A)BC excinuclease in a uniquely HMT-crosslinked M13mp19 circular (relaxed) plasmid (Figure 4-1). One approach was to treat the substrate with (A)BC excinuclease and then pol I, then digest the DNA to reduce the size of the fragment of interest from the entire 7253 basepairs to a 139/143-mer. By including [α-^{32}P]dCTP in the polymerase reaction mixture, we hoped to identify which strand had been incised. The 139-mer strand of the restriction fragment corresponded to the furan-side strand of the crosslink, the 143-mer strand to the pyrone-side. Once the strands had been isolated, the repair patch could be sequenced.

One potential source of background signal was (A)BC excinuclease incision of pyrimidine dimers that could have been introduced during the irradiation to convert the monoadducted M13mp19 to a crosslinked substrate. Two approaches were taken to quantitate this background damage. To estimate the extent to which the M13 substrate had been damaged during crosslinking, unmodified pBR322 plasmid was similarly irradiated and then transformed into HB101 (*recA*$^-$) *E. coli* cells. Damaged pBR322 was expected to show a reduced frequency of transformation. DNA photolyase (*phr* gene) was also used to repair dimers in the crosslinked M13mp19 and the repair patch signal from such samples was compared with that from untreated plasmid. DNA photolyases catalyze the photoreactivation (monomerization) of *cis-syn* cyclobutane rings of pyrimidine dimers [reviewed by Sancar and Sancar, 1988]. Another potential source of background signal was pol I nick-translation from random sites in the plasmid. Crosslinked substrate was therefore treated with polymerase and ligase to repair any random nicks or small gaps prior to the (A)BC excinuclease step.

Irradiated plasmid pBR322 showed no reduction in transformation efficiency, within experimental error, suggesting that little if any photodamage had been introduced during the crosslinking irradiations (data not shown). Transformation of CSR603 cells

with crosslinked M13mp19 yielded 22 colonies on a 10^{-3} dilution plate while the unmodified control yielded 2050 colonies on a 10^{-4} dilution plate. CSR603 cells are *uvrA*$^-$ and therefore deficient in nucleotide excision repair. The approximately 0.1% survival observed is attributable either to contaminating uncrosslinked substrate or to replicative bypass of crosslinks. Monoadduct lesions would not have been lethal because genetic information can be recovered through use of the undamaged strand as a template for replication [Koffel-Schwartz *et al.*, 1987]. With *uvr*$^+$ cells, Piette and colleagues [1988] observed a 1.7-1.8% survival of crosslinked substrate that had been prepared at the same time as that used in our own experiments. Of this, a maximum of 0.5% monoadduct contamination was estimated. A comparison of unmodified M13mp19 and one preparation of the crosslinked substrate, with and without photolyase treatment, also indicated that the resulting reduction in transformation frequency was primarily due to the psoralen adducts rather than to photodamage. In the *uvrA*$^+$ HB101 cells, a later preparation of the crosslinked M13mp19 yielded 18 colonies per ng M13 as compared to 700 per ng unmodified M13, equivalent to a 2.6% survival. This value is comparable to the 1.7-1.8% reported by Piette and coworkers [1988], suggesting that this later preparation of crosslinked M13mp19 was also approximately 0.5% in monoadduct. Piette and colleagues [1988] noted that the location of the crosslinked site within the *lacZ* gene meant that only frameshift mutations or large deletions would result in inactive β-galactosidase. We did not observe any white or pale colonies indicative of impaired β-galactosidase.

As Figure 4-4 indicates, repair patch synthesis by pol I yielded a family of [α-^{32}P]dCTP-labeled products. Closer examination of the pattern of pauses and termination revealed that the bands corresponded to the pattern of C's in the sequence of the (-) strand of the HindIII/PvuII fragment. This suggested that sequencing was not necessary. The fact that the pattern of bands in lanes 2-6 is the same as in lane 7 indicated that the furan-side strand of the crosslinked M13mp19 had been incised by (A)BC excinuclease. As indicated in Figure 4-5, the expected 5′ incision site follows C_{93}. This deoxycytidylate

lies at the 3′ end of the lowest molecular weight band in the crosslink lanes (2-6) in Figure 4-4. The 93-base paused/terminated product suggested that in a fraction of the sample population, pol I removed at least one additional base at the 5′ incision site before initiating strand synthesis. The observation that incorporation of [α-^{32}P]dCTP in the monoadducted sample (lane 8) began at n = 97 or 99 suggested that these repair patches were initiated from the 5′ (A)BC excinuclease incision site (between the 94th and 95th bases of the restriction fragment).

The data shown in Figure 4-4 contained several other notable features pertaining to the crosslink repair process. The band at approximately n = 93-94 bases disappeared in the presence of UvrD (helicase II), suggesting that this protein interfered with the 3′→5′ exonuclease activity of pol I at the 5′ incision site (compare lanes 3 and 4). RecA did not have the same effect (lane 5). In lane 1, the band at n = 101 bases may have resulted from synthesis by nick-translation along the furan-side strand that was stopped by the crosslinked thymine at position 102. The strong band at approximately n = 126 bases in lanes 1-6 appeared in other gels between n = 116-120 bases, and was later identified as undenatured crosslinked duplex (data not shown). Pretreatment of the crosslinked substrate with pol I and ligase to seal random nicks and gaps (lane 2) reduced the intensity of this band. The native PAGE gel (not shown) used to initially separate the HindIII/PvuII restriction fragments also indicated that [α-^{32}P]dCTP label had been incorporated throughout the plasmid, presumably from strand synthesis initiated at either random nicks or nicks introduced by (A)BC excinuclease. Samples that had been pretreated with DNA photolyase (not shown) or incubated with polymerase without prior (A)BC excinuclease digestion (as in lane 1 of Figure 4-4) did contain lower levels of label, but the background signal was not completely eliminated.

Subsequent efforts to examine the effect of UvrD were inconclusive. Although helicase II has been observed to have only a minor effect on the footprints of the UvrA and UvrB proteins and on polymerase activity, the protein appears to influence polymerase

Figure 4-4. Example of early data showing pattern of bands recovered from (A)BC excinuclease reactions and post-incision repair synthesis by pol I in the presence of [α-^{32}P]dCTP. As described under "Methods", a HindIII/PvuII restriction digest was used to focus on the region of interest. The patterns of bands from the monoadducted and crosslinked M13mp19 were compared to identify the strand preference for incision of the crosslinked substrate. To seal any nicks or gaps, the sample in lane 2 had been treated with pol I, dNTP's and ligase prior to the incision reaction. The full-length band is a 139-mer; termination after the last C yields a band at n = 138 bases. The band assignments were based upon the known sequence of the 139-mer (see Figures 4-1 and 4-5) and adjacent sequencing lanes (not shown) of a 107-mer standard. Also not shown are the series of bands at n < 50 bases that appeared in the monoadducted M13 lanes (see text).

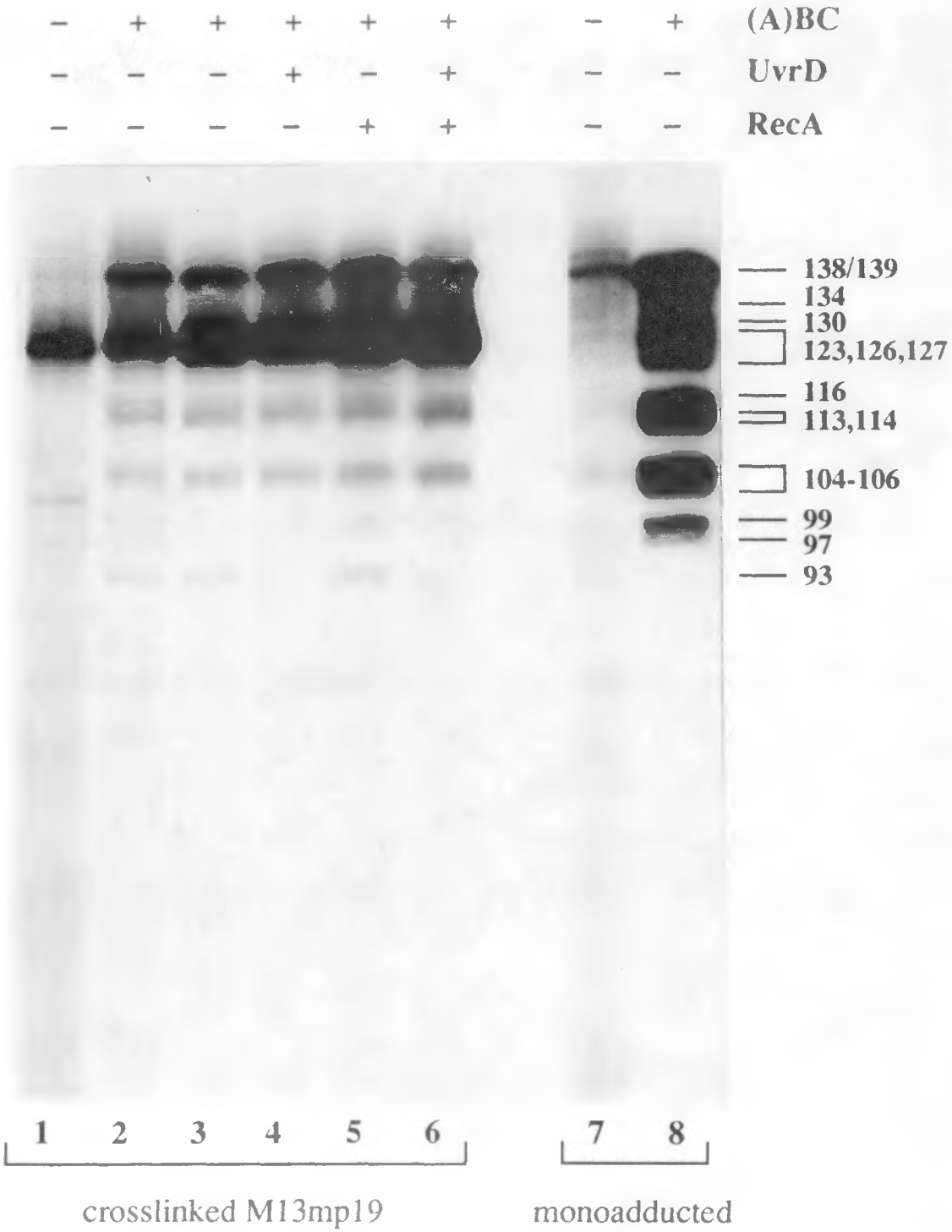
– + + + + + – + (A)BC
– – – + – + – – UvrD
– – – – + + – – RecA
138/139
134
130
123,126,127
116
113,114
104-106
99
97
93
1 2 3 4 5 6
7 8
crosslinked M13mp19
monoadducted

XBB903-2449

processivity and may interact with the DNA substrate at the 5′ incision site [Van Houten *et al.*, 1988].

Not shown in Figure 4-4 are lower molecular weight bands (n < 50 bases) in lanes (7 and 8) that contained repair patches from monoadducted M13mp19 samples. These bands could have arisen from synthesis in the nonadducted (+) strand (see Figure 4-1) originating upstream from the HindIII restriction site. The single band at n = 42-43 bases seen in lane 7 might represent termination of synthesis at the monoadducted thymidine (T_{41}) in the template strand (see Figure 4-5). Lane 8 contained a series of bands ending at C_{48}. In the nonadducted strand, this terminal deoxycytidylate is opposite the 5′ terminal base of the monoadducted 13-mer (Figure 2-2a) that was originally used to generate the monoadducted plasmid. An unligated nick at this position in the template might have led to termination of strand synthesis.

One interesting result illustrated in Figure 4-4 was that labeled 139-mer was obtained from crosslinked M13mp19. Full-length strands of the HindIII/PvuII restriction fragment (139 and 143 bases) that contained label introduced during post-incision repair synthesis could reflect either a background of uncrosslinked substrate in the sample or a low level of bypass synthesis. If replicative bypass could be detected, our interest was in the efficiency of such an event and in the sequence of nucleotides incorporated in the crosslinked region. Bypass of psoralen monoadducts has been previously reported [reviewed by Moustacchi, 1988]. A <1% *in vivo* bypass of an HMT crosslink may have been observed [Piette *et al.*, 1988], but no other data for crosslink bypass has been reported.

The sensitivity of each fragment to KpnI could be used to differentiate between products of bypass synthesis which would still be crosslinked and completely repaired molecules. As described in Chapter 3, the presence of the psoralen adduct within the KpnI site interferes with digestion. In a set of repaired samples, therefore, KpnI was added at the time of the HindIII and PvuII digestions. A schematic of the resulting

fragments is given in Figure 4-5. Incorporation of [α-^{32}P]dCTP into the furan-side strand beyond the 93rd base (5′ incision site for adducted T_{102}) would subsequently yield two labeled KpnI fragments, indicating that the psoralen had been excised. The results of such an assay are shown in Figures 4-6.

The samples in Figure 4-6 were isolated from the 139/143-mer HindIII/PvuII band on the native gel used to isolate restriction fragments. KpnI digestion resulted in two lower molecular weight bands that were isolated separately. The lengths of the 100/104-mer KpnI fragment (see Figure 4-5) were confirmed in lanes of the denaturing gels that are not shown. As calculated from the Cerenkov cpm (data not shown) of the DNA recovered from the native gel, lane 4 represents 47% of the HindIII/PvuII fragment that resisted KpnI digestion. Lane 6 represents 41% resistance, and lane 8 15%. The data for sample 8 suggests that in the presence of ligase, at least 85% of the monoadducts were fully repaired. The crosslinked samples could not be similarly quantitated because of the high and uneven background signal (unincorporated [α-^{32}P]dCTP) relative to the sample bands. The crosslink panel (lanes 9-16) in Figure 4-6 represents a film exposure nearly 20 times longer than that used for the monoadduct panel (lanes 1-8).

Figures 4-4 and 4-6 both suggested that full-length restriction fragments were produced at more than the 0.5% level of residual monoadducted M13mp19 estimated from the transformation data. Lanes 11-16 in Figure 4-6 contain more labeled 139-mer than the background levels attributable to pol I acting on uncrosslinked material (lanes 9 and 10). This suggested that bypass synthesis of incised crosslinks was detected. However, since we did observe incomplete KpnI digestion of patches produced during repair of the mono-adducted substrate, we could not unambiguously identify the source of the full-length fragments in the crosslinked M13 lanes 11-16.

We examined the role of the 5′→3′ exonuclease activity of pol I in generating background signal by comparing the pattern of bands from pol I-mediated synthesis with that from the Klenow fragment of pol I. Nonligatable products were reported to be

Figure 4-5. Schematic of the portion of the HindIII/PvuII restriction fragment that was used to analyze repair of the HMT crosslink site, before and after KpnI digestion. The 143/139-mer restriction fragment is shown in the same orientation as in Figure 4-1. Bases are numbered relative to the 5′ end of each strand. Possible (A)BC excinuclease incision sites are marked on both the pyrone- (P) and furan-side (F) strands; the terms "monoadduct incisions" and "crosslink incisions" refer to the positions of the incisions relative to the adducted thymidine on that strand. The location of incorporated [α-^{32}P]dCTP indicates which strand was incised and where repair patch synthesis began. In practice, the 143/139-mer was not isolated until after repair patch synthesis. Samples were simultaneously digested with HindIII, PvuII, and KpnI. The susceptibility of the repaired DNA to KpnI digestion reflects the completion of repair and restoration of the KpnI recognition site.

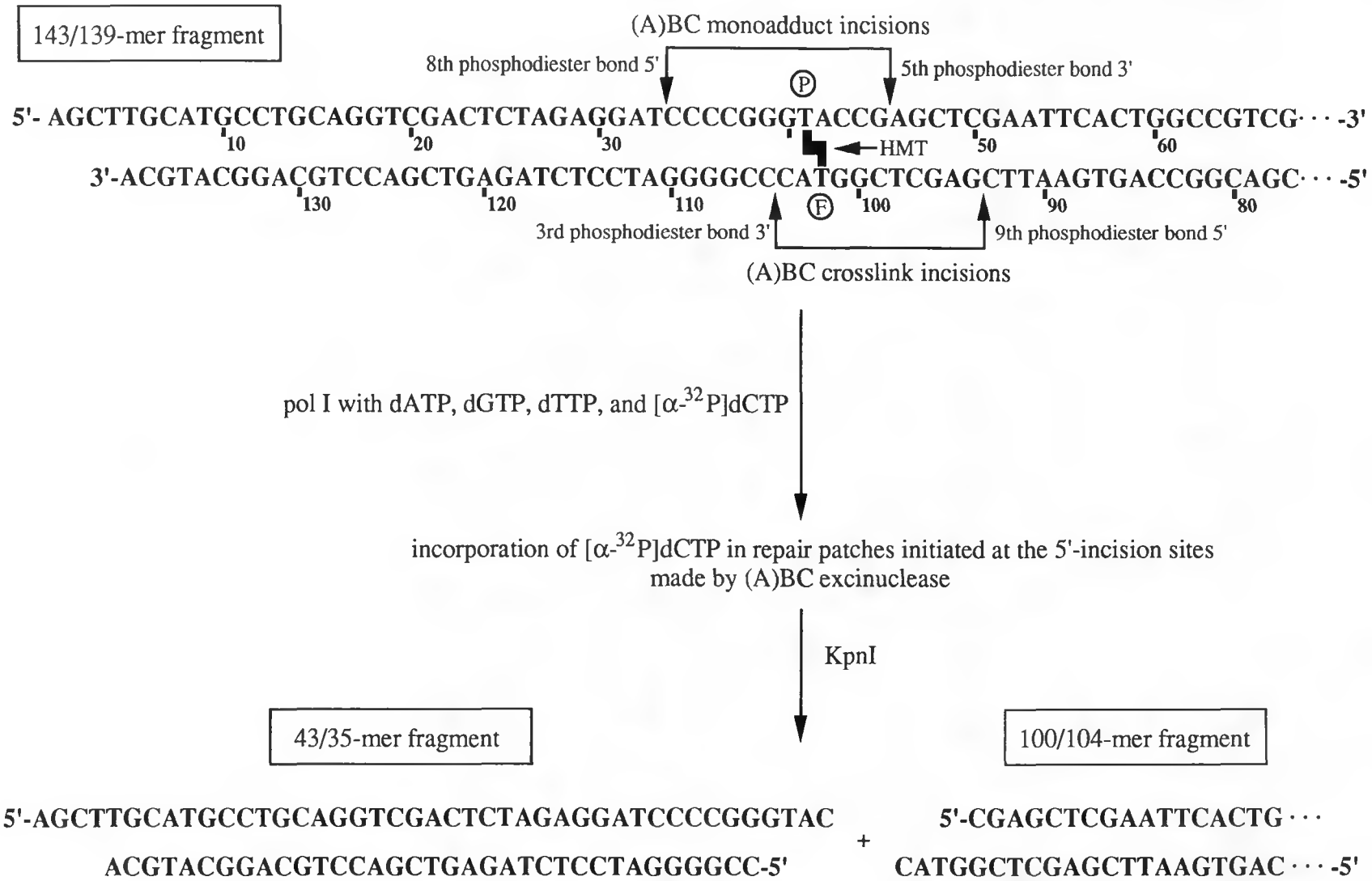
143/139-mer fragment
(A)BC monoadduct incisions
8th phosphodiester bond 5'
5th phosphodiester bond 3'
Ⓟ
5'- AGCTTGCATGCCTGCAGGTCGACTCTAGAGGATCCCCGGGTACCGAGCTCGAATTCACTGGCCGTCG· · · -3'
10 20 30 HMT 50 60
3'-ACGTACGGACGTCCAGCTGAGATCTCCTAGGGGCCCATGGCTCGAGCTTAAGTGACCGGCAGC· · · -5'
130 120 110 Ⓕ 100 90 80
3rd phosphodiester bond 3'
9th phosphodiester bond 5'
(A)BC crosslink incisions
pol I with dATP, dGTP, dTTP, and [α-32P]dCTP
incorporation of [α-32P]dCTP in repair patches initiated at the 5'-incision sites made by (A)BC excinuclease
KpnI
43/35-mer fragment
100/104-mer fragment
5'-AGCTTGCATGCCTGCAGGTCGACTCTAGAGGATCCCCGGGTAC
ACGTACGGACGTCCAGCTGAGATCTCCTAGGGGCC-5'
+
5'-CGAGCTCGAATTCACTG· · ·
CATGGCTCGAGCTTAAGTGAC· · · -5'

Figure 4-6. Repair of the monoadducted and crosslinked M13mp19 substrates, detected by KpnI digestion. Complete repair of the psoralen-adducted KpnI restriction site should restore susceptibility to this restriction endonuclease. Each M13mp19 substrate was treated with (A)BC excinuclease in the presence of UvrD or ligase, as indicated at the top. Post-incision repair synthesis was carried out by pol I in the presence of [α-^{32}P]-dCTP. For the even-numbered samples, KpnI was included in the HindIII/PvuII digests used to isolate the 143/139-mer fragment of interest. The duplex restriction fragments were separated on 8% native PAGE gels, and then analyzed on denaturing gels.

The native gel that preceded the 8% denaturing gels shown here also separated products of the KpnI digest from samples 4, 6, and 8; the sizes of these bands (100/104-mer and 43/35-mer) were confirmed in lanes not shown here. The 104-mer strand of the KpnI/PvuII fragment was more heavily labeled than its 100-mer complement, consistent with furan-side incision and repair. (Please refer to Figure 4-5.) Repair of the psoralen-adducted site and restoration of the KpnI site within the fragments that are shown in this figure is indicated by the reduced intensity of the bands in even-numbered lanes (digested with KpnI) relative to those in the corresponding odd-numbered lanes (undigested). The increased intensity of bands in sample 2 versus sample 1 is attributed to contamination from sample 3 during isolation from the native gel.

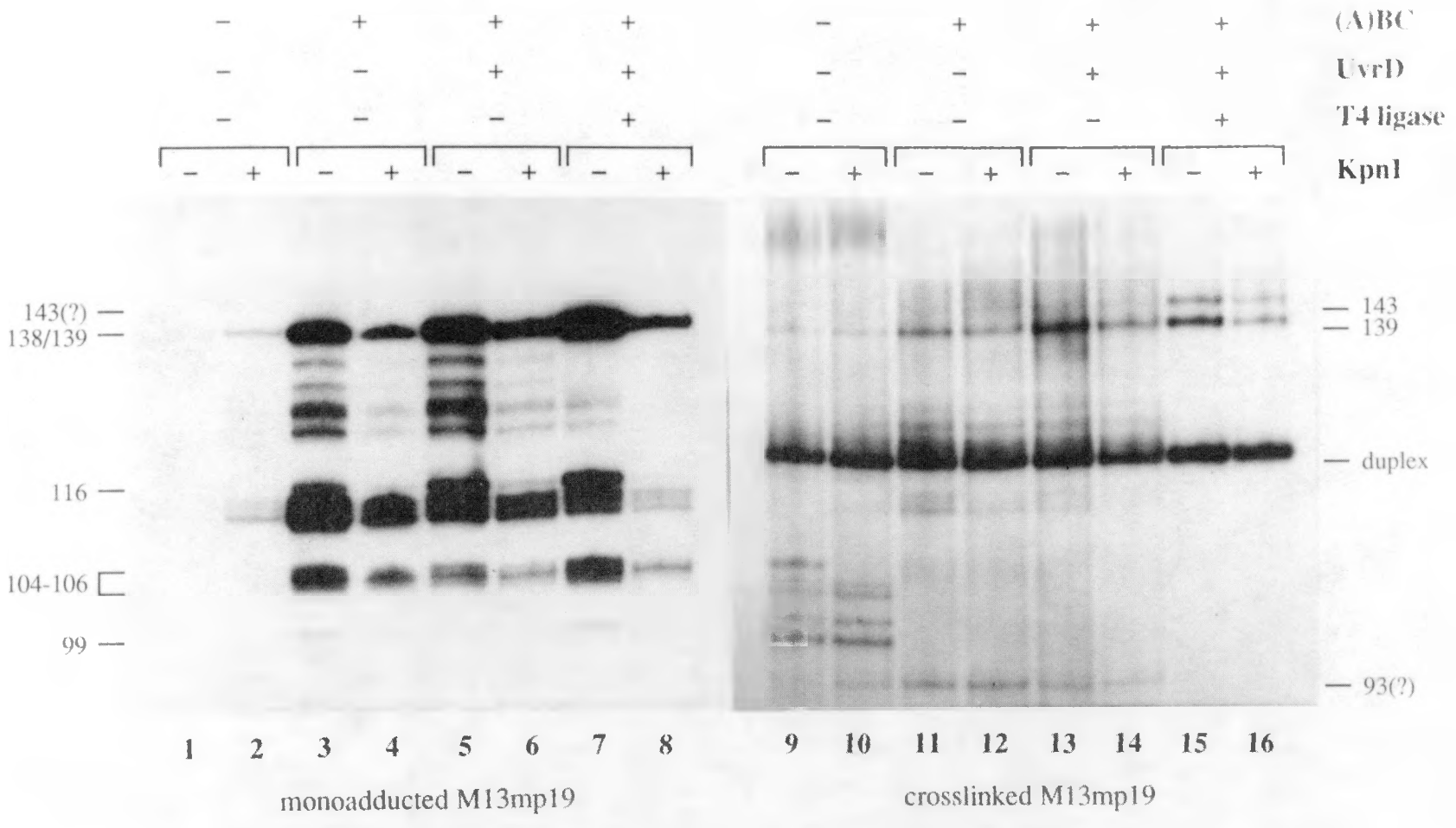
(A)BC
UvrD
T4 ligase
KpnI
143(?)
138/139
116
104-106
99
143
139
duplex
93(?)
1 2 3 4 5 6 7 8
9 10 11 12 13 14 15 16
monoadducted M13mp19
crosslinked M13mp19

XBB903-2450

produced by pol I mutants defective in the 5′→3′ exonuclease activity [Wahl *et al.*, 1983]. Such products could contribute to the observed incompleteness of patch synthesis (generation of a ladder of patch lengths) and subsequent KpnI digestion. Alternatively, (A)BC excinuclease bound to the DNA might interfere with strand synthesis. To evaluate these possibilites, repair synthesis in (A)BC excinuclease-incised monoadducted M13 was examined. As Figure 4-7 indicates, the majority of Klenow-generated fragments were converted to full-length fragments in the presence of ligase (compare lanes 11 and 13). This argues against an absolute requirement for the 5′→3′ exonuclease activity in pol I-mediated conversion of gaps to ligatable nicks. Furthermore, extractions to remove (A)BC excinuclease prior to the polymerase reactions had little effect on the pattern of bands (compare lanes 7 through 10 with lanes 3 through 6). The intensities of the bands from extracted samples in the absence of ligase (lanes 7 and 8) were also similar to those from untreated samples (lanes 3 and 4). As in Figure 4-6, bands that were susceptible to KpnI have already been separated and are therefore absent. The apparent resistance of extracted samples (lanes 9 and 10) may reflect salt-inactivation of the ligase; the extracted samples were ethanol-precipitated prior to the polymerase and ligase reactions. We again observed low molecular weight bands (not shown) corresponding to synthesis in the nonadducted strand up to the monoadducted thymidine. HMT-monoadducted templates were previously found to affect only the kinetics of polymerization; replication was not completely blocked [Piette and Hearst, 1983].

To analyze the sequence of the repair patch, the αS-dNTP sequencing method developed by Gish and Eckstein [Gish and Eckstein, 1988; Nakamaye *et al.*, 1988] was employed. Following incision by (A)BC excinuclease, repair patches were synthesized in the presence of αS-dNTP's. The strands of the isolated HindIII/PvuII restriction fragment were dephosphorylated and kinased, then gel-purified. Each sample was then treated with 2-iodoethanol to obtain the sequence-specific cleavage patterns. A representative result for monoadducted M13mp19 is shown in Figure 4-8. This autoradiogram

Figure 4-7. Analysis of pausing/termination phenomenon responsible for the [α-^{32}P]dCTP patterns observed (as in Figures 4-4 and 4-6). Only the monoadducted M13mp19 substrate was used for this purpose. Post-incision repair synthesis by pol I (lanes 3-6) was compared with synthesis by the Klenow fragment (lanes 11–14) and with synthesis following removal of (A)BC excinuclease by phenol-extraction (lanes 7–10). As in Figure 4-6, KpnI restriction digests were used to monitor completion of repair. Again, bands were assigned based upon adjacent sequencing of a standard and the known sequence of the 139-mer.

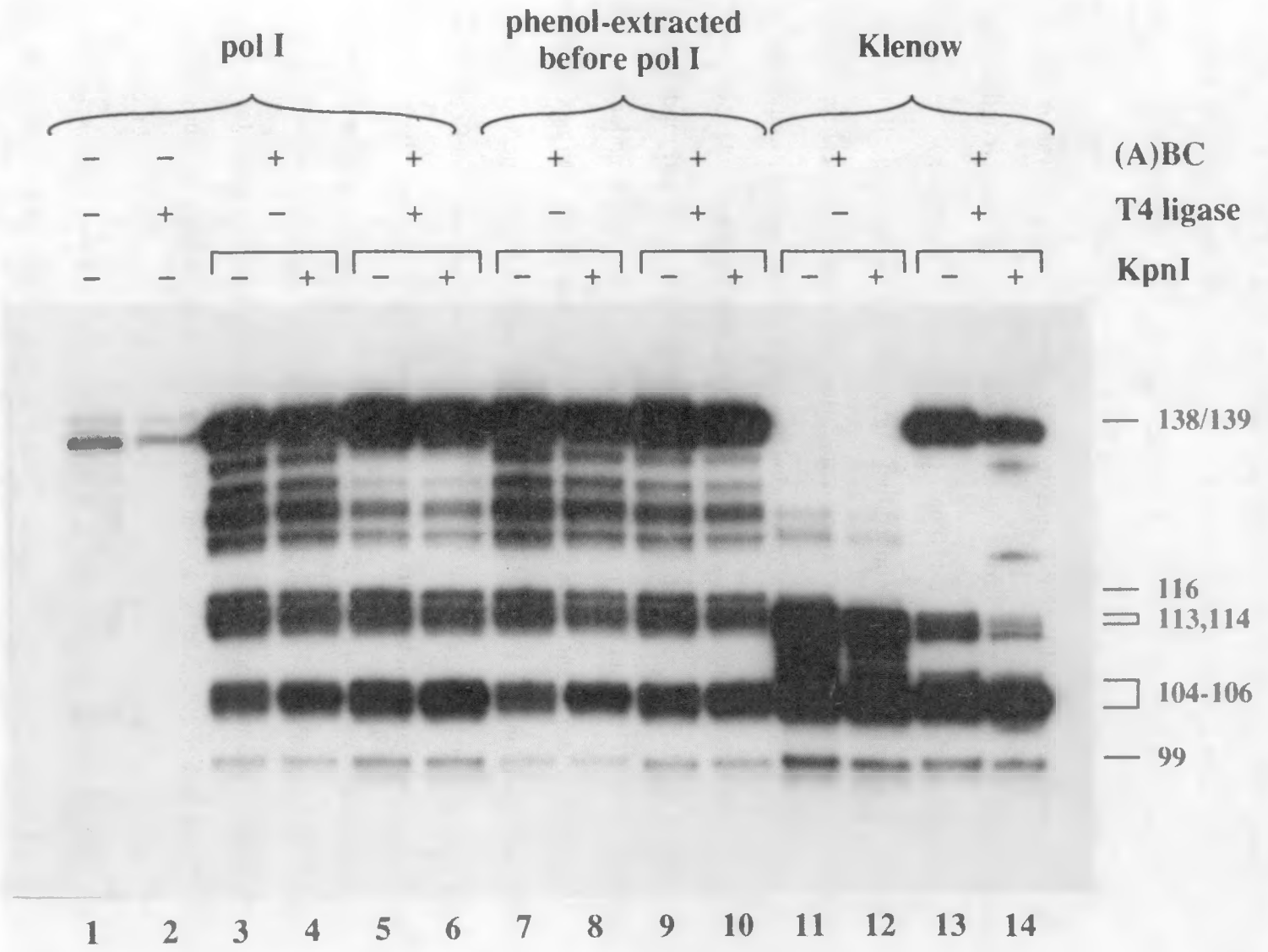
pol I
phenol-extracted before pol I
Klenow
(A)BC
T4 ligase
KpnI
138/139
116
113,114
104-106
99
1 2 3 4 5 6 7 8 9 10 11 12 13 14

XBB903-2451

represents an 11-day film exposure. Bands in the αS-dA lane 8 as short as 89-90 bases (visible only upon prolonged film exposure, and not included in Figure 4-8) indicated that at least some of the repair patches in the monoadduct samples began at the fifth or sixth base 5′ to the usual 5′ incision site (eighth bond from the adduct) of (A)BC excinuclease. (Please refer to the partial sequence in Figure 4-5.) This can be attributed to 5′→3′ exonuclease activity of pol I at the 5′ incision site. No effect of UvrD was observed. The presence of ligase did limit the size of the repair patch to less than 30 nucleotides (compare lanes 6 and 7 with others at $n \geq 120$ bases; additional data not shown). As Figure 4-8 illustrates, the sequence in the monoadduct samples could be followed. Bands from the crosslink samples were too faint. In principle, this method would reveal replicative bypass and identify nucleotide misincorporation caused by the unrepaired psoralen adducts.

To the extent that we were able to but did not detect pyrone-side incision of the crosslinked M13mp19, our results were consistent with the proposed model shown in Figure 3-1. (A)BC excinuclease preferentially incises the furan-side strand, and requires a three-stranded intermediate before it will incise the remaining strand. Our next goal was to duplicate conditions for RecA-mediated strand exchange with the incised crosslinked duplex. Sladek and coworkers [1989b] had previously demonstrated that RecA required a single-stranded gap which could be generated from the 3′ incision site by the 5′→3′ exonuclease activity of pol I. In addition to using pol I to create a gap following an (A)BC excinuclease reaction, we designed a uniquely gapped substrate to model the product (Figure 4-2). We attempted to carry out strand exchange reactions using these substrates and M13mp19 FIII (see 'Methods'), but met with little success (data not shown).

We then returned to the simpler system of an oligonucleotide and a circular plasmid. The crosslinked oligonucleotide was used to mimic the fragment excised from the furan-side strand during the first incision step in (A)BC excinuclease-mediated repair of a crosslinked duplex, as in Chapter 3. The KpnI/HindIII-gapped circular M13mp19 substrate was chosen as the duplex moiety because the KpnI restriction site corresponded to

Figure 4-8. Sample of αS-dNTP sequencing analysis on a denaturing 8% polyacrylamide gel. These are all monoadducted M13mp19 reaction samples; crosslinked sample reactions yielded bands too faint to interpret or show here. Each αS-dNTP was incorporated in a separate sample during post-incision strand synthesis, as indicated. As before, all samples were digested with HindIII and PvuII to focus on the repair patch. The isolated strands of the 143/139-mer restriction fragment were dephosphorylated and then 5′-end-labeled with kinase. Each was then heat-denaturated in the presence of 2-iodoethanol to produce the sequence-specific cleavage patterns seen here.

Lanes 2–6 and 7–11 reflect synthesis in the absence and presence of UvrD, respectively. Lanes 6 and 7 illustrate the effect of omitting ligase. Lane 12 contains a sample treated with KpnI following synthesis. Not shown is the lower portion of the autoradiogram which revealed the faintest of bands at n = 89 and 90 bases in lane 8. The far left lanes are G and C sequencing [Maxam and Gilbert, 1980] reactions of a 135-mer standard; the numbers on the far left refer to the nucleotide positions. The position of the formerly HMT-adducted residue (T_{102}) is highlighted in the sequence shown on the right. This sequence (from Figure 4-1 or 4-5) gives the expected order of bands; many of the bands were not resolvable. The diffuse nature of the bands is attributable, in part, to the 2-iodoethanol-mediated hydrolysis reactions which yield both 3′-OH and 3′-P termini [Gish and Eckstein, 1988].

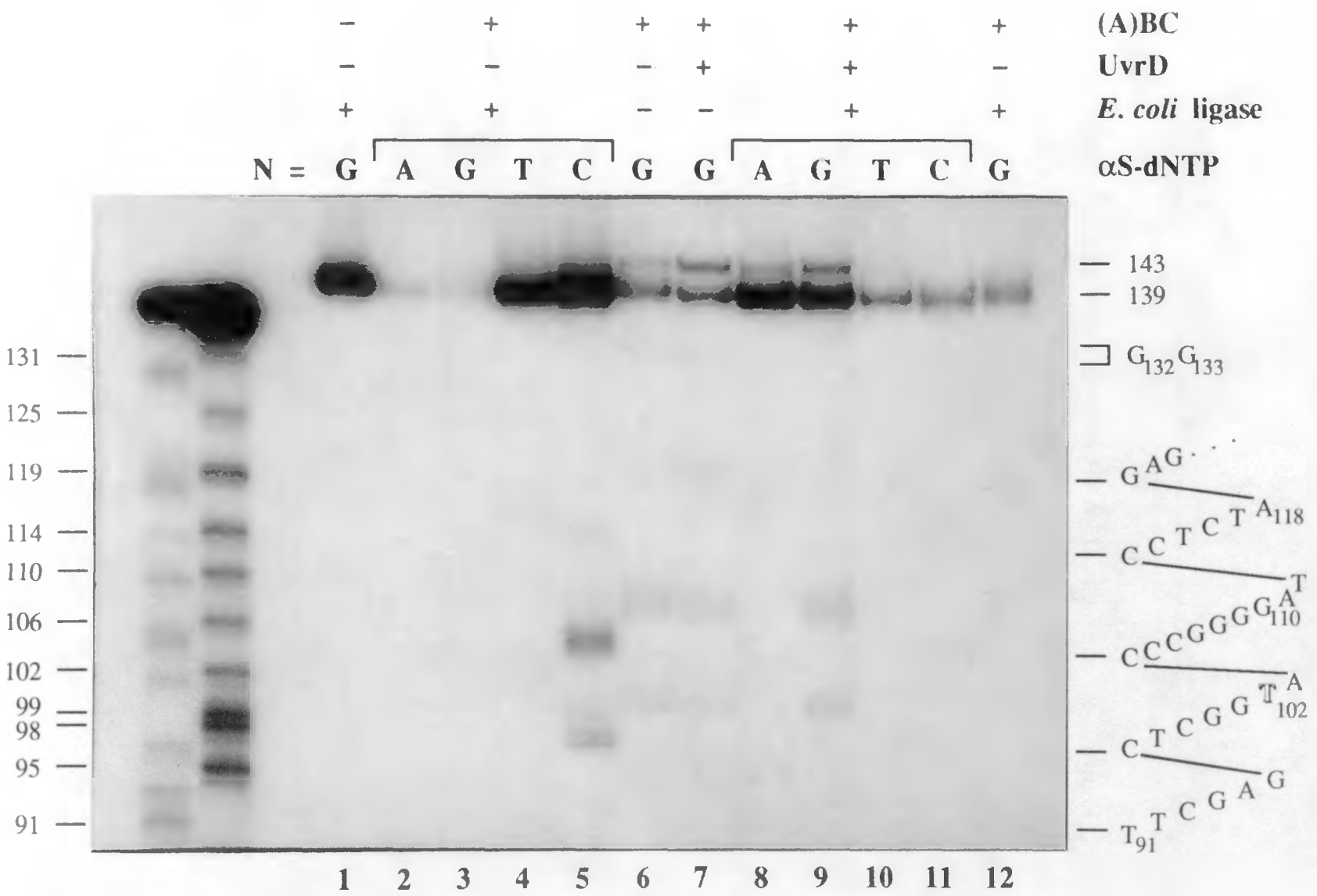
(A)BC
UvrD
E. coli ligase
αS-dNTP
N = G A G T C G G A G T C G
143
139
G132G133
131
125
119
114
110
106
102
99
98
95
91
1 2 3 4 5 6 7 8 9 10 11 12

the 3′ incision that (A)BC excinuclease would make on the furan-side strand, the third phosphodiester bond 3′ to the crosslink. In addition, the 35-base distance between the KpnI and HindIII restriction sites on the gapped strand was expected to be large enough to activate the substrate for RecA-mediated homologous pairing. Sladek and associates [1989b] have noted that the 11-12-base gap between (A)BC excinuclease incision sites is insufficient for the initiation of RecA-catalyzed strand exchange. The 40-mer (see Figure 2-2b) was chosen because it was the shortest of the oligomers to have a 5′ end very near the KpnI recognition site. The 50-mer was selected as well, since it was a more efficient substrate for RecA than either the 30- or the 40-mer (see Figure 2-5). Our previous data (see Figure 3-3) indicated that the length of the oligomer (between 30 and 107 nucleotides) had little, if any, effect on the ability of (A)BC excinuclease to recognize and incise the pyrone-side strand of the crosslink. The resulting crosslinked M13/40 and M13/50 complexes are pictured in Figure 4-3. These structures can be compared to the general three-stranded pUC19 complex pictured in Figure 2-3, keeping in mind that the three-stranded regions of these complexes has *not* been precisely characterized.

The experiment was designed to test the ability of a presynaptic mixture of RecA and a 107-mer (unmodified version of the oligomer in Figure 2-2b) to form a three-stranded intermediate at the KpnI site (the crosslink site) and thus induce (A)BC excinuclease to make pyrone-side incisions. As a control, three-stranded pUC19 complexes identical to those used for the work presented in Chapters 2 and 3 were also digested with (A)BC excinuclease. As in Chapter 3, only the 5′ ends of the 40- and 50-mers were ^{32}P-labeled. Furan-side incisions would therefore be indicated by the appearance of shortened oligomers while pyrone-side (plasmid strand) incisions would leave the labeled oligomer intact and crosslinked to the small fragment excised from the plasmid.

Figure 4-9 shows that "transient" formation of a complex between the homologous 107-mer and the crosslinked M13/40 and M13/50 substrates resulted in (A)BC excinuclease preferentially incising the pyrone-side strand, releasing fragments which migrate

Figure 4-9. Autoradiogram showing induced pyrone-side incisions. Gapped M13/40 and M13/50 complexes (Figure 4-3) were digested with (A)BC excinuclease in the presence of 107-mer complementary to the gap (lanes 3 and 10), RecA (lanes 4 and 11), or both (lanes 5 and 12). As positive controls for pyrone-side incision, the corresponding three-stranded pUC19 complexes were also digested with (A)BC excinuclease (lanes 7 and 14). In each complex, only the 40- or 50-mer was ^{32}P-labeled. Samples were analyzed on a denaturing 10% polyacrylamide gel. The crosslinked (XL) pyrone-side excision product is marked with an arrow. Uncrosslinked (either UM = unmodified or MA = monoadducted) oligonucleotide that had been retained by either the M13mp19 or pUC19 plasmid was released during the heat-denaturation step prior to loading of the gel.

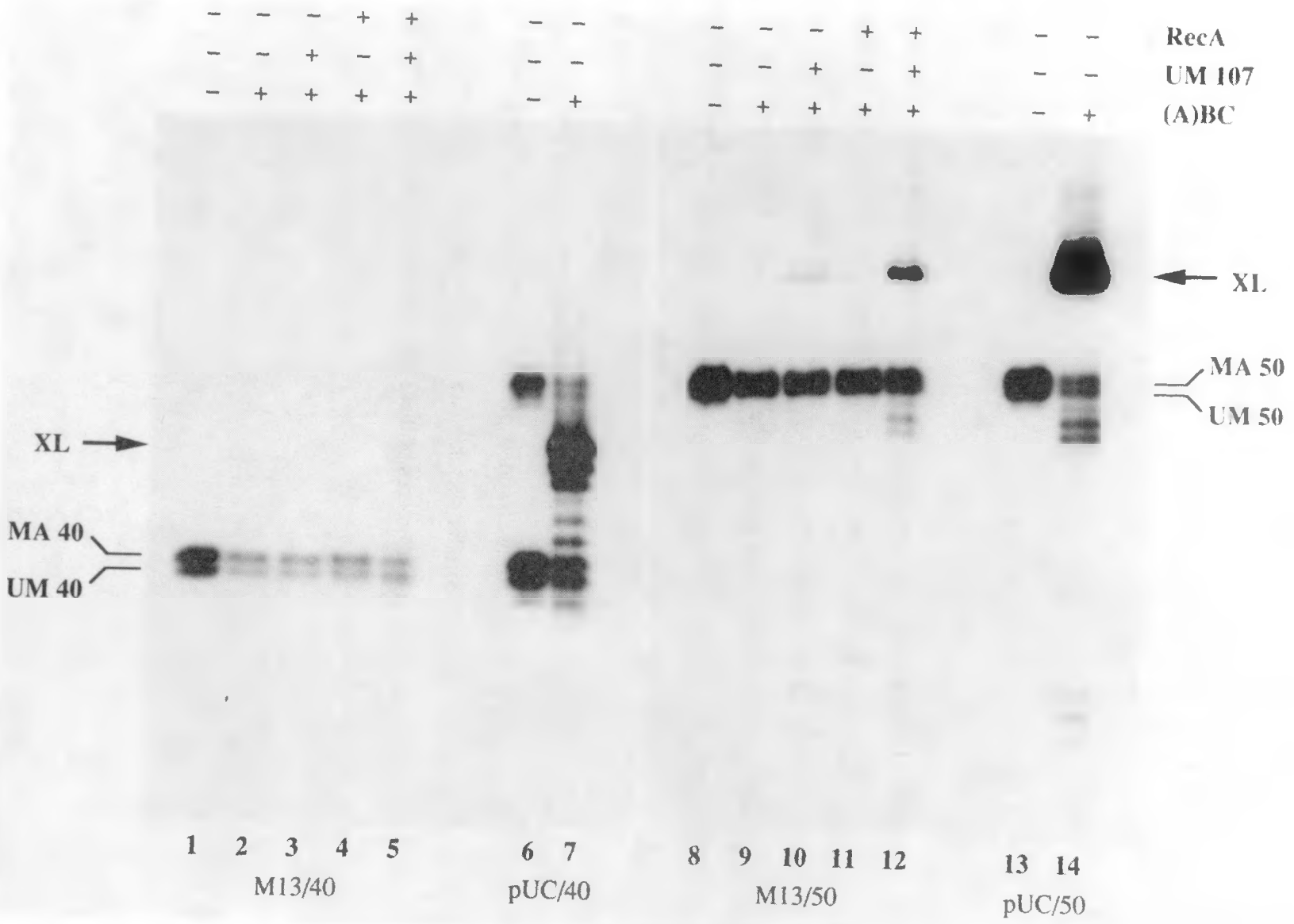
RecA
UM 107
(A)BC
XL
MA 50
UM 50
XL
MA 40
UM 40
1 2 3 4 5
M13/40
6 7
pUC/40
8 9 10 11 12
M13/50
13 14
pUC/50

Figure 4-10. Schematic illustrating the (A)BC excinuclease incisions induced by a three-stranded structure at the crosslink site in M13/40 and pUC/40. As was discussed in Chapter 3, the pUC/40 complex which is comprised of a supercoiled duplex circle and an oligonucleotide insert yields only pyrone-side (plasmid) strand incision products. For the M13/40 complex, the single-stranded region activates the substrate for RecA-mediated homologous pairing. (A)BC excinuclease incision of the three-stranded intermediate that results from synapsis between the M13/40 and a RecA-coated homologous 107-mer releases the 40-mer crosslinked to an excision fragment (Figure 4-9). This product co-migrates with that from the three-stranded pUC/40, indicating that the pyrone-side (plasmid) strand was incised. Similar sketches can be drawn for the M13/50 and pUC/50 complexes. Note that the actual structures of these complexes have not been determined. (F = furan side, P = pyrone side)

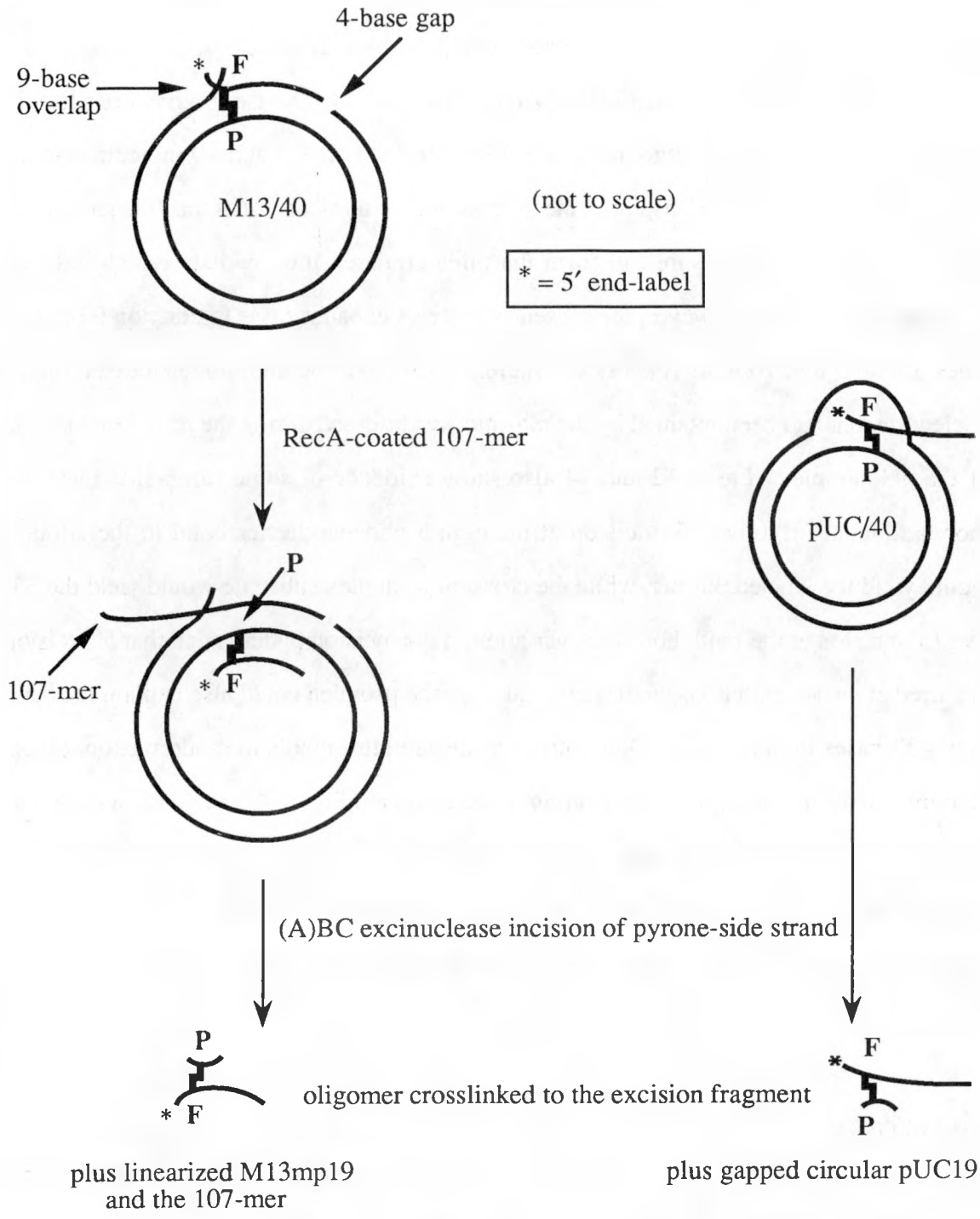

Figure 4-10. Induced pyrone-side incision of the crosslink

more slowly than intact 40- and 50-mer, respectively. More specifically, these fragments co-migrated with the excision products from the three-stranded pUC19 complexes (pUC/40 and pUC/50), previously shown to consist of an 11-12-base fragment of plasmid crosslinked to the labeled oligonucleotide (Chapter 3). Lanes 3 and 10 indicate that the 107-mer alone was able to "displace" the 50-mer, and to a lesser extent the 40-mer (apparent in a darker film exposure), to form the three-stranded intermediate which induced pyrone-side incision. However, the presence of RecA enhanced this interaction (compare lanes 3 with 5 and 10 with 12). As in Figure 3-3, unmodified and monoadducted oligonucleotide that had been retained by the plasmid was released during the heat-denaturation of the gel samples. Lanes 12 and 14 also show evidence of some furan-side incision; monoadducted oligomer (5′ incision at the eighth phosphodiester bond to the adduct) would yield the labeled 36-mer, while the crosslinked duplex substrate would yield the 35-mer (5′ incision at the ninth bond). A variation in the incision pattern such that 5′ incision occurred at the seventh phosphodiester bond from the psoralen could also explain the band at n = 37 bases in lanes 9-11. Other minor bands are attributable to random exonuclease activity. A schematic of the steps leading to the results in Figure 4-9 is given in Figure 4-10. The absence of pyrone-side incision of the M13/40 and M13/50 complexes in the absence of the 107-mer indicated that the overlap of the M13mp19 strand and the homologous 40- or 50-mer (Figure 4-3) was insufficient to produce the necessary three-stranded structure for such incision.

Discussion

Previous work with linear HMT-crosslinked duplexes indicated that (A)BC excinuclease preferentially incised the furan-side strand [Van Houten *et al.*, 1986b]. All of our results indicated that this was also true of the circular HMT-crosslinked M13mp19 substrate; the repair patch patterns were identical to those generated by the furan-side monoadducted substrate.

Jones and Yeung [1990] recently postulated that the GC content of sequences flanking a psoralen crosslink determines the binding and subsequent strand specificity of incisions by (A)BC excinuclease. In their study of various TMP-crosslinked duplexes, Jones and Yeung observed that a GC-rich sequence in the furan-side strand 6-12 bases to the 5′ side of TMP-crosslinked thymines led to preferential incision of the furan-side strand. If a GC-rich segment was on the 3′ side or absent entirely, then incision of both strands was observed. Jones and Yeung proposed that the UvrA and UvrB subunits may exhibit sequence-dependent modes of binding.

In our own work, we have examined (A)BC excinuclease incision of HMT-crosslinked molecules. The furan-side sequences flanking the crosslink site (underlined) are given below for a 137-basepair duplex (1) and the M13mp19 substrate (2).

5′-TA CGAATTC GAAGCTACGAGC TGAGGCC (1)

5′-GA ATTCGAG CTCGGTACCCGG GGATCCT (2)

Sequence (2) was also contained within the 40-mer oligonucleotide crosslinked into KpnI/HindIII-gapped M13mp19 to form M13/40; the 50-mer oligonucleotide in M13/50 began with the 3rd G in (2). Both of the above sequences are more GC-rich 6-12 bases 3′ to the crosslink than 5′; yet in both cases, only furan-side incisions were detected (data for sequence 1 not shown). With the M13/40 and M13/50 substrates, pyrone-side incisions were observed only in the presence of a third strand homologous to the furan-side strand.

We attribute the strand specificities noted by Jones and Yeung to their use of TMP. Unlike HMT, TMP lacks a 4′ substituent (see Figure 2-1) which is known to contribute to the asymmetry between the furan and pyrone ends of the psoralen diadduct [Tomic *et al.*, 1987]. Thus although sequence context may affect the incision of TMP crosslinks, our results with HMT-adducted substrates argue against this dependence for all psoralen crosslinks. As Jones and Yeung note, initial incision of a crosslinked duplex on the pyrone side could result in primarily error-prone repair through pol I strand synthesis. The

4′ substituent in HMT may block furan-side strand synthesis [Sladek *et al.*, 1989b] in favor of error-free recombinational repair.

The work described in this chapter represents our efforts to extend previous *in vitro* findings. We had observed (Chapter 3) that a crosslinked three-stranded complex in which the furan-side strand is an oligonucleotide will be preferentially incised by (A)BC excinuclease along the pyrone-side strand. Complete repair of the resulting excision gap could be carried out by DNA pol I and ligase. These observations were consistent with the sequential incision and recombination mechanism proposed for crosslink repair (Figure 3-1). By further investigating the transitions between the incision and recombination steps, to understand the interaction of the RecA protein with (A)BC excinuclease, we ultimately hoped to reconstitute crosslink repair *in vitro*.

The most promising results came from study of a model system comprised of a uniquely gapped M13mp19 circular duplex with a complementary oligonucleotide cross-linked to the plasmid near the 5′ end of the gap. The need for a gap to stimulate RecA-mediated homologous pairing had been noted by Sladek and coworkers [1989b]. The data presented here demonstrated that in the presence of a presynaptic complex between RecA and a complementary oligonucleotide, (A)BC excinuclease could be induced to incise the pyrone-side strand of the gapped crosslinked duplex. The incoming oligonucleotide did not need to be covalently attached to the plasmid, suggesting that a final recombination product may not be necessary for the second (A)BC excinuclease step in the crosslink repair process. The final product, however, is most likely necessary for completion of the repair process by polymerase and ligase.

One issue raised during early studies of the incision pattern of singly HMT-crosslinked M13mp19 was whether full-length product resulted from repair of residual monoadducted substrate in the crosslinked M13mp19 sample or from an ability of pol I to synthesize past the adducted thymine on the pyrone side (template strand). The transformation frequencies indicated that the amount of monoadduct present was less than the

apparent yield of full-length bands, suggesting that replicative bypass had indeed been detected. One approach to quantitate the bypass products was to assay for the restoration of the KpnI recognition site which would indicate complete crosslink repair. Results of this assay suggested that replicative bypass had been detected, but these results were not conclusive because repair patches from monoadducted samples exhibited some level of resistance to KpnI digestion as well. A second approach was to sequence the repair patches from (A)BC excinuclease-incised crosslinks. However, the sensitivity of the αS-dNTP sequencing analysis was too low to detect any nucleotide misincorporation that could reflect bypass. Recently, Taylor and O'Day [1990] reported that replicative bypass of *cis-syn* thymine dimers by pol I was observed at 100 μM each dNTP. At 1-10 μM levels of each dNTP, strand synthesis terminated at the dimer. By varying the enzyme concentration at 100 μM each dNTP, they observed a maximum of 20% bypass in one hour by the Klenow fragment. This suggests that replicative bypass of crosslinks might also be observable at high concentrations of each dNTP.

Our results do suggest several possible lines of research. The most immediate extension of the above work would require optimization of *in vitro* conditions for starting with a crosslinked duplex, creating a gapped post-furan-side-incision intermediate to serve as a substrate for RecA, and then forming a three-stranded intermediate which induces pyrone-side incisions. We have thus far been unable to detect the final excision fragment by beginning with the crosslinked M13mp19 and carrying out the steps of sequential incision and recombination. Incision of a psoralen-crosslinked plasmid may be significantly enhanced by supercoiling [cited in Pu *et al.*, 1989]. A next step would be to determine whether addition of pol I, dNTP's and ligase can complete the repair process from that point or if a final recombination product is necessary. These would certainly be significant steps towards *in vitro* crosslink repair. The recent results of Taylor and O'Day [1990] suggest that study of pol I strand synthesis at higher dNTP levels may reveal significant bypass of (A)BC excinuclease-incised HMT crosslinks. Finally, a possible

mechanism for SOS mutagenesis suggests that pol III replicative bypass of a psoralen crosslink may be detected in the presence of RecA and the UmuC and UmuD proteins.

Chapter 5

General Conclusions

Crosslink damage to DNA can result from a number of chemical agents including psoralens. Interstrand lesions are particularly dangerous for a cell because not only is the genetic information in both strands compromised, but essential processes such as replication and transcription are interrupted. Since crosslinks are potentially lethal lesions, it is of interest to understand how cells are able to repair this damage. In the preceding work, we have focused on the repair of psoralen diadducts by *Escherichia coli* proteins as a model for crosslink repair in general. Psoralen crosslinks are known to be mutagenic; yet there also exist mechanisms for error-free repair that rely upon homologous recombination to preserve the sequence at the crosslink site.

One model of nonmutagenic crosslink repair was originally developed in the 1970's through the work of Cole and colleagues. They determined that the *polA*, *recA*, *uvrA*, *uvrB*, and *uvrC* genes were all required for *E. coli* cells to survive psoralen damage. These results suggested a pathway involving pol I, RecA-mediated recombination, and *uvr*-dependent excision repair. A mechanism of sequential incision and recombination was therefore proposed [Cole, 1971 and 1973; Cole *et al.*, 1976]. Sancar and Rupp [1983] later clarified the role of the ABC excinuclease, the enzyme comprised of the products of the *uvrA*, *uvrB*, and *uvrC* genes. In nucleotide exision repair, the excinuclease makes a unique incision on each side of a lesion, enabling removal of the damage as a small oligonucleotide. Recent work revealed that the UvrA protein is required only for the initial damage recognition and association of the repair enzyme with a DNA lesion; the active incision complex consists only of the UvrB and UvrC proteins. The enzyme may therefore be more aptly named (A)BC excinuclease [Orren and Sancar, 1989]. Turnover and repair synthesis to fill and seal the excision gap require pol I and ligase, with the aid of helicase II (UvrD) [Van Houten *et al.*, 1988].

Van Houten and associates found that duplexes containing psoralen monoadducts (furan- and pyrone-side HMT adducts) were both incised by (A)BC excinuclease at the usual sites, the eighth phosphodiester bond on the 5′ side and the fifth bond on the 3′ side

of the adducted thymidine [Van Houten *et al.*, 1986a]. An HMT-crosslinked duplex, however, was incised only on the furan-side strand, and at the ninth phosphodiester bond on the 5′ side and the third bond on the 3′ side. This specificity of incision offered a clue as to how the mechanism of sequential incisions proposed by Cole could occur [Van Houten *et al.*, 1986b].

The work presented here extends those *in vitro* findings with regard to the details of error-free psoralen crosslink repair in *E. coli*. We observed that in the presence of a third strand, (A)BC excinuclease will recognize and preferentially incise the pyrone-side strand of an HMT crosslink. Initially, we used three-stranded substrates in which an HMT-monoadducted oligomer of between 30 and 107 nucleotides had been inserted into FI pUC19 plasmid by the RecA protein and subsequently irradiated to form a crosslink between the oligomer and its complement (Chapter 2). The crosslinked oligonucleotide represented the furan-side strand, thus modeling the oligomer excised by furan-side incisions of a crosslinked duplex. (A)BC excinuclease appeared indifferent to the length of this oligomer and incised only the pyrone-side (pUC19 complement to the oligomer) strand in each complex (Chapter 3). We then observed that this three-stranded complex need not be a final product of RecA-mediated homologous pairing, but that a recombination intermediate in the presence of RecA also selectively induced pyrone-side incisions at the crosslink site (Chapter 4). Whether this intermediate would also suffice for the replacement strand synthesis required for completion of the repair process is not clear. Most likely, DNA polymerase requires more than a "transient" template strand.

In the course of these studies, we also characterized parameters affecting the efficiency of RecA-mediated homologous pairing with oligonucleotide substrates and a supercoiled plasmid (Chapter 2). Both the length of the oligonucleotide and the internal location of the psoralen adduct affected the efficiency of complex formation. The tolerance that RecA exhibited for the presence of a psoralen adduct was perhaps not surprising since the protein had been observed to pair substrates despite the presence of pyrimidine dimers

[Livneh and Lehman, 1982] or mismatches and insertions [Bianchi and Radding, 1983]. The deproteinized three-stranded complexes showed a characteristic unwinding induced by the inserted oligonucleotide, but the precise structures of these complexes were not determined.

In summary, our work characterizes some of the molecular events of (A)BC excinuclease-mediated RecA-dependent crosslink repair. With uniquely psoralen-adducted substrates and purified proteins, we have found evidence for the sequential incision and recombination mechanism proposed to explain error-free crosslink repair (Figure 3-1). Mutagenic mechanisms certainly exist as well, possibly involving replicative bypass of crosslinked sites that have been incised on one strand but not the other.

Where do these results fit in the "big picture"? In principle, an understanding of events at a molecular level will enable reconstitution of crosslink repair pathways *in vitro*. Although there is no guarantee that any *in vitro* model will accurately depict the cellular process, such models certainly reflect functions that the component proteins are capable of having *in vivo*.

In a broader view, it is important too to note the extent to which an understanding of procaryotic DNA repair can facilitate the understanding of eucaryotic repair. From a more selfish reference point, DNA repair in humans may ultimately be understood. Procaryotic systems are simpler and hence more readily studied and characterized in detail. Parallels that do exist among bacteria, yeast and mammals support the idea that procaryotes can shed light on the analogous processes in eucaryotes. Intuitively, perhaps, repair mechanisms are the same in principle and differ primarily in their complexity, consistent with an organisms's evolutionary position (size and genetic complexity, for example).

In the yeast *Saccharomyces cerevisiae*, at least twelve genetic loci have been implicated in excision repair. Ten of these are unique to the nucleotide excision repair

epistasis group. This group, the RAD3 group, has been identified using yeast mutants with sensitivity to UV radiation. Mutations in a group of epistatically related genes result in the same degree of sensitivity whether just one or more than one gene is affected. The *RAD1*, *RAD2*, *RAD3*, *RAD4*, and *RAD10* genes, in particular, are absolutely required for nucleotide excision repair. All have been isolated and sequenced. Neither the nucleotide nor the amino acid sequences of any of these five show extensive homology with other proteins, but there are interesting regions of limited amino acid sequence homology. The Rad3 protein (~ 90 kilodaltons) shares homology with the *E. coli* UvrA, UvrB, and UvrD proteins over a 22-amino acid segment, and appears to have ATPase- and nucleotide-binding activities. The Rad10 protein may also bind DNA. Both the Rad3 and Rad10 proteins possess sequences suggestive of an α-helix–turn–α-helix motif for binding DNA, based upon comparison with a consensus sequence from procaryotic proteins. The *RAD3* gene appears to encode two distinct functions. One is essential to haploid cell viability, and one is associated with nucleotide excision repair. The latter is inactivated by point mutations, suggesting a particular sensitivity to conformational changes. [reviewed by Friedberg, 1987; Friedberg *et al.*, 1988; Myles and Sancar, 1989]

Mammalian systems represent yet another level of complexity. Two particularly useful human cell lines in the study of DNA excision repair are derived from the autosomal recessive disorders Fanconi's anemia (FA) and xeroderma pigmentosum (XP). XP cells are deficient in nucleotide excision repair, and FA cells exhibit a heightened sensitivity to agents which form interstrand crosslinks [reviewed by Averbeck *et al.*, 1988; Moustacchi *et al.*, 1988]. Rodent cell lines, particularly Chinese hamster ovary (CHO) mutants sensitive to UV radiation and deficient in excision repair also offer insight into the mammalian repair systems, and have been used in the isolation of human repair genes [reviewed by Friedberg, 1987; Thompson *et al.*, 1988]. The complexity of mammalian excision repair is suggested by the identification of nine XP and seven CHO complementation groups that at present appear to be completely distinct [Hoeijmakers *et al.*, 1988;

Thompson *et al.*, 1988].

The *ERCC-1* gene (*e*xcision *r*epair *c*ross *c*omplementing; Thompson and Bootsma, 1988) was isolated in 1984 using CHO cells [reviewed by Thompson *et al.*, 1988]. This gene shares significant homology with the C-terminal half of the Rad10 protein of *S. cerevisiae* [reviewed by Friedberg, 1987; Friedberg *et al.*, 1988]. Differences in the amino acid sequences of *ERCC-1* proteins predicted from the isolated mouse and human genes (85% identical overall) mostly map to the N-terminal portion, again suggesting that the C-terminal sequence is critical for the excision repair function(s) [Hoeijmakers *et al.*, 1988]. The predicted *ERCC-1* protein also shares a stretch of homology with the UvrC protein of *E. coli* [reviewed by Sancar and Sancar, 1988].

Efforts to correct excision repair deficiencies in *E. coli*, yeast or mammalian cells using proteins from the other species have thus far yielded only partial success with the *RAD10* gene and CHO mutants [Friedberg *et al.*, 1988]. Other approaches to investigate interspecies relationships include antibody recognition and *in vitro* repair studies with cell-free extracts or purified proteins [reviewed by Friedberg, 1987]. A nucleotide excision repair activity capable of *in vitro* repair of pyrimidine dimers and psoralen monoadducts has been recently identified in a HeLa cell-free extract [Sibghat-Ullah *et al.*, 1989; Sibghat-Ullah and Sancar, 1990] and in XP cells [Wood *et al.*, 1988].

Recombinational repair (RAD52 group) and mutagenic repair (RAD6 group) are two other major repair systems that have been identified in *S. cerevisiae*. As in *E. coli*, these are implicated as cellular responses to psoralen monoadducts and crosslinks in addition to the excision repair pathways. Recombination between sister chromatids may play a role in repair in mammalian cells as well. Glycosylase activities have been identified in *E. coli* and human cells [Boorstein *et al.*, 1989; Doetsch *et al.*, 1987; Weiss *et al.*, 1989], and in *S. cerevisiae* [Gossett *et al.*, 1988]. All three of these systems have also demonstrated a limited ability for replicative bypass of psoralen monoadducts. Evidence from both *E. coli* and *S. cerevisiae* suggests that an intermediate in the excision repair

pathway can serve as a common substrate for other repair processes. [reviewed by Moustacchi, 1988]

The phenomenon of selective repair was first observed in mammalian cells, but also appears to occur in bacteria. One study noted that psoralen crosslinks were removed nearly twice as quickly as monoadducts from the human dihydrofolate reductase (DHFR) gene [Vos and Hanawalt, 1987]. Repair of the *DHFR* gene, among others, has also been found to depend upon transcription. In particular, mammalian repair systems demonstrate a strand-specificity and preferentially target the actively transcribed strand within a transcriptionally active gene [Mellon *et al.*, 1987 and 1988]. This selectivity appears to be associated with transcription by RNA polymerase II rather than polymerase I [Vos, 1989], and may reflect a specific mechanism for overcoming blocked transcription [Mellon and Hanawalt, 1989; Vos, 1989]. In *E. coli*, Mellon and Hanawalt [1989] recently observed that selective repair of UV radiation damage in the lactose operon was detectable in cells exposed to an inducer, isopropyl-β-D-thiogalactoside (IPTG). The nontranscribed strand was repaired at a slower rate, comparable to the rate of repair of either strand in uninduced cells. Transcriptionally-activated excision repair may thus be a significant cellular pathway in all organisms.

Differential repair of psoralen crosslinks and monoadducts in eucaryotic systems may also explain *in vivo* observations of Averbeck and Papdopoulo. In *S. cerevisiae*, Averbeck [1988a and 1988b] noted that a mixture of crosslinks and monoadducts was more mutagenic than a population of monoadducts alone, and that bifunctional psoralen derivatives were more mutagenic than monofunctional ones. In normal human fibroblast cells, Papadopoulo and colleagues [1988] observed that TMP monoadducts can interfere with the efficiency of crosslink repair, as measured by incision of the DNA. In the repair-deficient FA cells, this effect was even more significant [Averbeck *et al.*, 1988]. The variations in the efficiencies of repair of adducts formed by TMP, 8-MOP, and 5-MOP have been attributed to the different levels of monoadduct versus crosslink damage

induced by 365 nm light [Averbeck, 1988b; Papadopoulo *et al.*, 1988].

Complete characterization of eucaryotic DNA repair is clearly much more difficult than for procaryotes as a consequence of the enormous complexity of eukaryotic systems. Similarities that have been noted do suggest that the understanding of *E. coli* excision repair processes can help elucidate the functions of the components of yeast and mammalian systems. Psoralen phototoxicity and the repair of psoralen damage in yeast and human cells, particularly in Fanconi's anemia cell lines, have been the subject of much study and this work has been recently reviewed [Averbeck, 1989]. The work presented in the preceding chapters represents our efforts to clarify the details of *E. coli* nucleotide excision repair using the model system of psoralen-crosslinked DNA.

Appendix 1. List of Abbreviations

5-MOP	5-methoxypsoralen
8-MOP	8-methoxypsoralen
(A)BC	ABC excinuclease, uvrABC endonuclease
ADP, dADP	adenosine 5′-diphosphate, deoxyadenosine 5′-diphosphate
AP	apurinic/apyrimidinic
ATP, dATP	adenosine 5′-triphosphate, deoxyadenosine 5′-triphosphate
ATPγS	adenosine 5′-*O*-(thiotriphosphate)
BSA	bovine serum albumin
CHO	Chinese hamster ovary
CPK	creatine phosphokinase
$\Delta\tau$, $\Delta\tau$*	center-to-center distance between densitometric peaks, in units of turns; please refer to Chapter 2 "Methods"
dCTP	deoxycytidine 5′-triphosphate
dNTP	deoxynucleoside 5′-triphosphate
DNA	deoxyribonucleic acid
ds	double-stranded
DTT	dithiothreitol
EDTA	ethylenediaminetetraacetic acid or [ethylenedinitrilo]tetraacetic acid
ERCC	excision repair cross complementing
FI	supercoiled, covalently closed form of circular DNA
FII	nicked circular DNA
FIII	linearized DNA
FA	Fanconi's anemia
gp	gene product
HMT	4′-hydroxymethyl-4,5′,8-trimethylpsoralen

IPTG	isopropyl-β-D-thiogalactopyranoside
PAGE	polyacrylamide gel electrophoresis
pol	polymerase
RF	replicative form
SDS	sodium dodecyl sulfate
ss	single-stranded
SSB	single-stranded DNA binding protein from *Escherichia coli*
TANE	40 mM Tris·acetate (pH 8 at 25°C), 5 mM NaCl, 1 mM EDTA
TBE	50 mM each Tris·HCl and boric acid, 1 mM EDTA
TMP	4,5′,8-trimethylpsoralen
Tris	Tris(hydroxymethyl)aminomethane or 2-amino-2-(hydroxymethyl)-1,3-propanediol
UV	ultraviolet
X-gal	5-bromo,4-chloro,3-indolyl-β-D-galactopyranoside
XP	xeroderma pigmentosum

Appendix 2. List of Figures

page

References

Abbotts, J., SenGupta, D.N., Zon, G., and Wilson, S.H. (1988) Studies on the mechanism of *Escherichia coli* DNA polymerase I large fragment. *J. Biol. Chem.* **263**: 15094-15103.

Amrein, M., Dürr, R., Stasiak, A., Gross, H., and Travaglini, G. (1989) Scanning tunneling microscopy of uncoated recA-DNA complexes. *Science* **243**: 1708-1711.

Amrein, M., Stasiak, A., Gross, H., Stoll, E., and Travaglini, G. (1988) Scanning tunneling microscopy of recA-DNA complexes coated with a conducting film. *Science* **240**: 514-516.

Averbeck, D. (1988a) Mutagenesis by psoralens on eukaryotic cells, *in Photosensitisation: Molecular, Cellular and Medical Aspects.* G. Moreno, R.H. Pottier and T.G. Truscott, ed. NATO ASI Series, Series H: Cell Biology, Vol. 15. Berlin: Springer-Verlag. pp. 279-291.

Averbeck, D. (1988b) Photomutagenicity induced by psoralens: Modulation of the photomutagenic response in eukaryotes. *Arch. Toxicol. Suppl.* **12**: 35-46.

Averbeck, D. (1989) Recent advances in psoralen phototoxicity mechanism. *Photochem. Photobiol.* **50**: 859-882.

Averbeck, D., Papadopoulo, D., and Moustacchi, E. (1988) Repair of 4,5′,8-trimethylpsoralen plus light-induced DNA damage in normal and Fanconi's anemia cell lines. *Cancer Res.* **48**: 2015-2020.

Bailone, A., Bäckman, A., Sommer, S., Célérier, J., Bagdasarian, M.M., Bagdasarian, M., and Devoret, R. (1988) PsiB polypeptide prevents activation of RecA protein in *Escherichia coli*. *Mol. Gen. Genet.* **214**: 389-395.

Banks, G.R. and Sedgwick, S.G. (1986) Direct ATP photolabeling of *Escherichia coli* RecA proteins: Identification of regions required for ATP binding. *Biochemistry* **25**: 5882-5889.

Battista, J.R., Nohmi, T., Donnelly, C.E., and Walker, G.C. (1988) Role of UmuD and UmuC in UV and chemical mutagenesis, *in Mechanisms and Consequences of DNA Damage Processing.* E.C. Friedberg and P.C. Hanawalt, ed. UCLA Symposia on Molecular and Cellular Biology, New Series, Vol. 83. New York: Alan R. Liss, Inc. pp. 455-459.

Beattie, K.L., Wiegand, R.C., and Radding, C.M. (1977) Uptake of homologous single-stranded fragments by superhelical DNA, II. Characterization of the reaction. *J. Mol. Biol.* **116**: 783-803.

Ben-Hur, E. and Song, P.-S. (1984) The photochemistry and photobiology of furocoumarins (psoralens). *Adv. Radiat. Biol.* **11**: 131-171.

Benedict, R.C. and Kowalczykowski, S.C. (1988) Increase of the DNA strand assimilation activity of recA protein by removal of the C terminus and structure-function studies of the resulting protein fragment. *J. Biol. Chem.* **263**: 15513-15520.

Bianchi, M., DasGupta, C., and Radding, C.M. (1983) Synapsis and the formation of paranemic joints by *E. coli* RecA protein. *Cell* **34**: 931-939.

Bianchi, M.E. and Radding, C.M. (1983) Insertions, deletions and mismatches in heteroduplex DNA made by RecA protein. *Cell* **35**: 511-520.

Blaho, J.A. and Wells, R.D. (1987) Left-handed Z-DNA binding by the recA protein of *Escherichia coli*. *J. Biol. Chem.* **262**: 6082-6088.

Blanar, M.A., Kneller, D., Clark, A.J., Karu, A.E., Cohen, F.E., Langridge, R., and Kuntz, I.D. (1984) A model for the core structure of the *Escherichia coli* RecA protein. *Cold Spring Harbor Symp. Quant. Biol.* **49**: 507-510.

Boiteux, S. and Laval, J. (1982) Coding properties of poly(deoxycytidylic acid) templates containing uracil or apyrimidinic sites: *In vitro* modulation of mutagenesis by deoxyribonucleic acid repair enzymes. *Biochemistry* **21**: 6746-6751.

Bonner, C.A., Randall, S.K., Rayssiguier, C., Radman, M., Eritja, R., Kaplan, B.E., McEntee, K., and Goodman, M.F. (1988) Purification and characterization of an inducible *Escherichia coli* DNA polymerase capable of insertion and bypass at abasic lesions in DNA. *J. Biol. Chem.* **263**: 18946-18952.

Boorstein, R.J., Hilbert, T.P., Cadet, J., Cunningham, R.P., and Teebor, G.W. (1989) UV-induced pyrimidine hydrates in DNA are repaired by bacterial and mammalian DNA glycosylase activities. *Biochemistry* **28**: 6164-6170.

Brenner, S.L., Mitchell, R.S., Morrical, S.W., Neuendorf, S.K., Schutte, B.C., and Cox, M.M. (1987) RecA protein-promoted ATP hydrolysis occurs throughout recA nucleoprotein filaments. *J. Biol. Chem.* **262**: 4011-4016.

Brenner, S.L., Zlotnick, A., and Griffith, J.D. (1988) RecA protein self-assembly. Multiple discrete aggregation states. *J. Mol. Biol.* **204**: 959-972.

Bryant, F.R. and Lehman, I.R. (1985) On the mechanism of renaturation of complementary DNA strands by the recA protein of *Escherichia coli*. *Proc. Natl. Acad. Sci. USA* **82**: 297-301.

Bryant, F.R., Menge, K.L., and Nguyen, T.T. (1989) Kinetic modeling of the RecA protein promoted renaturation of complementary DNA strands. *Biochemistry* **28**: 1062-1069.

Burckhardt, S.E., Woodgate, R., Scheuermann, R.H., and Echols, H. (1988) UmuD mutagenesis protein of *Escherichia coli*: Overproduction, purification, and cleavage by RecA. *Proc. Natl. Acad. Sci. USA* **85**: 1811-1815.

Caron, P.R. and Grossman, L. (1988a) Involvement of a cryptic ATPase activity of UvrB and its proteolysis product, UvrB* in DNA repair. *Nucl. Acids Res.* **16**: 10891-10902.

Caron, P.R. and Grossman, L. (1988b) Potential role of proteolysis in the control of UvrABC incision. *Nucl. Acids Res.* **16**: 10903-10912.

Caron, P.R., Kushner, S.R., and Grossman, L. (1985) Involvement of helicase II (*uvrD* gene product) and DNA polymerase I in excision mediated by the UvrABC protein complex. *Proc. Natl. Acad. Sci. USA* **82**: 4925-4929.

Cassuto, E., Gross, N., Bardwell, E., and Howard-Flanders, P. (1977) Genetic effects of photoadducts and photocross-links in the DNA of phage λ exposed to 360 nm light and tri-methylpsoralen or khellin. *Biochim. Biophys. Acta* **475**: 589-600.

Célérier, J., Sassanfar, M., Bailone, A., and Devoret, R. (1988) PsiB protein inhibits LexA protein cleavage, *in Mechanisms and Consequences of DNA Damage Processing*. E.C. Friedberg and P.C. Hanawalt, ed. UCLA Symposia on Molecular and Cellular Biology, New Series, Vol. 83. New York: Alan R. Liss, Inc. pp. 445-447.

Cheng, S., Gamper, H.B., and Hearst, J.E. (1989) RecA-directed hybridization of psoralen-monoadducted DNA oligonucleotides to duplex targets, *in Photochemical Probes in Biochemistry*. P.E. Nielsen, ed. NATO ASI Series, Series C, Vol. 272. Boston: Kluwer Academic Publishers. pp. 169-177.

Cheng, S., Van Houten, B., Gamper, H.B., Sancar, A., and Hearst, J.E. (1988a) Use of psoralen-modified oligonucleotides to trap three-stranded RecA-DNA complexes and repair of these cross-linked complexes by ABC excinuclease. *J. Biol. Chem.* **263**: 15110-15117.

Cheng, S., Van Houten, B., Gamper, H.B., Sancar, A., and Hearst, J.E. (1988b) Use of triple-stranded DNA complexes to study crosslink repair, *in Mechanisms and Consequences of DNA Damage Processing*. E.C. Friedberg and P.C. Hanawalt, ed. UCLA Symposia on Molecular and Cellular Biology, New Series, Vol. 83. New York: Alan R. Liss, Inc. pp. 105-113.

Chow, S.A., Honigberg, S.M., Bainton, R.J., and Radding, C.M. (1986) Patterns of nuclease protection during strand exchange. RecA protein forms heteroduplex DNA by binding to strands of the same polarity. *J. Biol. Chem.* **261**: 6961-6971.

Chow, S.A., Honigberg, S.M., and Radding, C.M. (1988) DNase protection by RecA protein during strand exchange. *J. Biol. Chem.* **263**: 3335-3347.

Christiansen, G. and Griffith, J. (1986) Visualization of the paranemic joining of homologous DNA molecules catalyzed by the RecA protein of *Escherichia coli*. *Proc. Natl. Acad. Sci. USA* **83**: 2066-2070.

Cimino, G.D., Gamper, H.B., Isaacs, S.T., and Hearst, J.E. (1985) Psoralens as photoactive probes of nucleic acid structure and function: Organic chemistry, photochemistry, and biochemistry. *Ann. Rev. Biochem.* **54**: 1151-1193.

Clark, J.M. and Beardsley, G.P. (1989) Template length, sequence context, and 3'–5' exonuclease activity modulate replicative bypass of thymine glycol lesions *in vitro*. *Biochemistry* **28**: 775-779.

Cole, R.S. (1971) Inactivation of *Escherichia coli*, F′ episomes at transfer, and bacteriophage lambda by psoralen plus 360-nm light: Significance of deoxyribonucleic acid cross-links. *J. Bacteriol.* **107**: 846-852.

Cole, R.S. (1973) Repair of DNA containing interstrand crosslinks in *Escherichia coli*: Sequential excision and recombination. *Proc. Natl. Acad. Sci. USA* **70**: 1064-1068.

Cole, R.S., Levitan, D., and Sinden, R.R. (1976) Removal of psoralen interstrand crosslinks from DNA of *Escherichia coli*: Mechanism and genetic control. *J. Mol. Biol.* **103**: 39-59.

Conley, E.C. and West, S.C. (1989) Homologous pairing and the formation of nascent synaptic intermediates between regions of duplex DNA by RecA protein. *Cell* **56**: 987-995.

Cooper, P.K. (1982) Characterization of long patch excision repair of DNA in ultraviolet-irradiated *Escherichia coli*: An inducible function under Rec-Lex control. *Mol. Gen. Genet.* **185**: 189-197.

Cox, M.M. and Lehman, I.R. (1981) Directionality and polarity in recA protein-promoted branch migration. *Proc. Natl. Acad. Sci. USA* **78**: 6018-6022.

Cox, M.M. and Lehman, I.R. (1987) Enzymes of general recombination. *Ann. Rev. Biochem.* **56**: 229-262.

Cox, M.M., Pugh, B.F., Schutte, B.C., Lindsley, J.E., Lee, J., and Morrical, S.W. (1987) On the mechanism of RecA protein-promoted DNA branch migration, *in DNA Replication and Recombination*. R. McMacken and T.J. Kelley, ed. UCLA Symposia on Molecular and Cellular Biology, New Series, Vol. 47. New York: Alan R. Liss, Inc. pp. 597-607.

Cunningham, R.P., Shibata, T., DasGupta, C., and Radding, C.M. (1979) Single strands induce recA protein to unwind duplex DNA for homologous pairing. *Nature* **281**: 191-195.

DasGupta, C. and Radding, C.M. (1982) Lower fidelity of RecA protein catalysed homologous pairing with a superhelical substrate. *Nature* **295**: 71-73.

Devoret, R., Bailone, A., Dutreix, M., Moreau, P.L., Sommer, S., and Bagdasarian, M. (1988) Regulation of activation of RecA protein in *E. coli*, *in Mechanisms and Consequences of DNA Damage Processing*. E.C. Friedberg and P.C. Hanawalt, ed. UCLA Symposia on Molecular and Cellular Biology, New Series, Vol. 83. New York: Alan R. Liss, Inc. pp. 437-443.

Di Capua, E., Engel, A., Stasiak, A., and Koller, T. (1982) Characterization of complexes between recA protein and duplex DNA by electron microscopy. *J. Mol. Biol.* **157**: 87-103.

Di Capua, E. and Müller, B. (1987) The accessibility of DNA to dimethylsulfate in complexes with RecA protein. *EMBO J.* **6**: 2493-2498.

Di Capua, E., Schnarr, M., and Timmins, P.A. (1989) The location of DNA in complexes of recA protein with double-stranded DNA. A neutron scattering study. *Biochemistry* **28**: 3287-3292.

Doetsch, P.W., Henner, W.D., Cunningham, R.P., Toney, J.H., and Helland, D.E. (1987) A highly conserved endonuclease activity present in *Escherichia coli*, bovine, and human cells recognizes oxidative DNA damage at sites of pyrimidines. *Mol. Cell. Biol.* **7**: 26-32.

Dombroski, D.F., Scraba, D.G., Bradley, R.D., and Morgan, A.R. (1983) Studies of the interaction of RecA protein with DNA. *Nucl. Acids Res.* **11**: 7487-7504.

Dunn, K., Chrysogelos, S., and Griffith, J. (1982) Electron microscopic visualization of RecA-DNA filaments: Evidence for a cyclic extension of duplex DNA. *Cell* **28**: 757-765.

Egelman, E.H. and Stasiak, A. (1986) Structure of helical RecA-DNA complexes. Complexes formed in the presence of ATP-gamma-S or ATP. *J. Mol. Biol.* **191**: 677-697.

Egelman, E.H. and Stasiak, A. (1988) Structure of helical RecA-DNA complexes, II. Local conformational changes visualized in bundles of RecA-ATPγS filaments. *J. Mol. Biol.* **200**: 329-349.

Egelman, E.H. and Yu, X. (1989) The location of DNA in RecA-DNA helical filaments. *Science* **245**: 404-407.

Egner, C., Azhderian, E., Tsang, S.S., Radding, C.M., and Chase, J.W. (1987) Effects of various single-stranded-DNA-binding proteins on reactions promoted by RecA protein. *J. Bacteriol.* **169**: 3422-3428.

El-Deiry, W.S., So, A.G., and Downey, K.M. (1988) Mechanisms of error discrimination by *Escherichia coli* DNA polymerase I. *Biochemistry* **27**: 546-553.

Ennis, D.G., Ossanna, N., and Mount, D.W. (1989) Genetic separation of *Escherichia coli recA* functions for SOS mutagenesis and repressor cleavage. *J. Bacteriol.* **171**: 2533-2541.

Fishel, R. and Rich, A. (1988) The role of left-handed Z-DNA in general genetic recombination, *in Mechanisms and Consequences of DNA Damage Processing*. E.C. Friedberg and P.C. Hanawalt, ed. UCLA Symposia on Molecular and Cellular Biology, New Series, Vol. 83. New York: Alan R. Liss, Inc. pp. 23-32.

Flory, J., Tsang, S.S., and Muniyappa, K. (1984) Isolation and visualization of active presynaptic filaments of recA protein and single-stranded DNA. *Proc. Natl. Acad. Sci. USA* **81**: 7026-7030.

Foster, P.L. and Sullivan, A.D. (1988) Interactions between epsilon, the proofreading subunit of DNA polymerase III, and proteins involved in the SOS response of *Escherichia coli*. *Mol. Gen. Genet.* **214**: 467-473.

Friedberg, E.C. (1985) *DNA Repair*. New York: W.H. Freeman and Co.

Friedberg, E.C. (1987) The molecular biology of nucleotide excision repair of DNA: Recent progress, *in Molecular Biology of DNA Repair*. A. Collins, R.T. Johnson and J.M. Boyle, ed. Journal of Cell Science Supplement, Vol. 6. Cambridge: The Company of Biologists, Ltd. pp. 1-23.

Friedberg, E.C. (1988) Deoxyribonucleic acid repair in the yeast *Saccharomyces cerevisiae*. *Microbiol. Rev.* **52**: 70-102.

Friedberg, E.C., Burtscher, H.J., Cooper, A.J., Couto, L.B., Harosh, I., Kalainov, D., Lambert, C., Naumovski, L., Robinson, G.W., Siede, W., Song, J.-M., and Weiss, W.A. (1988) *RAD* genes and Rad proteins for nucleotide excision repair in the yeast *Saccharomyces cerevisiae*: Recent progress, *in Mechanisms and Consequences of DNA Damage Processing*. E.C. Friedberg and P.C. Hanawalt, ed. UCLA Symposia on Molecular and Cellular Biology, New Series, Vol. 83. New York: Alan R. Liss, Inc. pp. 185-190.

Gamper, H., Piette, J., and Hearst, J.E. (1984) Efficient formation of a crosslinkable HMT monoadduct at the Kpn I recognition site. *Photochem. Photobiol.* **40**: 29-34.

Gamper, H.B., Cimino, G.D., and Hearst, J.E. (1987) Solution hybridization of cross-linkable DNA oligonucleotides to bacteriophage M13 DNA. Effect of secondary structure on hybridization kinetics and equilibria. *J. Mol. Biol.* **197**: 349-362.

Gish, G. and Eckstein, F. (1988) DNA and RNA sequence determination based on phosphorothioate chemistry. *Science* **240**: 1520-1522.

Gonda, D.K. and Radding, C.M. (1983) By searching processively RecA protein pairs molecules that share a limited stretch of homology. *Cell* **34**: 647-654.

Gonda, D.K. and Radding, C.M. (1986) The mechanism of the search for homology promoted by RecA protein. *J. Biol. Chem.* **261**: 13087-13096.

Gossett, J., Lee, K., Cunningham, R.P., and Doetsch, P.W. (1988) Yeast redoxyendonuclease, a DNA repair enzyme similar to *Escherichia coli* endonuclease III. *Biochemistry* **27**: 2629-2634.

Grafstrom, R.H. (1986) The repair of pyrimidine dimers via a DNA-glycosylase mechanism, *in Mechanisms of DNA Damage and Repair: Implications for Carcinogenesis and Risk Assessment*. M.G. Simic, L. Grossman and A.C. Upton, ed. Basic Life Sciences, Vol. 38. New York: Plenum Press. pp. 281-286.

Griffith, J.D. and Harris, L.D. (1988) DNA strand exchanges. *CRC Crit. Rev. Biochem.* **23, Supplement 1**: S43-S86.

Gruskin, E.A. and Lloyd, R.S. (1988) Molecular analysis of plasmid DNA repair within ultraviolet-irradiated *Escherichia coli*. II. UvrABC-initiated excision repair and photolyase-catalyzed dimer monomerization. *J. Biol. Chem.* **263**: 12738-12743.

Hahn, T.-R., West, S., and Howard-Flanders, P. (1988) RecA-mediated strand exchange reactions between duplex DNA molecules containing damaged bases, deletions, and insertions. *J. Biol. Chem.* **263**: 7431-7436.

Hanawalt, P.C., Cooper, P.K., Ganesan, A.K., and Smith, C.A. (1979) DNA repair in bacteria and mammalian cells. *Ann. Rev. Biochem.* **48**: 783-836.

Hearst, J.E. (1981) Psoralen photochemistry. *Ann. Rev. Biophys. Bioeng.* **10**: 69-86.

Hoeijmakers, J.H.J., van Duin, M., Weeda, G., van der Eb, A.J., Troelstra, C., Eker, A.P.M., Jaspers, N.G.J., Westerveld, A., and Bootsma, D. (1988) Analysis of mammalian excision repair: From mutants to genes and gene products, *in Mechanisms and Consequences of DNA Damage Processing*. E.C. Friedberg and P.C. Hanawalt, ed. UCLA Symposia on Molecular and Cellular Biology, New Series, Vol. 83. New York: Alan R. Liss, Inc. pp. 281-287.

Honigberg, S.M., Gonda, D.K., Flory, J., and Radding, C.M. (1985) The pairing activity of stable nucleoprotein filaments made from recA protein, single-stranded DNA, and adenosine 5′-(γ-thio)triphosphate. *J. Biol. Chem.* **260**: 11845-11851.

Honigberg, S.M. and Radding, C.M. (1988) The mechanics of winding and unwinding helices in recombination: Torsional stress associated with strand transfer promoted by RecA protein. *Cell* **54**: 525-532.

Howard-Flanders, P., West, S.C., Cassuto, E., Hahn, T.-R., and Egelman, E. (1987) Structure of RecA spiral filaments and their role in homologous pairing and strand exchange in genetic recombination, *in DNA Replication and Recombination.* R. McMacken and T.J. Kelley, ed. UCLA Symposia on Molecular and Cellular Biology, New Series, Vol. 47. New York: Alan R. Liss, Inc. pp. 609-617.

Howard-Flanders, P., West, S.C., Rusche, J.R., and Egelman, E.H. (1984a) Molecular mechanisms of general genetic recombination: The DNA-binding sites of RecA protein. *Cold Spring Harbor Symp. Quant. Biol.* **49**: 571-580.

Howard-Flanders, P., West, S.C., and Stasiak, A. (1984b) Role of RecA protein spiral filaments in genetic recombination. *Nature* **309**: 215-220.

Husain, I., Van Houten, B., Thomas, D.C., Abdel-Monem, M., and Sancar, A. (1985) Effect of DNA polymerase I and DNA helicase II on the turnover rate of UvrABC excision nuclease. *Proc. Natl. Acad. Sci. USA* **82**: 6774-6778.

Isaacs, S.T., Shen, C.-k.J., Hearst, J.E., and Rapoport, H. (1977) Synthesis and characterization of new psoralen derivatives with superior photoreactivity with DNA and RNA. *Biochemistry* **16**: 1058-1064.

Jones, B.K. and Yeung, A.T. (1988) Repair of 4,5′,8-trimethylpsoralen monoadducts and cross-links by the *Escherichia coli* UvrABC endonuclease. *Proc. Natl. Acad. Sci. USA* **85**: 8410-8414.

Jones, B.K. and Yeung, A.T. (1990) DNA base composition determines the specificity of UvrABC endonuclease incision of a psoralen cross-link. *J. Biol. Chem.* **265**: 3489-3496.

Kahn, R., Cunningham, R.P., DasGupta, C., and Radding, C.M. (1981) Polarity of heteroduplex formation promoted by *Escherichia coli* recA protein. *Proc. Natl. Acad. Sci. USA* **78**: 4786-4790.

Kawashima, H., Horii, T., Ogawa, T., and Ogawa, H. (1984) Functional domains of *Escherichia coli* recA protein deduced from the mutational sites in the gene. *Mol. Gen. Genet.* **193**: 288-292.

Keller, W. (1975) Determination of the number of superhelical turns in simian virus 40 DNA by gel electrophoresis. *Proc. Natl. Acad. Sci. USA* **72**: 4876-4880.

Khamis, M.I., Casas-Finet, J.R., and Maki, A.H. (1988) Binding of recA protein to single- and double-stranded polynucleotides occurs without involvement of its aromatic residues in stacking interactions with nucleotide bases. *Biochim. Biophys. Acta* **950**: 132-137.

Kim, J.-I., Heuser, J., and Cox, M.M. (1989) Enhanced recA protein binding to Z DNA represents a kinetic perturbation of a general duplex DNA binding pathway. *J. Biol. Chem.* **264**: 21848-21856.

Knight, K.L., Hess, R.M., and McEntee, K. (1988) Conservation of an ATP-binding domain among RecA proteins from *Proteus vulgaris, Erwinia carotovora, Shigella flexneri*, and *Escherichia coli* K-12 and B/r. *J. Bacteriol.* **170**: 2427-2432.

Knight, K.L. and McEntee, K. (1985) Covalent modification of the *recA* protein from *Escherichia coli* with the photoaffinity label 8-azidoadenosine 5′-triphosphate. *J. Biol. Chem.* **260**: 867-872.

Kobayashi, N., Knight, K., and McEntee, K. (1987) Evidence for nucleotide-mediated changes in the domain structure of the *RecA* protein of *Escherichia coli. Biochemistry* **26**: 6801-6810.

Kodadek, T. and Gamper, H. (1988) Efficient synthesis of a supercoiled M13 DNA molecule containing a site specifically placed psoralen adduct and its use as a substrate for DNA replication. *Biochemistry* **27**: 3210-3215.

Koffel-Schwartz, N., Maenhaut-Michel, G., and Fuchs, R.P.P. (1987) Specific strand loss in *N*-2-acetylaminofluorene-modified DNA. *J. Mol. Biol.* **193**: 651-659.

Konforti, B.B. and Davis, R.W. (1987) 3′ Homologous free ends are required for stable joint molecule formation by the RecA and single-stranded binding proteins of *Escherichia coli. Proc. Natl. Acad. Sci. USA* **84**: 690-694.

Kornberg, A. (1980) *DNA Replication.* San Francisco: W.H. Freeman and Co.

Kowalczykowski, S.C. (1986) Interaction of RecA protein with a photoaffinity analogue of ATP, 8-azido-ATP: Determination of nucleotide cofactor binding parameters and of the relationship between ATP binding and ATP hydrolysis. *Biochemistry* **25**: 5872-5881.

Kowalczykowski, S.C. (1987) Mechanistic aspects of the DNA strand exchange activity of *E. coli* recA protein. *Trends Biochem. Sci.* **12**: 141-145.

Kowalczykowski, S.C., Clow, J., and Krupp, R.A. (1987a) Properties of the duplex DNA-dependent ATPase activity of *Escherichia coli* RecA protein and its role in branch migration. *Proc. Natl. Acad. Sci. USA* **84**: 3127-3131.

Kowalczykowski, S.C., Clow, J., Somani, R., and Varghese, A. (1987b) Effects of the *Escherichia coli* SSB protein on the binding of *Escherichia coli* RecA protein to

single-stranded DNA. Demonstration of competitive binding and the lack of a specific protein-protein interaction. *J. Mol. Biol.* **193**: 81-95.

Kowalczykowski, S.C. and Krupp, R.A. (1987) Effects of *Escherichia coli* SSB protein on the single-stranded DNA-dependent ATPase activity of *Escherichia coli* RecA protein. Evidence that SSB protein facilitates the binding of RecA protein to regions of secondary structure within single-stranded DNA. *J. Mol. Biol.* **193**: 97-113.

Lackey, D., Krauss, S.W., and Linn, S. (1982) Isolation of an altered form of DNA polymerase I from *Escherichia coli* cells induced for *recA/lexA* functions. *Proc. Natl. Acad. Sci. USA* **79**: 330-334.

Lackey, D., Krauss, S.W., and Linn, S. (1985) Characterization of DNA polymerase I*, a form of DNA polymerase I found in *Escherichia coli* expressing SOS functions. *J. Biol. Chem.* **260**: 3178-3184.

Larson, K.L. and Strauss, B.S. (1987) Influence of template strandedness on *in vitro* replication of mutagen-damaged DNA. *Biochemistry* **26**: 2471-2479.

Leahy, M.C. and Radding, C.M. (1986) Topography of the interaction of recA protein with single-stranded deoxyoligonucleotides. *J. Biol. Chem.* **261**: 6954-6960.

Lin, J.-J. and Sancar, A. (1989) A new mechanism for repairing oxidative damage to DNA: (A)BC excinuclease removes AP sites and thymine glycols from DNA. *Biochemistry* **28**: 7979-7984.

Lin, P.-F., Bardwell, E., and Howard-Flanders, P. (1977) Initiation of genetic exchanges in λ phage-prophage crosses. *Proc. Natl. Acad. Sci. USA* **74**: 291-295.

Little, J.W. (1984) Autodigestion of LexA and phage λ repressors. *Proc. Natl. Acad. Sci. USA* **81**: 1375-1379.

Little, J.W. and Mount, D.W. (1982) The SOS regulatory system of *Escherichia coli*. *Cell* **29**: 11-22.

Livneh, Z. and Lehman, I.R. (1982) Recombinational bypass of pyrimidine dimers promoted by the recA protein of *Escherichia coli*. *Proc. Natl. Acad. Sci. USA* **79**: 3171-3175.

Lu, C. and Echols, H. (1987) RecA protein and SOS. Correlation of mutagenesis phenotype with binding of mutant RecA proteins to duplex DNA and LexA cleavage. *J. Mol. Biol.* **196**: 497-504.

Lu, C., Scheuermann, R.H., and Echols, H. (1986) Capacity of RecA protein to bind preferentially to UV lesions and inhibit the editing subunit (ε) of DNA polymerase III: A possible mechanism for SOS-induced targeted mutagenesis. *Proc. Natl. Acad. Sci. USA* **83**: 619-623.

Maki, S. and Kornberg, A. (1988) DNA polymerase III holoenzyme of *Escherichia coli*. III. Distinctive processive polymerases reconstituted from purified subunits. *J. Biol. Chem.* **263**: 6561-6569.

Maxam, A.M. and Gilbert, W. (1980) Sequencing end-labeled DNA with base-specific chemical cleavages. *Methods Enzymol.* **65**: 499-560.

McEntee, K. (1985) Kinetics of DNA renaturation catalyzed by the *RecA* protein of *Escherichia coli*. *Biochemistry* **24**: 4345-4351.

McEntee, K., Hesse, J.E., and Epstein, W. (1976) Identification and radiochemical purification of the *recA* protein of *Escherichia coli* K-12. *Proc. Natl. Acad. Sci. USA* **73**: 3979-3983.

McEntee, K. and Weinstock, G.M. (1981) The *recA* enzyme of *Escherichia coli* and recombination assays. *Enzymes* **14**: 445-470.

McEntee, K., Weinstock, G.M., and Lehman, I.R. (1981) DNA and nucleoside triphosphate binding properties of recA protein from *Escherichia coli*. *Prog. Nucl. Acid Res. Mol. Biol.* **26**: 265-279.

McKay, D.B., Steitz, T.A., Weber, I.T., West, S.C., and Howard-Flanders, P. (1980) Crystallization of monomeric recA protein. *J. Biol. Chem.* **255**: 6662.

Mellon, I. and Hanawalt, P.C. (1989) Induction of the *Escherichia coli* lactose operon selectively increases repair of its transcribed DNA strand. *Nature* **342**: 95-98.

Mellon, I., Spivak, G., and Hanawalt, P.C. (1987) Selective removal of transcription-blocking DNA damage from the transcribed strand of the mammalian *DHFR* gene. *Cell* **51**: 241-249.

Mellon, I., Spivak, G., and Hanawalt, P.C. (1988) Strand specificity of DNA repair in CHO cells expressing the human *ERCC-1* gene, *in Mechanisms and Consequences of DNA Damage Processing*. E.C. Friedberg and P.C. Hanawalt, ed. UCLA Symposia on Molecular and Cellular Biology, New Series, Vol. 83. New York: Alan R. Liss, Inc. pp. 263-266.

Menetski, J.P. and Kowalczykowski, S.C. (1985) Interaction of RecA protein with single-stranded DNA. Quantitative aspects of binding affinity modulation by nucleotide cofactors. *J. Mol. Biol.* **181**: 281-295.

Menetski, J.P. and Kowalczykowski, S.C. (1989) Enhancement of *Escherichia coli* RecA protein enzymatic function by dATP. *Biochemistry* **28**: 5871-5881.

Menetski, J.P., Varghese, A., and Kowalczykowski, S.C. (1988) Properties of the high-affinity single-stranded DNA binding state of the *Escherichia coli* RecA protein. *Biochemistry* **27**: 1205-1212.

Midden, W.R. (1988) Chemical mechanisms of the bioeffects of furocoumarins: The role of reactions with proteins, lipids, and other cellular constituents, *in Psoralen DNA Photobiology*. F.P. Gasparro, ed. Vol. 2. Boca Raton: CRC Press, Inc. pp. 1-49.

Modrich, P. (1989) Methyl-directed DNA mismatch correction. *J. Biol. Chem.* **264**: 6597-6600.

Moreau, P.L. (1985) Role of *Escherichia coli* RecA protein in SOS induction and post-replication repair. *Biochimie* **67**: 353-356.

Moreau, P.L. (1987) Effects of overproduction of single-stranded DNA-binding protein on RecA protein-dependent processes in *Escherichia coli*. *J. Mol. Biol.* **194**: 621-634.

Moreau, P.L. (1988) Overproduction of single-stranded-DNA-binding protein specifically inhibits recombination of UV-irradiated bacteriophage DNA in *Escherichia coli*. *J. Bacteriol.* **170**: 2493-2500.

Morrical, S.W., Lee, J., and Cox, M.M. (1986) Continuous association of *Escherichia coli* single-stranded DNA binding protein with stable complexes of *recA* protein and single-stranded DNA. *Biochemistry* **25**: 1482-1494.

Moustacchi, E. (1988) Photomutagenicity induced by psoralens: Mechanism of repair and photomutagenicity. *Arch. Toxicol. Suppl.* **12**: 26-34.

Moustacchi, E., Papadopoulo, D., Averbeck, D., Diatloff-Zito, C., Rousset, S., and Nocentini, S. (1988) Fanconi's anemia: Genetic and molecular studies, *in Mechanisms and Consequences of DNA Damage Processing*. E.C. Friedberg and P.C. Hanawalt, ed. UCLA Symposia on Molecular and Cellular Biology, New Series, Vol. 83. New York: Alan R. Liss, Inc. pp. 371-380.

Muniyappa, K., Shaner, S.L., Tsang, S.S., and Radding, C.M. (1984) Mechanism of the concerted action of recA protein and helix-destabilizing proteins in homologous recombination. *Proc. Natl. Acad. Sci. USA* **81**: 2757-2761.

Myles, G.M. and Sancar, A. (1989) DNA repair. *Chem. Res. Toxicol.* **2**: 197-226.

Nakamaye, K.L., Gish, G., Eckstein, F., and Vosberg, H.-P. (1988) Direct sequencing of polymerase chain reaction amplified DNA fragments through the incorporation of deoxynucleoside α-thiotriphosphates. *Nucl. Acids Res.* **16**: 9947-9959.

Navaratnam, S., Myles, G.M., Strange, R.W., and Sancar, A. (1989) Evidence from extended x-ray absorption fine structure and site-specific mutagenesis for zinc fingers in UvrA protein of *Escherichia coli*. *J. Biol. Chem.* **264**: 16067-16071.

Nohmi, T., Battista, J.R., Dodson, L.A., and Walker, G.C. (1988) RecA-mediated cleavage activates UmuD for mutagenesis: Mechanistic relationship between transcriptional derepression and posttranslational activation. *Proc. Natl. Acad. Sci. USA* **85**: 1816-1820.

O'Farrell, P. (1981) Replacement synthesis method of labeling DNA fragments. *BRL Focus* **3**: 1-3.

Orren, D.K. and Sancar, A. (1989) The (A)BC excinuclease of *Escherichia coli* has only the UvrB and UvrC subunits in the incision complex. *Proc. Natl. Acad. Sci. USA* **86**: 5237-5241.

Orren, D.K. and Sancar, A. (1990) Formation and enzymatic properties of the UvrB–DNA complex. *submitted*

Ossanna, N., Peterson, K.R., and Mount, D.W. (1987) UV-inducible SOS response in *Escherichia coli*. *Photochem. Photobiol.* **45**: 905-908.

Papadopoulo, D., Averbeck, D., and Moustacchi, E. (1988) High levels of 4,5′,8-trimethylpsoralen photoinduced furan-side monoadducts can block cross-link removal in normal human cells. *Photochem. Photobiol.* **47**: 321-326.

Parsons, B.J. (1980) Psoralen photochemistry. *Photochem. Photobiol.* **32**: 813-821.

Peterson, K.R., Ossanna, N., Thliveris, A.T., Ennis, D.G., and Mount, D.W. (1988) Derepression of specific genes promotes DNA repair and mutagenesis in *Escherichia coli*. *J. Bacteriol.* **170**: 1-4.

Phizicky, E.M. and Roberts, J.W. (1981) Induction of SOS functions: Regulation of proteolytic activity of *E. coli* RecA protein by interaction with DNA and nucleoside triphosphate. *Cell* **25**: 259-267.

Piette, J., Gamper, H.B., van de Vorst, A., and Hearst, J.E. (1988) Mutagenesis induced by site specifically placed 4′-hydroxymethyl-4,5′,8-trimethylpsoralen adducts. *Nucl. Acids Res.* **16**: 9961-9977.

Piette, J.G. and Hearst, J.E. (1983) Termination sites of the *in vitro* nick-translation reaction on DNA that had photoreacted with psoralen. *Proc. Natl. Acad. Sci. USA* **80**: 5540-5544.

Pu, W.T., Kahn, R., Munn, M.M., and Rupp, W.D. (1989) UvrABC incision of *N*-methylmitomycin A–DNA monoadducts and cross-links. *J. Biol. Chem.* **264**: 20697-20704.

Pugh, B.F. and Cox, M.M. (1987a) RecA protein binding to the heteroduplex product of DNA strand exchange. *J. Biol. Chem.* **262**: 1337-1343.

Pugh, B.F. and Cox, M.M. (1987b) Stable binding of recA protein to duplex DNA. *J. Biol. Chem.* **262**: 1326-1336.

Pugh, B.F., Schutte, B.C., and Cox, M.M. (1989) Extent of duplex DNA underwinding induced by RecA protein binding in the presence of ATP. *J. Mol. Biol.* **205**: 487-492.

Pustell, J. and Kafatos, F.C. (1982) A convenient and adaptable package of DNA sequence analysis programs for microcomputers. *Nucl. Acids Res.* **10**: 51-59.

Rabkin, S.D., Moore, P.D., and Strauss, B.S. (1983) *In vitro* bypass of UV-induced lesions by *Escherichia coli* DNA polymerase I: Specificity of nucleotide incorporation. *Proc. Natl. Acad. Sci. USA* **80**: 1541-1545.

Radding, C.M. (1982) Homologous pairing and strand exchange in genetic recombination. *Ann. Rev. Genet.* **16**: 405-437.

Radding, C.M. (1989) Helical RecA nucleoprotein filaments mediate homologous pairing and strand exchange. *Biochim. Biophys. Acta* **1008**: 131-145.

Radding, C.M., Flory, J., Wu, A., Kahn, R., DasGupta, C., Gonda, D., Bianchi, M., and Tsang, S.S. (1982) Three phases in homologous pairing: Polymerization of *recA* protein on single-stranded DNA, synapsis, and polar strand exchange. *Cold Spring Harbor Symp. Quant. Biol.* **47**: 821-828.

Ramdas, J., Mythili, E., and Muniyappa, K. (1989) RecA protein promoted homologous pairing *in vitro*. *J. Biol. Chem.* **264**: 17395-17400.

Register, J.C., III, Christiansen, G., and Griffith, J. (1987) Electron microscopic visualization of the RecA protein-mediated pairing and branch migration phases of DNA strand exchange. *J. Biol. Chem.* **262**: 12812-12820.

Register, J.C., III and Griffith, J. (1985a) 10 nm RecA protein filaments formed in the presence of Mg^{2+} and ATPγS may contain RNA. *Mol. Gen. Genet.* **199**: 415-420.

Register, J.C., III and Griffith, J. (1985b) The direction of RecA protein assembly onto single strand DNA is the same as the direction of strand assimilation during strand exchange. *J. Biol. Chem.* **260**: 12308-12312.

Register, J.C., III and Griffith, J. (1988) Direct visualization of RecA protein binding to and unwinding duplex DNA following the D-loop cycle. *J. Biol. Chem.* **263**: 11029-11032.

Riddles, P.W. and Lehman, I.R. (1985a) The formation of paranemic and plectonemic joints between DNA molecules by the recA and single-stranded DNA-binding proteins of *Escherichia coli*. *J. Biol. Chem.* **260**: 165-169.

Riddles, P.W. and Lehman, I.R. (1985b) The formation of plectonemic joints by the recA protein of *Escherichia coli*. Requirement for ATP hydrolysis. *J. Biol. Chem.* **260**: 170-173.

Roman, L.J. and Kowalczykowski, S.C. (1986) Relationship of the physical and enzymatic properties of *Escherichia coli* RecA protein to its strand exchange activity. *Biochemistry* **25**: 7375-7385.

Roman, L.J. and Kowalczykowski, S.C. (1989) Formation of heteroduplex DNA promoted by the combined activities of *Escherichia coli* recA and recBCD proteins. *J. Biol. Chem.* **264**: 18340-18348.

Rusche, J.R., Konigsberg, W., and Howard-Flanders, P. (1985) Isolation of altered recA polypeptides and interaction with ATP and DNA. *J. Biol. Chem.* **260**: 949-955.

Saffran, W.A. (1988) Genotoxic effects of psoralen, *in Psoralen DNA Photobiology*. F.P. Gasparro, ed. Vol. 2. Boca Raton: CRC Press, Inc. pp. 73-85.

Saffran, W.A. and Cantor, C.R. (1984a) The complete pattern of mutagenesis arising from the repair of site-specific psoralen crosslinks: Analysis by oligonucleotide hybridization. *Nucl. Acids Res.* **12**: 9237-9248.

Saffran, W.A. and Cantor, C.R. (1984b) Mutagenic SOS repair of site-specific psoralen damage in plasmid pBR322. *J. Mol. Biol.* **178**: 595-609.

Sage, E., Le Doan, T., Boyer, V., Helland, D.E., Kittler, L., Helene, C., and Moustacchi, E. (1989) Oxidative DNA damage photo-induced by 3-carbethoxypsoralen and other furocoumarins. Mechanisms of photo-oxidation and recognition by repair enzymes. *J. Mol. Biol.* **209**: 297-314.

Sancar, A., Franklin, K.A., Sancar, G., and Tang, M.-s. (1985) Repair of psoralen and acetylaminofluorene DNA adducts by ABC excinuclease. *J. Mol. Biol.* **184**: 725-734.

Sancar, A. and Rupp, W.D. (1983) A novel repair enzyme: UvrABC excision nuclease of *Escherichia coli* cuts a DNA strand on both sides of the damaged region. *Cell* **33**: 249-260.

Sancar, A. and Sancar, G.B. (1988) DNA repair enzymes. *Ann. Rev. Biochem.* **57**: 29-67.

Sancar, A., Stachelek, C., Konigsberg, W., and Rupp, W.D. (1980) Sequences of the *recA* gene and protein. *Proc. Natl. Acad. Sci. USA* **77**: 2611-2615.

Schaaper, R.M., Kunkel, T.A., and Loeb, L.A. (1983) Infidelity of DNA synthesis associated with bypass of apurinic sites. *Proc. Natl. Acad. Sci. USA* **80**: 487-491.

Schutte, B.C. and Cox, M.M. (1987) Homology-dependent changes in adenosine 5′-triphosphate hydrolysis during *recA* protein promoted DNA strand exchange: Evidence for long paranemic complexes. *Biochemistry* **26**: 5616-5625.

Schutte, B.C. and Cox, M.M. (1988) Homology-dependent underwinding of duplex DNA in RecA protein generated paranemic complexes. *Biochemistry* **27**: 7886-7894.

Seeley, T.W. and Grossman, L. (1989) Mutations in the *Escherichia coli* UvrB ATPase motif compromise excision repair capacity. *Proc. Natl. Acad. Sci. USA* **86**: 6577-6581.

Selby, C.P. and Sancar, A. (1988) ABC excinuclease incises both 5′ and 3′ to the CC-1065–DNA adduct and its incision activity is stimulated by DNA helicase II and DNA polymerase I. *Biochemistry* **27**: 7184-7188.

Shaner, S.L., Flory, J., and Radding, C.M. (1987a) The distribution of *Escherichia coli* recA protein bound to duplex DNA with single-stranded ends. *J. Biol. Chem.* **262**: 9220-9230.

Shaner, S.L., Flory, J., and Radding, C.M. (1987b) Nucleation of binding of RecA protein to duplex DNA by single-stranded tails in the presence of ATP, *in DNA Replication and Recombination.* R. McMacken and T.J. Kelley, ed. UCLA Symposia on Molecular and Cellular Biology, New Series, Vol. 47. New York: Alan R. Liss, Inc. pp. 629-636.

Shavitt, O. and Livneh, Z. (1989) The β subunit modulates bypass and termination at UV lesions during *in vitro* replication with DNA polymerase III holoenzyme of *Escherichia coli*. *J. Biol. Chem.* **264**: 11275-11281.

Shi, Y.-b. and Hearst, J.E. (1986) Thermostability of double-stranded deoxyribonucleic acids: Effects of covalent additions of a psoralen. *Biochemistry* **25**: 5895-5902.

Shibata, T., DasGupta, C., Cunningham, R.P., Williams, J.G.K., Osber, L., and Radding, C.M. (1981) Homologous pairing in genetic recombination: The pairing reaction catalyzed by *Escherichia coli* RecA protein. *J. Biol. Chem.* **256**: 7565-7572.

Shibata, T., Makino, O., Ikawa, S., Ohtani, T., Iwabuchi, M., Shibata, Y., Maeda, H., and Ando, T. (1984) Roles of processive unwinding in recombination reactions promoted by RecA protein of *Escherichia coli*: A study using a monoclonal antibody. *Cold Spring Harbor Symp. Quant. Biol.* **49**: 541-551.

Shinagawa, H., Iwasaki, H., Kato, T., and Nakata, A. (1988) RecA protein-dependent cleavage of UmuD protein and SOS mutagenesis. *Proc. Natl. Acad. Sci. USA* **85**: 1806-1810.

Shure, M., Pulleyblank, D.E., and Vinograd, J. (1977) The problems of eukaryotic and prokaryotic DNA packaging and *in vivo* conformation posed by superhelix density heterogeneity. *Nucl. Acids Res.* **4**: 1183-1205.

Shwartz, H. and Livneh, Z. (1987) Dynamics of termination during *in vitro* replication of ultraviolet-irradiated DNA with DNA polymerase III holoenzyme of *Escherichia coli*. *J. Biol. Chem.* **262**: 10518-10523.

Shwartz, H. and Livneh, Z. (1989) RecA protein inhibits *in vitro* replication of single-stranded DNA with DNA polymerase III holoenzyme of *Escherichia coli*. *Mutat. Res.* **213**: 165-173.

Shwartz, H., Shavitt, O., Hevroni, D., Tadmor, Y., Cohen, O., and Livneh, Z. (1988a) *In vitro* replication of damaged DNA: A model for SOS-mutagenesis, *in Mechanisms and Consequences of DNA Damage Processing*. E.C. Friedberg and P.C. Hanawalt, ed. UCLA Symposia on Molecular and Cellular Biology, New Series, Vol. 83. New York: Alan R. Liss, Inc. pp. 471-475.

Shwartz, H., Shavitt, O., and Livneh, Z. (1988b) The role of exonucleolytic processing and polymerase–DNA association in bypass of lesions during replication *in vitro*. *J. Biol. Chem.* **263**: 18277-18285.

Sibghat-Ullah, Husain, I., Carlton, W., and Sancar, A. (1989) Human nucleotide excision repair *in vitro*: Repair of pyrimidine dimers, psoralen and cisplatin adducts by HeLa cell-free extract. *Nucl. Acids Res.* **17**: 4471-4484.

Sibghat-Ullah and Sancar, A. (1990) Substrate overlap and functional competition between human nucleotide excision repair and *E. coli* photolyase and (A)BC excision nuclease. *submitted*

Sladek, F.M. (1988) *Psoralen Interstrand Crosslinks: Intermediates in Repair and Mutagenesis in Escherichia coli.* Ph.D. dissertation, Yale University.

Sladek, F.M., Melian, A., and Howard-Flanders, P. (1989a) Incision by UvrABC excinuclease is a step in the path to mutagenesis by psoralen crosslinks in *Escherichia coli*. *Proc. Natl. Acad. Sci. USA* **86**: 3982-3986.

Sladek, F.M., Munn, M.M., Rupp, W.D., and Howard-Flanders, P. (1989b) *In vitro* repair of psoralen-DNA cross-links by RecA, UvrABC, and the 5′-exonuclease of DNA polymerase I. *J. Biol. Chem.* **264**: 6755-6765.

Smith, C.A. (1988) Repair of DNA containing furocoumarin adducts, *in Psoralen DNA Photobiology*. F.P. Gasparro, ed. Vol. 2. Boca Raton: CRC Press, Inc. pp. 87-116.

Smith, G.R. (1989) Homologous recombination in *E. coli*: Multiple pathways for multiple reasons. *Cell* **58**: 807-809.

Smith, K.C. and Sharma, R.C. (1987) A model for the *recA*-dependent repair of excision gaps in UV-irradiated *Escherichia coli*. *Mutat. Res.* **183**: 1-9.

Smith, K.C. and Wang, T.-c.V. (1989) *recA*-dependent DNA repair processes. *BioEssays* **10**: 12-16.

Smith, K.C., Wang, T.-c.V., and Sharma, R.C. (1987) *recA*-dependent DNA repair in UV-irradiated *Escherichia coli*. *J. Photochem. Photobiol. B: Biol.* **1**: 1-11.

Song, P.-S. and Tapley, K.J., Jr. (1979) Photochemistry and photobiology of psoralens. *Photochem. Photobiol.* **29**: 1177-1197.

Stasiak, A. and Di Capua, E. (1982) The helicity of DNA in complexes with RecA protein. *Nature* **299**: 185-186.

Stasiak, A., Di Capua, E., and Koller, T. (1981) Elongation of duplex DNA by recA protein. *J. Mol. Biol.* **151**: 557-564.

Stasiak, A. and Egelman, E.H. (1986) Structure and dynamics of RecA protein-DNA complexes as determined by image analysis of electron micrographs. *Biophys. J.* **49**: 5-7.

Stasiak, A. and Egelman, E.H. (1987) RecA protein-DNA interactions in recombination, *in DNA Replication and Recombination*. R. McMacken and T.J. Kelley, ed. UCLA Symposia on Molecular and Cellular Biology, New Series, Vol. 47. New York: Alan R. Liss, Inc. pp. 619-628.

Stasiak, A., Egelman, E.H., and Howard-Flanders, P. (1988) Structure of helical RecA-DNA complexes, III. The structural polarity of RecA filaments and functional polarity in the RecA-mediated strand exchange reaction. *J. Mol. Biol.* **202**: 659-662.

Stasiak, A., Stasiak, A.Z., and Koller, T. (1984) Visualization of RecA-DNA complexes involved in consecutive stages of an *in vitro* strand exchange reaction. *Cold Spring Harbor Symp. Quant. Biol.* **49**: 561-570.

Takahashi, M., Kubista, M., and Nordén, B. (1989) Binding stoichiometry and structure of RecA-DNA complexes studied by flow linear dichroism and fluorescence

spectroscopy. Evidence for multiple heterogeneous DNA co-ordination. *J. Mol. Biol.* **205**: 137-147.

Takahashi, M., Strazielle, C., Pouyet, J., and Daune, M. (1986) Co-operativity value of DNA-RecA protein interaction. Influence of the protein quaternary structure on the binding analysis. *J. Mol. Biol.* **189**: 711-714.

Taylor, J.-S. and O'Day, C.L. (1990) *Cis-syn* thymine dimers are not absolute blocks to replication by DNA polymerase I of *Escherichia coli in vitro*. *Biochemistry* **29**: 1624-1632.

Tessman, J.W., Isaacs, S.T., and Hearst, J.E. (1985) Photochemistry of the furan-side 8-methoxypsoralen–thymidine monoadduct inside the DNA helix. Conversion to diadduct and to pyrone-side monoadduct. *Biochemistry* **24**: 1669-1676.

Thomas, D.C., Kunkel, T.A., Casna, N.J., Ford, J.P., and Sancar, A. (1986) Activities and incision patterns of ABC excinuclease on modified DNA containing single-base mismatches and extrahelical bases. *J. Biol. Chem.* **261**: 14496-14505.

Thomas, D.C., Levy, M., and Sancar, A. (1985) Amplification and purification of UvrA, UvrB, and UvrC proteins of *Escherichia coli*. *J. Biol. Chem.* **260**: 9875-9883.

Thompson, L. and Bootsma, D. (1988) Designation of mammalian complementation groups and repair genes, *in Mechanisms and Consequences of DNA Damage Processing*. E.C. Friedberg and P.C. Hanawalt, ed. UCLA Symposia on Molecular and Cellular Biology, New Series, Vol. 83. New York: Alan R. Liss, Inc. pp. 279.

Thompson, L.H., Weber, C.A., and Carrano, A.V. (1988) Human DNA repair genes, *in Mechanisms and Consequences of DNA Damage Processing*. E.C. Friedberg and P.C. Hanawalt, ed. UCLA Symposia on Molecular and Cellular Biology, New Series, Vol. 83. New York: Alan R. Liss, Inc. pp. 289-293.

Thresher, R.J., Christiansen, G., and Griffith, J.D. (1988) Assembly of presynaptic filaments. Factors affecting the assembly of RecA protein onto single-stranded DNA. *J. Mol. Biol.* **201**: 101-113.

Tomic, M.T., Wemmer, D.E., and Kim, S.-H. (1987) Structure of a psoralen cross-linked DNA in solution by nuclear magnetic resonance. *Science* **238**: 1722-1725.

Tsang, S.S., Muniyappa, K., Azhderian, E., Gonda, D.K., Radding, C.M., Flory, J., and Chase, J.W. (1985) Intermediates in homologous pairing promoted by recA protein. Isolation and characterization of active presynaptic complexes. *J. Mol. Biol.* **185**: 295-309.

Van Houten, B., Gamper, H., Hearst, J.E., and Sancar, A. (1986a) Construction of DNA substrates modified with psoralen at a unique site and study of the action mechanism of ABC excinuclease on these uniformly modified substrates. *J. Biol. Chem.* **261**: 14135-14141.

Van Houten, B., Gamper, H., Hearst, J.E., and Sancar, A. (1988) Analysis of sequential steps of nucleotide excision repair in *Escherichia coli* using synthetic substrates containing single psoralen adducts. *J. Biol. Chem.* **263**: 16553-16560.

Van Houten, B., Gamper, H., Holbrook, S.R., Hearst, J.E., and Sancar, A. (1986b) Action mechanism of ABC excision nuclease on a DNA substrate containing a psoralen crosslink at a defined position. *Proc. Natl. Acad. Sci. USA* **83**: 8077-8081.

Van Houten, B., Gamper, H., Sancar, A., and Hearst, J.E. (1987) DNase I footprint of ABC excinuclease. *J. Biol. Chem.* **262**: 13180-13187.

Voigt, J.M., Van Houten, B., Sancar, A., and Topal, M.D. (1989) Repair of O^6-methylguanine by ABC excinuclease of *Escherichia coli in vitro*. *J. Biol. Chem.* **264**: 5172-5176.

Vos, J.-M.H. (1989) Differential processing of DNA damage on functional mammalian sequences. *Photochem. Photobiol.* **49, Supplement**: 53S-54S.

Vos, J.-M.H. and Hanawalt, P.C. (1987) Processing of psoralen adducts in an active human gene: Repair and replication of DNA containing monoadducts and interstrand cross-links. *Cell* **50**: 789-799.

Wahl, A.F., Hockensmith, J.W., Kowalski, S., and Bambara, R.A. (1983) Alternative explanation for excision repair deficiency caused by the *polA*ex1 mutation. *J. Bacteriol.* **155**: 922-925.

Walker, G.C. (1985) Inducible DNA repair systems. *Ann. Rev. Biochem.* **54**: 425-457.

Walker, J.E., Saraste, M., Runswick, M.J., and Gay, N.J. (1982) Distantly related sequences in the α- and β-subunits of ATP synthase, myosin, kinases and other ATP-requiring enzymes and a common nucleotide binding fold. *EMBO J.* **1**: 945-951.

Walter, R.B., Pierce, J., Case, R., and Tang, M.-s. (1988) Recognition of the DNA helix stabilizing anthramycin-N2 guanine adduct by UvrABC nuclease. *J. Mol. Biol.* **203**: 939-947.

Wang, T.-c.V. and Smith, K.C. (1989) The roles of RecBCD, Ssb and RecA proteins in the formation of heteroduplexes from linear-duplex DNA *in vitro*. *Mol. Gen. Genet.* **216**: 315-320.

Wang, W.-B., Sassanfar, M., Tessman, I., Roberts, J.W., and Tessman, E.S. (1988a) Activation of protease-constitutive RecA proteins of *Escherichia coli* by all of the common nucleoside triphosphates. *J. Bacteriol.* **170**: 4816-4822.

Wang, W.-B. and Tessman, E.S. (1986) Location of functional regions of the *Escherichia coli* RecA protein by DNA sequence analysis of RecA protease-constitutive mutants. *J. Bacteriol.* **168**: 901-910.

Wang, W.-B., Tessman, E.S., and Tessman, I. (1988b) Activation of protease-constitutive RecA proteins of *Escherichia coli* by rRNA and tRNA. *J. Bacteriol.* **170**: 4823-4827.

Weinstock, G.M., McEntee, K., and Lehman, I.R. (1979) ATP-dependent renaturation of DNA catalyzed by the recA protein of *Escherichia coli*. *Proc. Natl. Acad. Sci. USA* **76**: 126-130.

Weinstock, G.M., McEntee, K., and Lehman, I.R. (1981) Hydrolysis of nucleoside triphosphates catalyzed by the recA protein of *Escherichia coli*. Characterization of ATP hydrolysis. *J. Biol. Chem.* **256**: 8829-8834.

Weiss, R.B., Gallagher, P.E., Brent, T.P., and Duker, N.J. (1989) Cytosine photoproduct–DNA glycosylase in *Escherichia coli* and cultured human cells. *Biochemistry* **28**: 1488-1492.

West, S.C. (1988) Protein-DNA interactions in genetic recombination. *Trends Genet.* **4**: 8-13.

West, S.C., Cassuto, E., and Howard-Flanders, P. (1981) Heteroduplex formation by recA protein: Polarity of strand exchanges. *Proc. Natl. Acad. Sci. USA* **78**: 6149-6153.

West, S.C., Cassuto, E., and Howard-Flanders, P. (1982a) Postreplication repair in *E. coli*: Strand exchange reactions of gapped DNA by RecA protein. *Mol. Gen. Genet.* **187**: 209-217.

West, S.C., Cassuto, E., and Howard-Flanders, P. (1982b) Role of SSB protein in RecA promoted branch migration reactions. *Mol. Gen. Genet.* **186**: 333-338.

West, S.C., Cassuto, E., Mursalim, J., and Howard-Flanders, P. (1980) Recognition of duplex DNA containing single-stranded regions by recA protein. *Proc. Natl. Acad. Sci. USA* **77**: 2569-2573.

West, S.C., Countryman, J.K., and Howard-Flanders, P. (1983) Enzymatic formation of biparental figure-eight molecules from plasmid DNA and their resolution in *E. coli*. *Cell* **32**: 817-829.

Williams, J.G.K., Shibata, T., and Radding, C.M. (1981) *Escherichia coli* RecA protein protects single-stranded DNA or gapped duplex DNA from degradation by RecBC DNase. *J. Biol. Chem.* **256**: 7573-7582.

Williams, R.C. and Spengler, S.J. (1986) Fibers of RecA protein and complexes of RecA protein and single-stranded ϕX174 DNA as visualized by negative-stain electron microscopy. *J. Mol. Biol.* **187**: 109-118.

Wood, R.D., Robins, P., and Lindahl, T. (1988) Complementation of the xeroderma pigmentosum DNA repair defect in cell-free extracts. *Cell* **53**: 97-106.

Woodgate, R., Rajagopalan, M., Lu, C., and Echols, H. (1989) UmuC mutagenesis protein of *Escherichia coli*: Purification and interaction with UmuD and UmuD′. *Proc. Natl. Acad. Sci. USA* **86**: 7301-7305.

Wu, A.M., Bianchi, M., DasGupta, C., and Radding, C.M. (1983) Unwinding associated with synapsis of DNA molecules by RecA protein. *Proc. Natl. Acad. Sci. USA* **80**: 1256-1260.

Wu, A.M., Kahn, R., DasGupta, C., and Radding, C.M. (1982) Formation of nascent heteroduplex structures by RecA protein and DNA. *Cell* **30**: 37-44.

Yanisch-Perron, C., Vieira, J., and Messing, J. (1985) Improved M13 phage cloning vectors and host strains: Nucleotide sequences of the M13mp18 and pUC19 vectors. *Gene* **33**: 103-119.

Yarranton, G.T. and Sedgwick, S.G. (1982) Cloned truncated *recA* genes in *E. coli*, II. Effects of truncated gene products on *in vivo* $recA^+$ protein activity. *Mol. Gen. Genet.* **185**: 99-104.

Yatagai, F., Horsfall, M.J., and Glickman, B.W. (1987) Defect in excision repair alters the mutational specificity of PUVA treatment in the *lacI* gene of *Escherichia coli*. *J. Mol. Biol.* **194**: 601-607.

Yeung, A.T., Jones, B.K., Capraro, M., and Chu, T. (1987) The repair of psoralen monoadducts by the *Escherichia coli* UvrABC endonuclease. *Nucl. Acids Res.* **15**: 4957-4971.

Zhen, W.-P., Jeppesen, C., and Nielsen, P.E. (1986) Repair in *Escherichia coli* of a psoralen–DNA interstrand crosslink site specifically introduced into $T_{410}A_{411}$ of the plasmid pUC19. *Photochem. Photobiol.* **44**: 47-51.